

Dissertation zur Erlangung des Doktorgrades
der Fakultät für Chemie und Pharmazie
der Ludwig-Maximilians-Universität München



IAP antagonism as a novel approach to target endothelial activation

Bettina Angela Mayer
aus Bad Reichenhall

2010

Erklärung

Diese Dissertation wurde im Sinne von §13 Abs. 3 bzw. 4 der Promotionsordnung vom 29. Januar 1998 von Frau Prof. Dr. Angelika M. Vollmar am Lehrstuhl für Pharmazeutische Biologie betreut.

Ehrenwörtliche Versicherung

Diese Dissertation wurde selbstständig und ohne unerlaubte Hilfe erarbeitet.

München, den 14. Mai 2010

Bettina Angela Mayer

Dissertation eingereicht am:	14. Mai 2010
1. Gutachter:	Prof. Dr. Angelika M. Vollmar
2. Gutachter:	PD Dr. Stefan Zahler
Mündliche Prüfung am:	11. Juni 2010

meinen Eltern

CONTENTS

1	INTRODUCTION	10
1.1	Background and aim of the study	11
1.2	Inhibitor of Apoptosis Proteins	13
1.2.1	Apoptosis	13
1.2.2	The IAP family	14
1.2.3	Structural elements of IAPs	14
1.2.3.1	The structure and functions of the BIR domains.....	14
1.2.3.2	The UBA and the CARD domains	16
1.2.3.3	The RING domain.....	16
1.2.3.4	IAPs in TNFR signaling.....	16
1.2.4	IAP antagonists.....	18
1.2.4.1	Smac.....	18
1.2.4.2	Synthetic monovalent Smac mimetics	19
1.3	Endothelium.....	20
1.3.1	Endothelial permeability.....	21
1.3.2	Endothelium and inflammation	22
1.3.2.1	Leukocyte recruitment	23
1.3.2.2	Signaling involved in inflammatory activation of endothelial cells.....	24
2	MATERIALS AND METHODS	28
2.1	Materials	29
2.1.1	Biochemicals and inhibitors, dyes and cell culture reagents.....	29
2.2	Cell culture	32
2.2.1	Solutions and reagents	32
2.2.2	Endothelial cells.....	32
2.2.2.1	HMEC-1 (Human microvascular endothelial cells)	33
2.2.2.2	HUVECs (Human umbilical vein endothelial cells)	33
2.2.3	Passaging	33
2.2.4	Freezing and thawing	34
2.2.5	Isolation of human neutrophil granulocytes	34
2.3	Preparation of protein samples.....	35
2.3.1	Total cell lysates	35
2.3.2	Immunoprecipitation	36
2.3.3	Membrane fractionation	37
2.3.4	Extraction of nuclear proteins	37
2.4	Western blot analysis.....	38

2.4.1	Protein quantification	38
2.4.1.1	Bicinchoninic (BCA) Protein Assay	38
2.4.1.2	Bradford Assay	38
2.4.2	SDS-PAGE	39
2.4.3	Tank electroblotting	40
2.4.4	Protein detection	40
2.4.4.1	Enhanced chemiluminescence	41
2.4.4.2	Infrared imaging	41
2.5	Electrophoretic mobility shift assay (EMSA)	42
2.5.1	Binding reaction and electrophoretic separation	42
2.6	Flow cytometry	43
2.6.1	Analysis of ICAM-1 expression on cell surface	44
2.6.2	Determination of cell surface expression of CD11b	44
2.6.3	Determination of ROS production in granulocytes	44
2.6.4	Quantification of apoptosis rate	45
2.7	Transfection of cells	45
2.7.1	Transfection with siRNA	45
2.7.2	Transfection with plasmids	46
2.8	Dual Luciferase [®] Reporter Assay System	46
2.9	Macromolecular permeability assay	47
2.10	Confocal microscopy	48
2.11	Leukocyte adhesion assay	48
2.11.1	Adhesion assay	48
2.11.2	Myeloperoxidase (MPO) activity	48
2.12	<i>In vivo</i> assays	49
2.12.1	Animals	49
2.12.2	Murine antigen-induced arthritis	49
2.12.3	Analysis of leukocyte adhesion and transmigration by intravital microscopy of mouse cremaster muscle	50
2.12.4	Statistical analysis	51

3	RESULTS	52
3.1	ABT abolishes antigen-induced arthritis in mice and inhibits leukocyte transmigration <i>in vivo</i>	53
3.2	ABT does not exert proapoptotic effects in HUVECs	55
3.3	Influence of ABT on endothelial barrier function	56
3.3.1	ABT inhibits macromolecular hyperpermeability	56
3.3.2	Impact of ABT on adhesion junctions and the contractile machinery of endothelial cells	57
3.4	Effects of ABT on leukocyte adhesion to endothelial cells	58
3.4.1	Influence of ABT on CD11b expression and oxidative burst of neutrophil granulocytes	58
3.5	Role of IAPs in TNF α -induced adhesion molecule expression	60
3.5.1	ABT reduces TNF α -induced expression of an endothelial adhesion molecule	60
3.5.2	The IAP inhibitors Smac066 and Smac085 are capable of reducing TNF α -induced expression of ICAM-1	61
3.5.3	Impact of the pan-caspase inhibitor Q-VD-OPh on ICAM-1 expression induced by TNF α	62
3.6	Interactions of ABT with the NF κ B signaling	63
3.6.1	ABT does not influence phosphorylation and degradation of I κ B α	63
3.6.2	The translocation of p65 is not impaired by ABT	63
3.6.3	ABT does not affect the DNA-binding capacity of NF κ B	64
3.6.4	NF κ B-dependent promoter activity is not influenced by ABT	65
3.7	Interactions of ABT with MAPK signaling	66
3.7.1	ABT affects TNF α -induced activation of MAPKs	66
3.7.2	Inhibition of p38 and JNK influence ICAM-1 expression	66
3.7.3	ABT controls the activity of the MAP3K TAK1	67
3.7.4	Impact of ABT on the interactions of TAK1 binding protein (TAB1) with XIAP	68
3.8	Silencing of XIAP does not reduce ICAM-1 expression	69
3.9	Interactions of ABT with the TNF receptor signaling	70
3.9.1	ABT induces degradation of cIAP1 and cIAP2	70
3.9.2	The proteasomal degradation of cIAP1 and cIAP2 is responsible for the anti-inflammatory effect of ABT	71

3.9.3	Influence of ABT on the participants of the TNFR1-associated complex TRAF2 and TRAF5.....	72
4	DISCUSSION	73
4.1	The link between IAPs and inflammation.....	74
4.2	Anti-inflammatory effects of ABT <i>in vivo</i>	74
4.3	Effects of ABT on endothelial activation <i>in vitro</i>	75
4.3.1	Functional <i>in vitro</i> assays	75
4.3.1.1	Endothelial permeability.....	76
4.3.1.2	ICAM-1 mediated endothelium leukocyte interactions.....	76
4.3.1.3	Specificity of the ICAM-1-attenuating effect of ABT	77
4.3.2	Signaling	78
4.3.2.1	NF κ B/MAPK signaling	78
4.3.2.2	Role of XIAP	79
4.3.2.3	Role of cIAP1 and cIAP2	80
4.3.2.4	TNFR-associated signaling.....	81
5	SUMMARY AND CONCLUSION	82
6	ANP	85
7	REFERENCES	99
8	APPENDIX	112
8.1	Publications	113
8.1.1	Original publications	113
8.1.2	Abstracts.....	113
8.1.3	Grants	114
8.2	Curriculum vitae.....	115
8.3	Acknowledgements.....	116

Introductory remark

The main part of this work refers to the investigation of the role of inhibitor of apoptosis proteins (IAPs) in inflammatory processes of endothelial cells and the effects of an IAP antagonist in inflammation. The second part corresponds to the project I worked on before that and consists of the published manuscript dealing with the influence of ANP on endothelial hyperpermeability.

1 INTRODUCTION

1.1 Background and aim of the study

XIAP, cIAP1 and cIAP2 are the best characterized mammalian members of the inhibitor of apoptosis protein (IAP) family, whose common feature is the appearance of variable numbers of baculoviral IAP repeat (BIR) domains. The IAPs, in particular XIAP, are implicated in the regulation of apoptosis by interaction with caspases via their BIR domains.^{1, 2} Due to the fact that IAPs often are over-expressed in human malignancies,^{3, 4} they became attractive targets for the development of anti-cancer therapeutics based on the structure of the endogenous IAP antagonist Smac.⁵ The peptidic Smac mimetic A-410099.1 (ABT), which we used as a tool for this work, is a high affinity, proteolytic stable, small molecule inhibitor modelled to bind to the BIR3 domain of XIAP with an affinity in a nanomolar K_d range and has been employed for anti-cancer strategies.⁶

Besides their anti-apoptotic function, IAPs interact with a variety of signaling molecules and pathways: The BIR1 domain of XIAP participates in the activation of the MAP3-kinase TAK1,⁷ whereas the BIR1 domain of cIAP1 and cIAP2 interacts with the INF -receptor associated proteins TRAF1 and TRAF2.^{8, 9} Additionally to the BIR motifs, XIAP, cIAP1 and cIAP2 contain a RING (really interesting new gene) domain with E3-ubiquitin protein ligase activity that promotes the transfer of ubiquitin chains to target proteins.¹⁰ The ubiquitination of proteins can on the one hand promote proteasomal degradation or on the other hand contribute to signaling processes. By providing ubiquitin platforms, cIAP1 and cIAP2 are important players in the INF receptor 1 (TNFR1) signaling. They contribute to the recruitment of TNFR1-associated signaling complexes like TAK/TAB (activation of MAPK and $\text{NF}\kappa\text{B}$ signaling) or IKK/NEMO (activation of $\text{NF}\kappa\text{B}$ signaling).^{11, 12}

The TNF receptor-associated signaling is a key factor in the induction of inflammatory processes. Acute and chronic inflammation is implicated in a number of severe diseases like atherosclerosis, arthritis or sepsis. The endothelium, which regulates the recruitment of circulating leukocytes and promotes their transmigration from blood to the tissue, is a crucial player in inflammation.¹³ Despite the involvement of cIAP1 and cIAP2 in TNFR signaling, there is as yet nothing known about their role in inflammatory processes.

These facts led us to the hypothesis that IAP antagonists function not only as inducers of apoptosis but might also have an anti-inflammatory potential and that the IAPs are involved in the regulation of inflammatory events.

The **aims of the study** were:

1. to elucidate if IAP antagonists have an anti-inflammatory potential and
2. to unravel the role of IAPs in inflammatory processes in endothelial cells.

1.2 Inhibitor of Apoptosis Proteins

1.2.1 Apoptosis

Apoptosis is a process of programmed cell death which is of physiological importance for tissue homeostasis and control of proliferation. In many human disorders apoptosis is dysregulated as demonstrated by the excessive cell death in neurodegenerative disorders or the insufficient apoptosis in cancer.¹⁴ The main actors in apoptosis are caspases, a family of proteases, which occur in the cell as inactive zymogens (procaspases). The activity of the initiator caspases (caspases 8 and caspases 9) is induced upon proapoptotic stimuli and they activate the downstream effector caspases (caspases 3 and 7) by proteolytic cleavage.¹⁵ The extrinsic pathway triggers apoptosis upon binding of proapoptotic ligands to cell surface receptors from the tumor necrosis factor receptor (TNFR) family. This results in a recruitment of adaptor proteins (TRADD, FADD, Fas) which form the death inducing signaling complex (DISC) and activate the procaspase-8.¹⁶ Apoptosis goes along with a release of proapoptotic factors like cytochrome c (cyt c), or the second mitochondria-derived activator of caspases (Smac) from the mitochondrion. There exist several specific cellular inhibitors that prevent inappropriate induction of cell death like the inhibitor of apoptosis proteins (Figure 1).

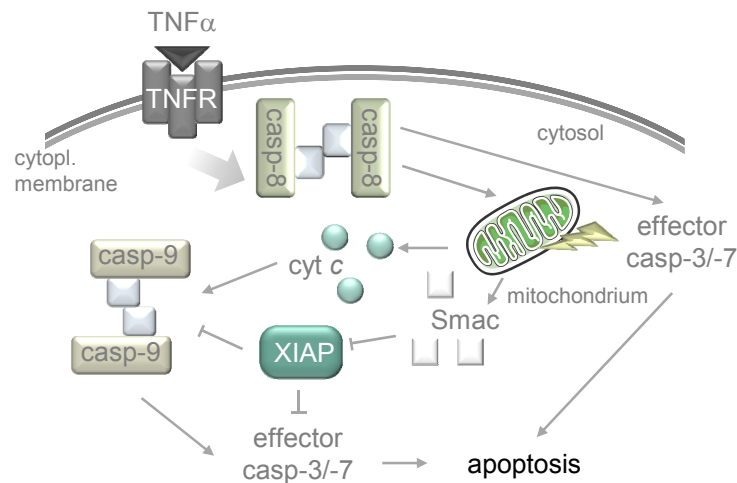


Figure 1 Apoptotic pathways. The extrinsic pathway triggers apoptosis upon binding of a ligand to a receptor from the TNFR family resulting in an activation of caspase-8. Caspase-8 on the one hand directly activates the caspases-3 and -7. On the other hand caspase-8 can amplify the apoptotic signal via inducing the release of proapoptotic substances (Smac, cytochrome c) from the mitochondrion, like the intrinsic activation of apoptosis does, and thereby mobilizes the effector caspases-3 and -7. The inhibitor of apoptosis proteins block the activation of caspase-3, -7 and -9.

1.2.2 The IAP family

The inhibitor of apoptosis proteins (IAPs) have been identified in many different organisms like in yeast, nematodes, flies and higher vertebrates. The *iap* gene was discovered 17 years ago by Miller and colleagues as a gene that inhibits apoptosis in virally-infected *Spodoptera frugiperda* cells.¹⁷ The name of the IAPs derives from their ability to suppress apoptosis that is triggered by a variety of stimuli.¹⁸⁻²⁰ New insights from deletion experiments in mice and *Drosophila melanogaster* disclose that the IAPs also are involved in many other cellular events including signal transduction, proliferation and differentiation processes.²¹ There are at least 8 mammalian members of the IAP family: NAIP, ILP2, BRUCE, survivin, livin, X-linked IAP (XIAP), cellular IAP1 (cIAP1) and cellular IAP2 (cIAP2). XIAP, cIAP1 and cIAP2 are the best-characterized members²²⁻²⁴. In mammalian cells IAPs are not inevitable for inhibition of apoptosis but regulate the apoptotic response under stress conditions.²⁵ The knockout of XIAP in mice does not induce spontaneous apoptosis²⁶ but XIAP exhibits protective effects in the survival of post-mitotic neurons²⁷ and cardiomyocytes²⁸.

1.2.3 Structural elements of IAPs

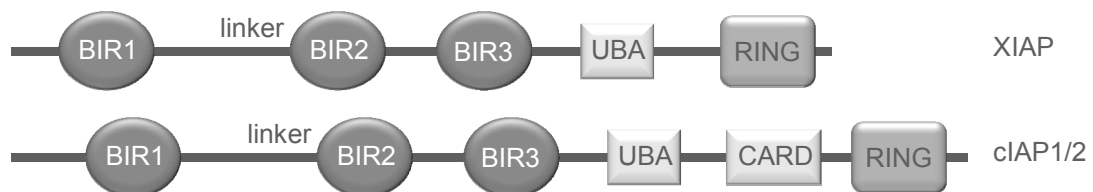


Figure 2 Domain organization of IAPs. (BIR: baculoviral IAP repeat, UBA: ubiquitin-associated, CARD: caspase recruitment domain, RING: really interesting new gene)

1.2.3.1 The structure and functions of the BIR domains

The common feature of all IAPs is the occurrence of one to three copies of baculoviral IAP repeat (BIR) domains.²⁹ The BIR domains comprise 70 to 80 amino acids and contain a conserved C2HC-type zinc finger motif.^{29, 30} XIAP, cIAP1 and cIAP2 consist of three N-terminal BIR domains. Most of the BIR domains contain a surface groove that is called IBM-interacting exosite and interacts with N-terminal IAP binding motifs

(IBMs). IBMs occur for example in Smac, the cellular IAP antagonist, and in the caspases-3, -7, and -9.³¹

Generally, there are specific sequence differences in the BIR domains that result in distinct binding properties. Therefore, IAPs containing different BIR domains are able to interact with multiple proteins. BIR domains also show association properties. The BIR1 domain of XIAP for example forms homodimers.⁷

XIAP, cIAP1 and cIAP2 regulate the activity of both, initiator and effector caspases. The BIR domains of cIAP1 and cIAP2 efficiently bind to caspases-3, -7, and -9. However they most likely do not inhibit them via an interaction between their BIR domains and the caspases because they do not possess the precise structural elements required for the inhibition of those enzymes.³² Instead, cIAP1 and cIAP2 are believed to regulate cell survival by influencing TNFR signaling and caspase-8 signaling.¹¹

Most likely, XIAP is the only direct inhibitor of the caspases-3, -7, and -9.^{32, 33} XIAP interacts with caspase-3 via the linker region preceding the BIR2 domain.³⁴ The interaction with caspase-7 is mediated by the linker region and the BIR2 domain.³⁵ The BIR3 domain interferes with caspase-9.²

Besides their direct binding to caspases, the IAPs have been shown to interact with a number of adaptor proteins and therefore are involved in the regulation of different signaling pathways like heavy metal metabolism, cell division, morphogenesis, mitogen-activated protein kinase (MAPK) pathways and nuclear factor κ B (NF κ B) activation. In contrast to BIR2 and BIR3, the BIR1-domain of XIAP, cIAP1 and cIAP2 does not bind caspases but functions in several signaling pathways via an oligomerization of binding partners.³⁶ The interaction of the XIAP BIR-1 domain with the TGF β -activated kinase 1 (TAK1) binding protein 1 (TAB1) for example can activate the MAP kinase kinase kinase (MAP3K) TAK1⁷ and therefore NF κ B signaling. The BIR1 domains of cIAP1 and cIAP2 similarly interact with TRAF1 and TRAF2,^{8, 37-39} adapter proteins that are associated with TNFR signaling complexes.

Despite structural similarity, the BIR domains are multifaceted protein-protein-interaction domains that can bind numerous proteins that are involved in diverse apoptotic and signaling processes.³¹

1.2.3.2 The UBA and the CARD domains

The last BIR domains of IAPs (like cIAP1, cIAP2 and XIAP) are followed by a domain that is homologous to ubiquitin-associated (UBA) domains. It enables IAPs to bind ubiquitin residues.³¹

Some members of the IAP family, like cIAP1 and cIAP2, are characterized by the occurrence of a homotypic dimerization domain, the caspase recruitment domain (CARD).⁴⁰ This domain is recognized in a increasing number of proteins that participate in apoptotic or inflammatory signaling complexes.⁴¹

1.2.3.3 The RING domain

The C-terminal really interesting new gene (RING) zinc-finger domain possesses E3 ubiquitin ligase activity which mediates IAP autoubiquitination as well as the ubiquitination of other proteins like caspases-3, -7, and -9,^{42, 43} TRAF1, TRAF2 and RIP,^{37, 44} Smac,⁴³ and NEMO/IKK γ .^{10, 45, 46} The conjugation of ubiquitin requires an ubiquitin-activating enzyme (E1), an ubiquitin-conjugating enzyme (E2), and an ubiquitin protein ligase (E3).⁴⁷ E3 ligases facilitate the generation of an isopeptide bond between the C-terminus of ubiquitin and the amino group of a reactive side chain of the substrate, mostly a lysine residue (K).⁴⁸ The seven K residues of ubiquitin can accept further attachment of ubiquitin resulting in a formation of polyubiquitin chains. The linkage of the ubiquitin chains determines the fate of the modified protein. K48-linked polyubiquitin chains render the modified protein to degradation by the 26S proteasome.⁴⁴ In contrast, K63-linked polyubiquitin chains as well as monoubiquitination are involved in a variety of nondegradative signaling processes. They often serve as a kind of scaffold for the association of other proteins in order to build signaling platforms³⁴⁻³⁶ or alter the activation of the modified protein (NEMO/IKK γ).^{46, 49}

The ubiquitination processes exerted by their RING domains (K48 and K63) allow cIAP1 and cIAP2 to contribute to several signaling pathways, for instance the TNFR signaling.

1.2.3.4 IAPs in TNFR signaling

Many biological responses are achieved by TNF α signaling. The cytokine can be involved in the induction of other pro-inflammatory cytokines, cell proliferation, differentiation or cell death.⁵⁰ The pathogenesis of many human diseases like cancer,

sepsis, diabetes and autoimmune diseases involves inadequate TNF α signaling.⁵¹ Notably, most cancer cells pass on to autocrine TNF α signaling.^{52, 53} TNF α binds to two cell surface receptors: TNFR1 and TNFR2. The TNFR1 is the best-characterized receptor for TNF α and mediates most of the TNF α -induced effects whereby ubiquitination processes play an important role.⁵⁴ TNFR1 activates caspase-8, the transcription factor NF κ B and MAPKs like p38 and JNK.^{36, 55}

The association of cIAP1 and cIAP2 with the RING domain-containing proteins TRAF1 and TRAF2 assigns cIAP1/2 to be components of TNFR1-associated signaling complex.^{23, 56-59} Binding of TNF α induces a trimerization of TNFR1 and stimulates the formation of the TNFR-associated signaling complex I. This involves the death domain-mediated binding of the adapter protein TNF receptor-associated protein with death domain (TRADD) to the cytoplasmic tail of TNFR1.⁶⁰ TRADD immediately recruits TRAF2, the receptor-interacting protein 1 (RIP1) and cIAP1 and cIAP2.^{12, 61-64} cIAP1 ubiquitinates several components of the TNFR-associated complex I, including itself and RIP1 (K63-linked ubiquitination), which facilitates the recruitment of the I κ B kinase (IKK) complex and the TAB/TAK complex. The outcome of this is the activation of NF κ B and MAPK signaling promoting prosurvival and proinflammatory transcriptional response.^{53, 65}

In cancer cells, cIAP1 and cIAP2 seem to be crucial for the induction of the TNF α -caused NF κ B activation and therefore protect the cells from TNF α -mediated cell death.^{52, 58} Additionally, the presence of cIAP1 and cIAP2 in the TNFR1-associated signaling complex is essential for the inhibition of caspase-8.^{23, 66} The K63-linked ubiquitination of RIP1 seems to prevent its release from the TNFR-associated complex and therefore the recruitment and activation of FADD and caspase-8.^{57, 67, 68}

Thus, cIAP1 and cIAP2 are crucial players in TNFR1 signaling (Figure 3) and important regulators of apoptosis although they are not able to directly inhibit the activation of caspases via their BIR2 and BIR3 domains.

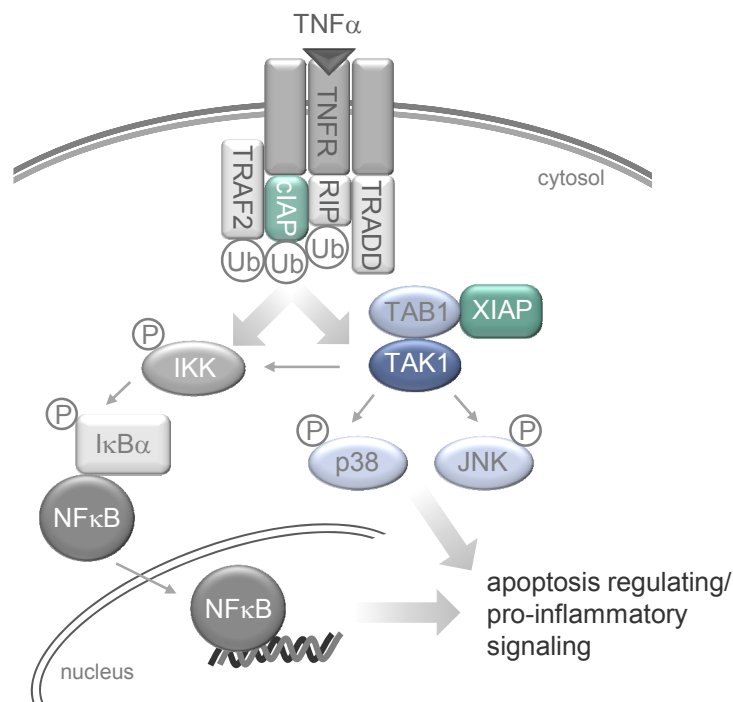


Figure 3 IAPs in TNFR-associated signaling.

1.2.4 IAP antagonists

In many human malignancies IAPs are often overexpressed going along with a poor survival prognosis for the patient (cIAP1: multipla myeloma, various carcinomas; cIAP2: MALT lymphoma, multiple myeloma, various carcinoma; XIAP: X-linked lymphoproliferative disorder).⁶⁸ The upregulation of IAPs causes resistance of cancer cells to chemotherapy and radiation.⁶⁹ Therefore, the IAPs are interesting targets for the development of new anti-cancer drugs, such as small molecule IAP antagonists. These IAP antagonists are designed on the basis of the interaction of Smac, the endogenous IAP inhibitor, with XIAP.⁶

1.2.4.1 Smac

Smac is encoded by a nuclear gene and is subsequently imported into mitochondria. Mature Smac is generated by cleavage of the N-terminus.^{70, 71} It is released from the mitochondrion upon proapoptotic stimuli to inhibit the activity of IAPs and to enable the induction of apoptosis. The Ala1-Val2-Pro3-Ile4 (AVPI) residues exposed at the N-

terminus of mature, dimeric Smac interacts with a surface groove in the BIR2 and BIR3 but not with the BIR1 domain of XIAP.⁷² Smac competes with caspase-9 for binding to the BIR3 domain of XIAP and therefore gives rise to induction of apoptosis.^{5, 72, 73} Even though Smac does not interact with the BIR1 domain, Smac binding to the BIR2 and BIR 3 domains of XIAP, respectively, induces changes affecting the BIR1 interactions with its downstream targets. In particular, Smac prevents full-length XIAP BIR1/TAB1 interactions.⁷

Recent studies showed that, besides preventing the XIAP-caspases-9 interaction, Smac and synthetic Smac mimetics target cIAP1 and cIAP2 by induction of their autoubiquitination followed by their proteasomal degradation.^{59, 74} In the contrary, Smac (and some of the IAP antagonists) does not induce the degradation of XIAP.^{74, 75} As members of the TNFR1-associated signaling complex, cIAP1 and cIAP2 suppress the activation of caspase-8. The Smac- or IAP antagonist-induced loss of cIAP1 and cIAP2 alters TNFR signaling regarding ubiquitination processes and NF κ B activation and therefore sensitizes cells to TNF α -mediated apoptosis.^{11, 67}

1.2.4.2 Synthetic monovalent Smac mimetics

Since the therapeutic use of peptides is constraint by proteolytic stability, limited cell permeation and poor pharmacokinetics the development of synthetic Smac mimetics aims in achieving cell permeable, high affinity and proteolytic stable IAP antagonists. Oost *et al.* 2004⁶ used the pentapeptide N-terminus AVPFY of the functional Smac homologue HID (head involution deficiency), which is characterized by a better binding affinity for the XIAP BIR3 domain than AVPI, as a starting point for the generation of four peptide libraries. In these peptide libraries each of the first four residues had been varied, while the other four were left unchanged. By analyzing the structure-activity relationships (SAR), they gained a series of proteolytically stable, capped tripeptides comprised of unnatural amino acids that are shown to bind to the XIAP BIR3 domain with low nanomolar affinity. One of these synthetic peptides, the compound 11 (also called: A-410099.1 or in the following: ABT) is depicted in Figure 4 and was used for this work. It exhibits cytotoxic effects in cancer cell lines and was successfully applied in a MDA-MB-231 breast cancer mouse xenograft model. It binds to the BIR3 domain of XIAP with a K_d of 16 nM.

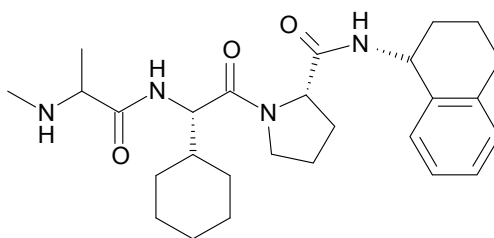


Figure 4 Synthetic IAP antagonist: A-10099.1 (ABT, Compound 11; Oost *et al.* 2004)

Recently, IAP antagonists have come into the focus of attention of many research groups. On the one hand, IAP antagonists sensitize cancer cells to TNF α -induced apoptosis and, therefore, they render the IAPs to be an outstanding therapeutical target.⁷⁶ The Smac mimetics developed by the companies Aegara (Human Genome Sciences, Rockvill, MD, USA) and Genentech (San Francisco, CA, USA/Abbott) have already reached clinical trials phase I.^{68, 69} On the other hand, IAP antagonists are designed and used by several other research groups to uncover the exact role of IAPs and TNFR signaling in apoptotic processes.^{68, 77, 78}

Despite the knowledge about the participation of IAPs in NF κ B and TNFR signaling, which are not only involved in apoptosis but also critical mediators of inflammation, until now there is nothing known about the role of IAPs in inflammatory processes of endothelial cells.

1.3 Endothelium

The endothelium is the innermost cell monolayer of blood vessels separating the lumen from the tissue. It is not just like a wall paper lining the vessels but fulfills, not at least due to its strategic position, important functions regarding vessel tone homeostasis, the supply of the tissue with nutrients and gasses, tissue fluid homeostasis, hemostasis, and angiogenesis, and host defense.⁷⁹⁻⁸¹ To implement the tasks of macromolecular transport, tissue fluid homeostasis and regulation of leukocyte transmigration the endothelium shows the properties of a semi-permeable barrier.⁸⁰

1.3.1 Endothelial permeability

Under physiological conditions, the endothelial cell barrier tightly regulates the permeation of liquids and solutes. Macromolecules like plasma proteins are transported on the vesicle-mediated transcellular pathway. The endothelium allows the passive paracellular diffusion of small macromolecules but restricts the free passage of bigger macromolecules through the minute gaps that arise from the interendothelial junctions (IEJ).⁸² The endothelial barrier function is maintained by a balance between adhesive forces represented by the IEJs, which are connected to the actin cytoskeleton and the contractile forces, that result from the interaction of myosin with the actin cytoskeleton.⁸⁰ The interendothelial junctions consist of tight junctions and mainly of adherens junctions (AJ). These are composed of vascular endothelial cadherin (VE-cadherin).⁸⁰ VE-cadherin interacts homotypically and this interaction is Ca^{2+} -dependent. Changes in the phosphorylation state of VE-cadherin, for example evoked by protein kinase C (PKC), regulate the AJ stability by inducing the internalization of VE-cadherin.⁸³ The juxtamembrane domain of VE-cadherin is linked to p120 catenin whereas the C-terminal domain binds α - and β -catenin, which link VE-cadherin to the actin cytoskeleton.⁸⁴ p120 provides a scaffold function and controls the interaction of VE-cadherin with important regulators of vascular endothelial permeability like Rho-GTPases or phosphatases. The interaction of VE-cadherin with the cortical actin cytoskeleton stabilizes the AJ while the reorganization of actin into stress fibers mediates cellular contraction and disrupts the AJ.⁸⁰ These contractile forces are generated by the interaction of the stress fiber components myosin II and actin induced by a phosphorylation of the regulatory myosin light chain 2 (MLC2). MLC2 is phosphorylated by the Ca^{2+} /calmodulin-dependent MLC kinase (MLCK). The phosphorylation of MLC2 can also be influenced by the downstream effector of the small GTPase RhoA, Rho Kinase (ROCK), that inhibits the MLC2 phosphatase (MYPT) activity.⁸⁵ While RhoA activity and intracellular increase of Ca^{2+} show barrier disrupting properties, the activity of the small Rho GTPase Rac1 and an increase of intracellular cAMP levels result in a barrier protection.⁸⁰

Several inflammatory mediators like thrombin, histamine, or VEGF induce endothelial barrier dysfunction, which causes an uncontrolled efflux of fluid and macromolecules to the tissue causing edema formation.⁸⁰

Besides its involvement in blood clotting, the procoagulant serine protease thrombin induces endothelial hyperpermeability and is a frequently used stimulus for the investigation of vascular endothelial permeability.⁸⁶ Thrombin mediates its barrier

disrupting effects by cleavage of the protease-activated receptor (PAR1) receptor which results in an increase of intracellular Ca^{2+} levels. The rising of Ca^{2+} causes the activation of MLCK and PKC. In turn, PKC induces phosphorylation of VE-cadherin as well as the activation of RhoA (Figure 5). Therefore, thrombin evokes a loss of barrier integrity by internalization of VE-cadherin and induction of cell contraction.⁸⁰

The damage of endothelial barrier function is a hallmark of inflammatory diseases like sepsis or respiratory distress syndrome. It leads to organ dysfunction by edema formation or promotes disease progression by exposure of the underlying tissue to pro-inflammatory and coagulation mediators.⁸⁷⁻⁸⁹

Thus, to effectively treat inflammatory diseases it would be of great advantage if an anti-inflammatory drug shows barrier protective properties as well.

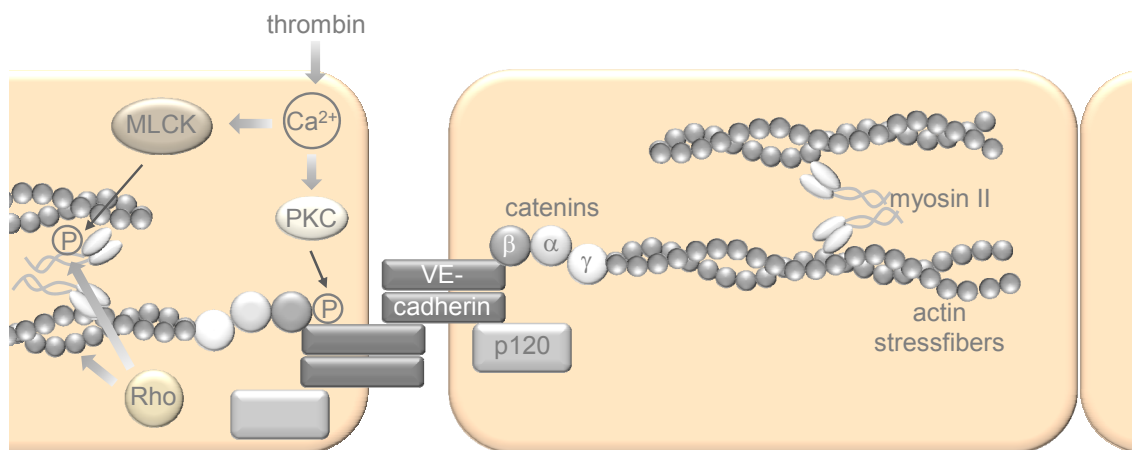


Figure 5 Structural organization of endothelial barrier function and barrier disruptive processes induced by thrombin.

1.3.2 Endothelium and inflammation

Inflammation is important for the host defense or for repairing tissue damage but it shows detrimental properties in chronic diseases like atherosclerosis, rheumatoid arthritis or asthma. The endothelium is a crucial player in inflammatory diseases because it is involved in the recruitment and transmigration of leukocytes to the site of inflammation in the tissue. After clearance of an infection, normally the leucocytes disappear and the endothelium readopts its quiescent state.⁹⁰

1.3.2.1 Leukocyte recruitment

The immune response to pathogens depends on the production of chemokines and cytokines that are released upon recognition of pathogens. The inflammatory response results in the recruitment of activated phagocytes. It is mediated by adhesion molecules that are induced on the cell surface of cytokine-activated endothelium.⁹¹ The first leukocytes that are recruited to the endothelium are the neutrophils followed by the monocytes that differentiate to macrophages in the tissue.⁹¹ The leukocyte recruitment and transmigration can be divided into 4 steps in the innate as well as in the adaptive immune response: 1. Selectin-mediated rolling adhesion, 2. Activation by chemokines 3. Integrin-mediated firm adhesion/arrest and 4. Transmigration (Figure 6).⁹² At inflammatory sites, blood flow is slowed down due to vasodilation, which enables the leukocytes to leave the bloodstream and get in contact with the endothelium. The initial rolling of the leukocytes on the endothelium is due to transient weak interactions and involves L-selectin, which is expressed on leukocytes, and P- and E-selectin expressed on endothelial cells.⁹³⁻⁹⁵ The process of leukocyte rolling and the following firm adhesion involves the leukocyte $\beta 1$ and $\beta 2$ integrins very late antigen-4 (VLA-4), lymphocyte function-associated antigen-1 (LFA-1/CD11a-CD18) and CD11b-CD18 (MAC1) which interact with the immunoglobulin family adhesion molecules vascular cell adhesion molecule-1 (VCAM-1) and intercellular adhesion molecule-1 (ICAM-1) expressed on endothelial cells. The leukocytes locally secrete cytokines like $TNF\alpha$, which causes the upregulation of adhesion molecule expression on endothelial cells (ICAM-1 and VCAM-1) and elicits the endothelial production of additional, specific cytokines (like IL-8). These cytokines rapidly trigger a structural change of the $\beta 1$ and $\beta 2$ integrins resulting in a firm interaction of VLA-4 with VCAM-1 and of LFA1, or MAC-1 with ICAM-1.⁹⁶⁻¹⁰⁰ The final step of leukocyte transmigration is the diapedesis of the leukocytes through the vessel wall into the inflamed tissue. ICAM-1 and CD11-CD18 participate in the crawling of leukocytes into the blood vessel. Inflammatory cytokines and the interaction with the leukocytes cause a transient opening of the intercellular contacts (adhesion junctions and tight junctions) and facilitate the paracellular transmigration.^{92, 101} The immunoglobulin family proteins ICAM-1, the platelet/endothelial cell adhesion molecule-1 (PECAM-1) and the tight junction proteins junctional adhesion molecules (JAMs) are responsible for the leukocyte transendothelial migration. Thereby, LFA-1 constitutes the binding partner of ICAM-1, PECAM-1 interacts homo-typically, and JAMs can associate with integrins.¹⁰² Lastly, leukocytes have to pervade the perivascular basement membrane. This occurs in

regions of low matrix protein deposition and seems to involve proteases like neutrophil elastase.¹⁰³

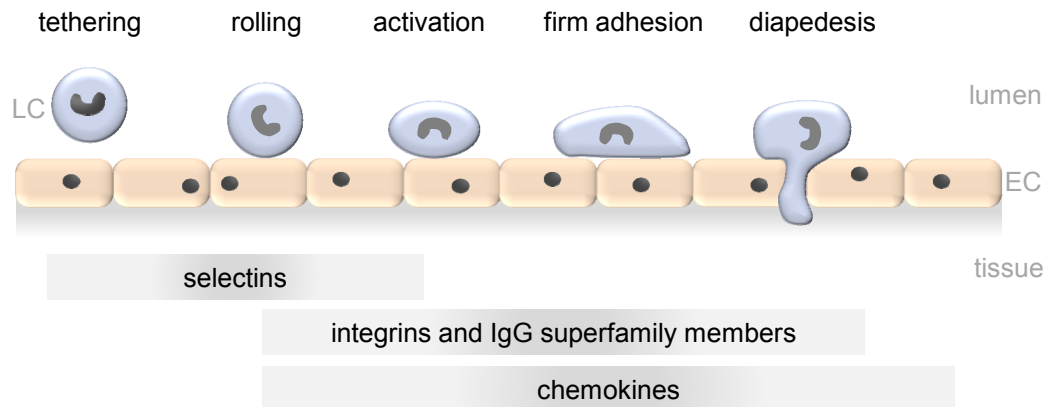


Figure 6 Leukocyte recruitment and transmigration. (LC: leukocyte; EC: endothelial cell)

Thus, endothelial cells actively participate in all steps of leukocyte recruitment in the innate and adaptive immune response. Thereby, a tight regulation of this process and the integrity of cell junctions is necessary to avoid diseases like atherosclerosis, rheumatoid arthritis, or chronic inflammation.⁹²

1.3.2.2 Signaling involved in inflammatory activation of endothelial cells

As mentioned in 1.2.3.4 “IAPs in TNFR signaling”, the cytokine $\text{TNF}\alpha$ is involved in diverse signaling processes and it is a key regulator in apoptosis and inflammatory response. $\text{TNF}\alpha$ stimulates the inflammatory activation of endothelial cells in terms of facilitating leukocyte recruitment, vascular leakage and it promotes thrombosis. It is produced by a wide variety of cells.¹⁰⁴ TNFR1 initiates the majority of $\text{TNF}\alpha$ biological activities.^{52, 105} The activation of TNFR1 induces the association of the intracellular death domain of TNFR1 with the death domain of TRADD, which is followed by the recruitment of TRAF2, RIP1, cIAP1 and cIAP2 including several ubiquitination processes exerted by the cIAPs and TRAF2. As described above, this causes an ubiquitin-dependent recruitment of the TAB/TAK and IKK complex and results in an activation of $\text{NF}\kappa\text{B}$ and of MAPK signaling initiating the pro-inflammatory activation of the endothelium.¹⁰⁶

NF κ B signaling

The transcription factor NF κ B is a central player in initiation and maintenance of inflammation because it regulates the further expression of genes encoding for cytokines and endothelial adhesion molecules like E-selectin, VCAM and ICAM-1.¹⁰⁷ It binds to DNA sequences called κ B elements in promoters and enhancers of transcription.¹⁰⁸ There are 5 mammalian members of the NF κ B family, RelA (p65), RelB, cRel, p50/p105 (NF κ B1) and p52/p100 (NF κ B2) which form homodimeric and heterodimeric complexes. In the canonical pathway induced by TNF α (Figure 7), the inhibitor of NF κ B α (I κ B α) retains the NF κ B p50/p65 dimer in the cytoplasm. The activated I κ B Kinase (IKK) complex phosphorylates I κ B α resulting in its subsequent proteasomal degradation. This is followed by a release of the NF κ B dimer which then can translocate to the nucleus.^{109, 110} The IKK complex consisting of the catalytic subunits IKK α and IKK β and the regulatory subunit IKK γ /NEMO is activated upon recruitment to the TNFR-associated signaling complex where NEMO is ubiquitinated (K63).¹⁰⁶ Moreover, the MAP3K TAK1 can activate IKK β when on the one hand the activity of the TAB/TAK complex is induced by hooking on the ubiquitin platform of TNFR-associated signaling complex¹¹¹ or on the other hand, by the direct interaction of XIAP with TAB1⁷.

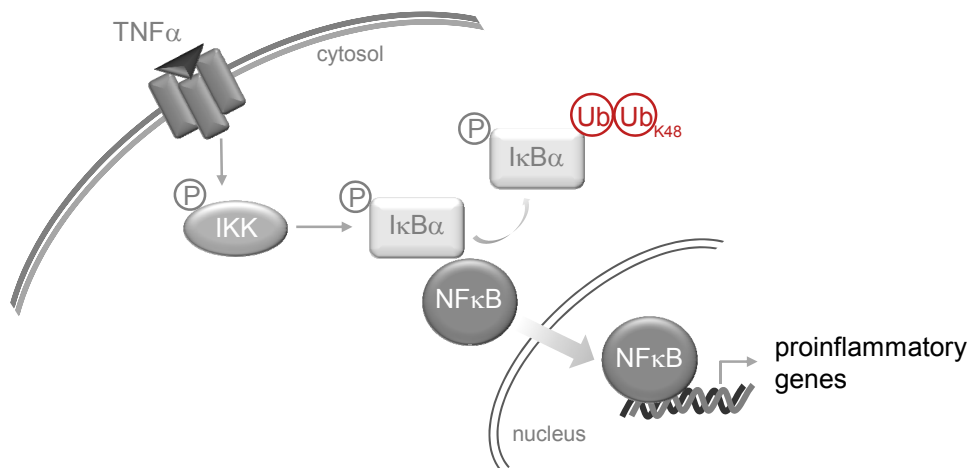


Figure 7 NF κ B signaling.

MAPK signaling

Like NF κ B signaling, the MAPK signaling integrates various stimuli and regulates a variety of cellular processes ranging from survival and apoptosis, differentiation and proliferation to cellular stress and inflammation.^{112, 113} Besides NF κ B, the TNF α -induced activation of MAPKs plays an important role in endothelial activation and in inflammatory processes.¹¹⁴ The mammalian MAPKs comprise 3 major groups consisting of extracellular signal regulated kinase 1/2 (ERK1/2), p38 and c-Jun N-terminal kinase (JNK). The activity of the MAPKs (ser/thr kinases) is regulated by an upstream MAPK phosphorylation cascade. The MAPKs all share a T-X-Y motif where they are dually phosphorylated by MAPK kinases (MAPKKs or MEKs). In turn, MAPKKs are activated by MAPKK kinases (MAPKKKs or MEKKs), whose activation is usually induced by a ligand binding to a receptor, like the TNFR1.^{112 115} (Figure 8) The MAPKKs for p38 are MKK3/6, while JNK is phosphorylated by MKK4/7. The MAPKKs of JNK and p38 are activated by the MAPKKK TAK1, ASK1 and MEKK1-4. These MAPKKK respond to TNFR signaling as shown above for TAK1, which is not only implicated in NF κ B but also p38 and JNK activation.¹¹⁶ ERK, p38 and JNK are all known to be induced by the cytokines TNF α and IL-1.¹¹⁷ Despite ERK is mainly implicated in the response to growth factors, *in vivo* and *in vitro* data also indicate an involvement of ERK in inflammation.¹¹⁵ The activated MAPKs bind and phosphorylate their targets in cytoplasm or translocate to the nucleus and induce gene transcription.¹¹⁸ p38 and JNK activate the transcription factors c-Jun (TSFs), Elk-1, ATF2 and STAT3,^{115, 119} while ERK1/2 phosphorylates the transcription factor Elk-1.¹¹⁷ Elk-1 and STAT3 are required for the activation of the c-fos promoter and ATF2 and c-Jun induce the transcription from the c-Jun promoter. This results in expression of members of the Fos and Jun family of transcription factors. Heterodimers of the Fos and Jun family constitute the transcription factor AP-1. Since the ICAM-1 promoter contains several AP-1 binding sites, the MAPKs ERK, p38 and JNK are involved in the regulation of ICAM-1 expression.^{13, 119}

Because of their activities in TNFR signaling and in TAK activation cIAP1, cIAP2 and XIAP are involved in the induction of MAPK and NF κ B signaling.^{7, 56, 58}

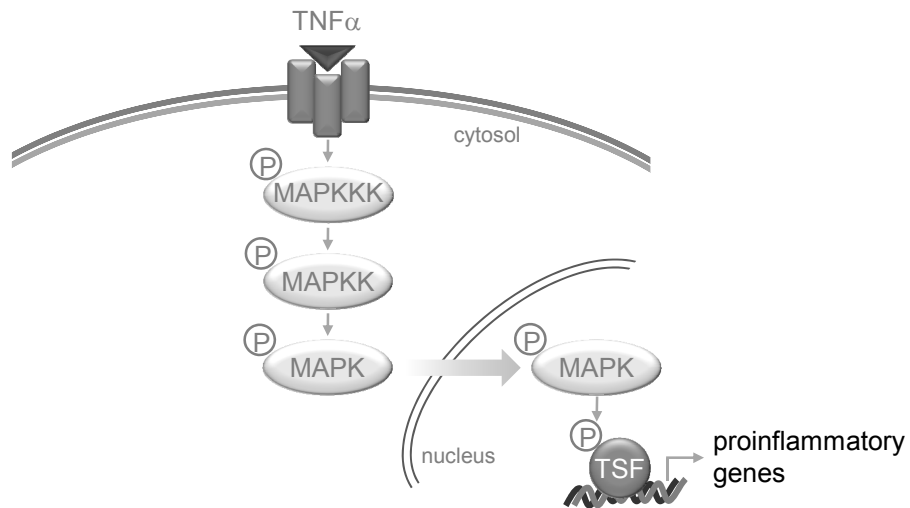


Figure 8 MAPK signaling cascade. (TSF: transcription factor)

To sum up, the inhibitor of apoptosis proteins can interact with a variety of proteins and therefore participate in several signaling pathways. These pathways are often closely interconnected like inflammation and apoptosis. Despite the clear involvement of XIAP, cIAP1 and cIAP2 in NF κ B and TNFR signaling, which are the basis for apoptotic and inflammatory processes, until now the role of the IAPs has been only recognized with a view to apoptosis.

2 MATERIALS AND METHODS

2.1 Materials

2.1.1 Biochemicals and inhibitors, dyes and cell culture reagents

Table 1 Biochemicals, inhibitors, dyes, and cell culture reagents

Reagent	Producer
Accustain [®] formaldehyde	Sigma-Aldrich, Taufkirchen, Germany
Amphotericin B	PAA Laboratories, Pasching, Austria
BC Assay reagent	Interdim, Montulocon, France
Bradford Reagent [™]	Bio-Rad, Munich, Germany
Collagen A/G	Biochrom AG, Berlin, Germany
Collagenase A	Biochrom AG, Berlin, Germany
Complete [®]	Roche diagnostics, Penzberg, Germany
Dianisidinehydrochlorid	Sigma-Aldrich, Taufkirchen, Germany
Dihydrorhodamine-123 (DHR)	Invitrogen, Karlsruhe, Germany
DMSO	Sigma-Aldrich, Taufkirchen, Germany
Endothelial Cell Growth Medium (ECGM)	Provitro, Berlin, Germany
FCS gold	PAA Laboratories, Pasching, Austria
fMLP	Sigma-Aldrich, Taufkirchen, Germany
Formaldehyde, 16% ultrapure	Polysciences Europe GmbH, Eppelheim, Germany
M199 Medium	PAA Laboratories, Pasching, Austria
NaF	Merck, Darmstadt, Germany
Na ₃ VO ₄	ICN Biomedicals, Aurora, Ohio, USA
Page Ruler [™] Prestained Protein Ladder	Fermentas, St. Leon-Rot, Germany
Penicillin	PAA Laboratories, Pasching, Austria
Propidium iodide	Sigma-Aldrich, Taufkirchen, Germany
PermaFluor mounting medium	Beckman Coulter, Krefeld, Germany
PMSF	Sigma Aldrich, Munich, Germany
Q-VD-OPh	R&D Systems, Wiesbaden, Germany
SB203580	Enzo Life Sciences, Lörrach, Germany
SP600125	Enzo Life Sciences, Lörrach, Germany
Streptomycin	PAA Laboratories, Pasching, Austria
Thrombin	Sigma Aldrich, Taufkirchen, Germany

Reagent	Producer
Tumor necrosis factor α (TNF α)	PeptoTech GmbH, Hamburg, Germany
Triton X-100	Merck, Darmstadt, Germany

Table 2 IAP antagonists

Compunds	Producer
A-410099.1 (ABT)	Abbott Bioresearch Corp. Worcester, MA, USA
Smac066 (monomeric IAP antagonist) ¹²⁰	P. Seneci, Milano, Italy
Smac085 (dimeric IAP antagonist)	P. Seneci, Milano, Italy

Table 3 Commonly used buffers

HEPES buffer (pH 7.4)		PBS ⁺ Ca ²⁺ /Mg ²⁺ (pH 7.4)	
NaCl	125 mM	NaCl	137 mM
KCl	3 mM	KCl	2.68mM
NaH ₂ PO ₄	1.25 mM	Na ₂ HPO ₄	8.10 mM
CaCl ₂	2.5 mM	KH ₂ PO ₄	1.47 mM
MgCl ₂	1.5 mM	MgCl ₂	0.25 mM
glucose	10 mM	H ₂ O	
HEPES	10 mM		
H ₂ O		PBS (pH 7.4)	
		NaCl	132.2 mM
		Na ₂ HPO ₄	10.4 mM
		KH ₂ PO ₄	3.2 mM
		H ₂ O	

Table 4 Technical equipment

Name	Device	Producer
AB7300 RT-PCR	Real-time PCR system	Applied Biosystems, Foster City, CA, USA
Axioskop	Upright microscope	Zeiss, Jena, Germany
Culture flasks, plates, dishes	Disposable cell culture material	TPP, Trasadingen, Switzerland
Curix 60	Tabletop film processor	Agfa, Cologne, Germany
Cyclone	Storage Phosphor Screens	Canberra-Packard, Schwadorf, Austria
FACSCalibur	Flow cytometer	Becton Dickinson, Heidelberg, Germany
ibidi slides	Microscope slide	ibidi GmbH, Munich, Germany
LSM 510 Meta	Confocal laser scanning microscope	Zeiss, Jena, Germany
Mikro 22R	Table centrifuge	Hettich, Tuttlingen, Germany
Nanodrop [®] ND-1000	Spectrophotometer	Peqlab, Wilmington, DE, USA
Nucleofector II	Electroporation device	Lonza GmbH, Cologne, Germany
Odyssey 2.1	Infrared Imaging System	LI-COR Biosciences, Lincoln, NE, USA
Orion II Microplate Luminometer	Luminescence	Berthold Detection Systems, Pforzheim, Germany
Polytron PT1200	Ultrax homogenizer	Kinematica AG, Lucerne, Switzerland
SpectraFluor Plus [™]	Microplate multifunction reader	Tecan, Männedorf, Austria
Sunrise [™]	Microplate absorbance reader	Tecan, Männedorf, Austria
Vi-Cell [™] XR	Cell viability analyzer	Beckman Coulter, Fullerton, CA, USA

2.2 Cell culture

2.2.1 Solutions and reagents

The following solutions and reagents were used for the isolation as well as for the cultivation of endothelial cells.

Table 5 Solutions and reagents for cell culture

Growth medium		Stopping medium	
ECGM	500 ml	M 199	500 ml
Supplement	23.5 ml	FCS	50 ml
FCSgold	50 ml		
Antibiotics	3.5 ml		
Trypsin/EDTA (T/E)		Collagen A	
Trypsin	0.05%	Collagen A	10%
EDTA	0.20%	PBS	
PBS			
Collagen G			
Collagen G	0.001%		
PBS			

For heat inactivation, FCSgold was partially thawed for 30 min at room temperature. Subsequently, it was totally thawed at 37°C. Finally, FCS was inactivated at 56°C for 30 min. FCS was stored at -20°C.

2.2.2 Endothelial cells

Endothelial cells (ECs) were cultured under constant humidity at 37°C and with 5% CO₂ in an incubator (Heraeus, Hanau, Germany). Cells were routinely tested for contamination with mycoplasma using the PCR detection kit VenorGeM (Minerva Biolabs, Berlin, Germany).

2.2.2.1 HMEC-1 (Human microvascular endothelial cells)

The cell line CDC/EU.HMEC-1 was kindly provided by the Centers for Disease Control and Prevention (Atlanta, GA, USA). The immortalized HMEC-1 cell line was created by transfection of human dermal microvascular endothelial cells with a plasmid coding for the transforming SV40 large T-antigen. HMEC-1 were shown to retain endothelial morphologic, phenotypic, and functional characteristics.^{77, 78} HMECs were used for macromolecular permeability assays.

2.2.2.2 HUVECs (Human umbilical vein endothelial cells)

Human umbilical cords were kindly provided by Klinikum München Pasing, Frauenklinik Dr. Wilhelm Krüsmann, and Rotkreuzklinikum München. After childbirth, umbilical cords were placed in PBS+Ca²⁺/Mg²⁺ containing penicillin (100 U/ml) and streptomycin (100 µg/ml), and stored at 4°C. Cells were freshly isolated every week. The umbilical vein was washed with PBS+Ca²⁺/Mg²⁺, filled with 0.1 g/l collagenase A, and incubated for 45 min at 37°C. To isolate endothelial cells, the vein was flushed with stopping medium and the eluate was centrifuged (1,000 rpm, 5 min). Afterwards, cells were resuspended in growth medium and plated in a 25 cm² flask. After reaching confluence, cells were trypsinized and plated in a 75 cm² flask. Experiments were performed using cells at passage 3. HUVECs were used for all assays except for the macromolecular permeability assay.

2.2.3 Passaging

After reaching confluency, cells were either sub-cultured 1:3 in 75 cm² culture flasks or seeded either in multiwell-plates or dishes for experiments. For passaging, medium was removed and cells were washed twice with PBS before incubation with trypsin/ethylene diamine tetraacetic acid (EDTA) (T/E) for 1-2 min at 37°C. Thereafter, cells were gradually detached and the digestion was stopped using stopping medium. After centrifugation (1,000 rpm, 5 min, 20°C), the pellet was resuspended in growth medium and cells were plated.

2.2.4 Freezing and thawing

For freezing, confluent HMECs from a 75 cm² flask were trypsinized, centrifuged (1,000 rpm, 5 min, 20°C) and resuspended in 3 ml ice-cold freezing medium. 1.5 ml aliquots were frozen in cryovials. After storage at -80°C for 24 h, aliquots were moved to liquid nitrogen for long term storage.

For thawing, a cryovial was warmed to 37°C and the content was immediately dissolved in prewarmed growth medium. In order to remove DMSO, cells were centrifuged, resuspended in growth medium and transferred to a 75 cm² culture flask.

2.2.5 Isolation of human neutrophil granulocytes

Human neutrophil granulocytes were separated from heparinized peripheral blood of healthy volunteers. The blood samples were centrifuged (1,400 rpm, 15 min, without additional deceleration) to separate the blood cells from the plasma. The “buffy coat” (the layer between the erythrocytes and plasma where the granulocytes are sedimented) was collected and CD15 MicroBeads (Mini-Macs, Miltenyi Biotec GmbH, Bergisch Gladbach, Germany) were added for 30 min at 4°C and for magnetic tagging of the neutrophil granulocytes (the main population of CD15⁺ cells). Using MACS[®] column technology (Miltenyi Biotec, Bergisch Gladbach, Germany), CD15⁺ cells were separated and collected in granulocyte isolation buffer. Cells were counted and kept at room temperature in HEPES buffer or granulocyte medium until use (usually within 30 min). Assays using neutrophils were performed at 37°C.

Table 6 Buffer and medium for granulocyte isolation

Granulocyte isolation buffer		Granulocyte medium	
PBS	500 ml	M 199	500 ml
BSA	2.5 ml	FCS	10 ml
EDTA	2 mM	Antibiotics	3.5 ml

2.3 Preparation of protein samples

2.3.1 Total cell lysates

Endothelial cells were treated as indicated, washed once with icecold PBS and subsequently lysed in RIPA lysis buffer or in modified RIPA lysis buffer (phospho-proteins). Immediately, cells were frozen at -80°C . Afterwards, cells were scraped off and transferred to Eppendorf tubes (Peske, Aindling-Arnhofen, Germany) before centrifugation (14,000 rpm, 10 min, 4°C). Protein concentration was determined in the supernatant using the BCA and the Bradford assay, respectively. Afterwards, Laemmli sample buffer (3x) or 5x SDS sample buffer was added and samples were heated at 95°C for 5 min. Samples were kept at -20°C until Western blot analysis.

Table 7 Buffers for the preparation of total cell lysates

RIPA buffer		Lysis buffer for phospho-proteins	
Tris/HCl	50 mM	Tris/HCl	50 mM
NaCl	150 mM	NaCl	150 mM
Nonidet NP 40	1%	Nonidet NP 40	1%
Deoxycholic acid	0.25%	Deoxycholic acid	0.25%
SDS	0.10%	SDS	0.10%
H ₂ O		Na ₃ VO ₄	0.3 mM
Complete [®]	4.0 mM	NaF	1.0 mM
PMSF	1.0 mM	β-Glycerophosphate	3.0 mM
Na ₃ VO ₄	1.0 mM	Pyrophosphate	10 mM
NaF	1.0 mM	H ₂ O	
		Complete [®]	4.0 mM
		PMSF	1.0 mM
		H ₂ O ₂	600 μM

Table 8 Sample buffer

5x SDS-sample buffer		3x Laemmli buffer	
Tris/HCl	3.125 M, pH 6.8	Tris/HCl	187.5 mM
Glycerol	10 ml	SDS	6%
SDS	5%	Glycerol	30%
DTT	2%	Bromphenolblue	0.025%
Pryonin Y	0.025%	H ₂ O	
H ₂ O		β-Mercaptoethanol	12.5%

2.3.2 Immunoprecipitation

For immunoprecipitations Protein A Agarose beads (Sigma-Aldrich, Munich, Germany) were incubated with TAB1 antibody (Cell Signaling Technology/NEB, Frankfurt am Main, Germany) (2 µg per 50 µl unpacked beads) at 4°C overnight. Cells were scraped in non-denaturing lysis buffer and kept on ice for 30 min. Thereafter, the samples were centrifuged and protein concentrations were determined in the supernatants. Cell lysates were incubated with the Protein A Agarose beads (Sigma-Aldrich, München Germany) for 2 h at 4°C. After three washing steps with non-denaturing lysis buffer, proteins were extracted from the beads with Laemmli sample buffer and subjected to Western blot analysis.

Table 9 Non-denaturing lysis buffer for immunoprecipitations

Non-denaturing lysis buffer	
Tris/HCl	300 mM
NaCl	5 mM
EDTA	1 mM
Triton-X100	1%
Complete [®]	4.0 mM
PMSF	1.0 mM
Na ₃ VO ₄	1.0 mM
NaF	1.0 mM
H ₂ O	

2.3.3 Membrane fractionation

HUVEC lysates were separated into a soluble (cytosolic) and a particulate (membranous) fraction, as described previously by Li H *et al.*¹²¹ HUVECs were treated as indicated, washed twice with ice-cold PBS, and homogenized in lysis buffer. Lysates were centrifuged at 100,000 g for 1 h. The supernatant (cytosolic fraction) was collected. The pellet was washed in lysis buffer containing 1.0 M NaCl and centrifuged at 100,000 g for 30 min. The supernatant was discarded and the pellet was solubilized with lysis buffer containing 20 mM CHAPS at 4°C for 30 min. After centrifugation at 100,000 g for 1 h, the supernatant was kept as membranous fraction. The membranous fraction was used for Western blotting.

Table 10 Buffer for membrane fractionation

Membrane lysis buffer

Tris/HCl, pH 7.5	0.05 M
EDTA	0.5 M
EGTA	0.5 M
Glutathione	0.7 M
Glycerol	10%
H ₂ O	
PMSF	1.0 mM
Complete [®]	4 mM

2.3.4 Extraction of nuclear proteins

For nuclear preparation, HUVECs were treated as indicated and washed twice with ice-cold PBS. The PBS was removed completely and cells were lysed by adding 400 µl nuclear extraction buffer A. Cells were scraped off the plate/dish and transferred to 1.5 ml reaction tubes. Cells were allowed to swell on ice for 15 min. Nonidet P-40 (0.625%) was added, followed by 10 s of vigorous vortexing. Probes were centrifuged (14,000 rpm, 1 min, 4°C), supernatants removed, and pellets incubated for 30 min under agitation at 4°C in 40 µl nuclear extraction buffer B. After centrifugation (14,000 rpm, 5 min, 4°C), supernatants were collected and frozen at -80°C. Protein concentrations were determined by Bradford assay.

Table 11 Extraction buffers for nuclear proteins

Extraction Buffer A		Extraction Buffer B	
HEPES, pH 7.9	10 mM	HEPES, pH 7.9	20 mM
KCl	10 mM	NaCl	0.4 mM
EDTA	0.1 mM	EDTA	0.1 mM
EGTA	0.1 mM	EGTA	0.1 mM
DTT	1.0 mM	DTT	1.0 mM
PMSF	0.5 mM	PMSF	0.5 mM
		Glycerol	25%

2.4 Western blot analysis

2.4.1 Protein quantification

In order to employ equal amounts of proteins in all samples for Western blot analysis, protein concentrations were determined using either the Bicinchoninic Protein Assay or Bradford Assay. After measurement, protein concentration was adjusted by adding Laemmli sample buffer (1x) or 1x SDS sample buffer.

2.4.1.1 Bicinchoninic (BCA) Protein Assay

Bicinchoninic (BCA) Protein Assay (BC Assay reagents, Interdim, Montulocon, France) was performed as described previously.¹²² 10 μ l protein samples were incubated with 200 μ l BC Assay reagent for 30 min at 37°C. Absorbance of the blue complex was measured photometrically at 550 nm (Tecan Sunrise Absorbance reader, TECAN, Crailsheim, Germany). Protein standards were obtained by diluting a stock solution of bovine serum albumin (BSA, 2 mg/ml). Linear regression was used to determine the actual protein concentration of each sample.

2.4.1.2 Bradford Assay

Bradford Assay (Bradford solution, Bio-Rad, Munich, Germany) was performed as described previously.¹²³ It employs Coomassie Brilliant Blue as a dye, which binds to proteins. 10 μ l protein samples were incubated with 190 μ l Bradford solution (1:5 dilution in water) for 5 min. Thereafter, absorbance was measured photometrically at

592 nm (Tecan Sunrise Absorbance reader, TECAN, Crailsheim, Germany). Protein standards were achieved as described above (BCA Assay).

2.4.2 SDS-PAGE

Proteins were separated by discontinuous SDS-polyacrylamid gel electrophoresis (SDS-PAGE) according to Laemmli.¹²⁴ Equal amounts of protein were loaded on discontinuous polyacrylamide gels, consisting of a separation and stacking gel, and separated using the Mini-PROTEAN 3 electrophoresis module (Bio-Rad, Munich, Germany). The concentration of Rotiphorese™ Gel 30 (acrylamide) in the separating gel was adjusted for an optimal separation of the proteins depending on their molecular weights. Electrophoresis was carried out at 100 V for 21 min for protein stacking and 200 V for 45 min for protein separation. The molecular weight of proteins was determined by comparison with the prestained protein ladder PageRuler™.

Table 12 Acrylamide concentration in the separation gel

Protein		Acrylamide concentration	
phospho-MLC2, di-phospho-MLC2		15%	
phospho-p38, phospho-JNK, phospho-ERK, phospho-VE-cadherin, ICAM-1, β -actin, TRAF2, TRAF5, cIAP1, cIAP2, XIAP, I κ B α , phospho-I κ B α		10%	
Separation gel 10%/15%		Stacking gel	
Rotiphorese™ Gel 30	33.3/5%	Rotiphorese™ Gel 30	40%
Tris (pH 8.8)	375 mM	Tris (pH 6.8)	125 mM
SDS	0.1%	SDS	0.1%
TEMED	0.1%	TEMED	0.2%
APS	0.05%	APS	0.1%
H ₂ O		H ₂ O	

Table 13 Electrophoresis buffer**Electrophoresis buffer**

Tris	4.9 mM
Glycine	38 mM
SDS	0.1%
H ₂ O	

2.4.3 Tank electroblotting

After protein separation, proteins were transferred onto a nitrocellulose membrane (Hybond-ECL™, Amersham Bioscience, Freiburg, Germany) by electro tank blotting.¹²⁵ A blotting sandwich was prepared in a box filled with 1x tank buffer to avoid bubbles as follows: cathode–pad–blotting paper–separating gel (from SDS-PAGE)–nitrocellulose membrane–blotting paper–pad–anode. The membrane was equilibrated with 1x tank buffer 15 minutes prior to running the tank blot. Sandwiches were mounted in the Mini Trans-Blot® system (Bio-Rad, Munich, Germany), ice-cold 1x tank buffer filled the chamber and a cooling pack was inserted to avoid excessive heat. Transfers were carried out at 4°C, 100 V for 90 min.

Table 14 Tank blotting buffer

5x Tank buffer		1x Tank buffer	
Tris base	240 mM	5x Tank buffer	20%
Glycine	195 mM	Methanol	20%
H ₂ O		H ₂ O	

2.4.4 Protein detection

Prior to the immunological detection of the relevant proteins, unspecific protein binding sites were blocked. Therefore, the membrane was incubated in non-fat dry milk powder (Blotto) 5% or BSA 5% for 2 h at room temperature. Afterwards, detection of the proteins was performed by incubating the membrane with the respective primary antibody at 4°C overnight (Table 15). After three washing steps with PBS containing 0.1% Tween (PBS-T), the membrane was incubated with the secondary antibody,

followed by 3 additional washing steps. All steps regarding the incubation of the membrane were performed under gentle agitation. In order to visualize the proteins, two different methods have been used depending on the labels of the secondary antibodies.

2.4.4.1 Enhanced chemiluminescence

Membranes were incubated for 2 h with HRP-conjugated secondary antibodies (Table 15). For detection, luminol was used as a substrate. The membrane was incubated with ECL (enhanced chemiluminescence) solution for 1 minute (ECL Plus Western Blotting Detection Reagent RPN 2132, GE Healthcare, Munich, Germany). The appearing luminescence was detected by exposure of the membrane to an X-ray film (Super RX, Fuji, Düsseldorf, Germany) and subsequently developed with a Curix 60 Developing system (Agfa-Gevaert AG, Cologne, Germany).

2.4.4.2 Infrared imaging

Secondary antibodies coupled to IRDye™ 800 and Alexa Fluor® 680 with emission at 800 and 700 nm, respectively, were used. Membranes were incubated for 1 h. Protein bands of interest were detected using the Odyssey imaging system (Li-COR Biosciences, Lincoln, NE). Secondary antibodies used for this type of protein detection are listed in (Table 16).

Table 15 Primary antibodies

Antigen	Source	Dilution	In	Provider
β-actin	Mouse monocl.	1:1,000	Blotto 1%	Chemicon
IκBα	Rabbit polycl.	1:1,000	Blotto 1%	Cell Signaling
phos.-IκBα ^{S32}	Rabbit polycl.	1:1,000	Blotto 1%	Santa Cruz
phos.-MLC2 ^{S19}	Rabbit polycl.	1:1,000	BSA 5%	Cell Signaling
phos.-MLC2 ^{T18/S19}	Rabbit polycl.	1:1,000	BSA 5%	Cell Signaling
MLC2	Rabbit polycl.	1:500	Blotto 5%	Santa Cruz
phos.-TAK1 ^{T184/Y187}	Rabbit monocl.	1:1,000	BSA 5%	Cell Signaling
phos.-p38 ^{T180/Y182}	Rabbit polycl.	1:1,000	BSA 5%	Cell Signaling
phos.-JNK ^{T183/Y185}	Mouse monocl.	1:500	BSA 5%	Cell Signaling
TRAF2	Rabbit polycl.	1:1,000	Blotto 5%	Cell Signaling

Antigen	Source	Dilution	In	Provider
TRAF5	Mouse monocl.	1:200	Blotto 5%	Cell Signaling
cIAP1	Goat polycl.	1:1,000	Blotto 5%	Epitomics
cIAP2	Rabbit monocl.	1:500	BSA 5%	R&DSYSTEMS
XIAP	Mouse monocl.	1:1,000	Blotto 5%	BD Bioscience
phos.-VE-cad. ^{Y731}	Rabbit polycl.	1:1,000	BSA 3%	Biosource
MKP-1	Rabbit polycl.	1:1,000	Blotto 5%	Santa Cruz
phos.-ERK ^{T202/Y204}	Rabbit polycl.	1:1,000	BSA 5%	Cell Signaling

Table 16 Secondary antibodies

Antibody	Dilution	in	Provider
Goat anti-mouse IgG1: HRP	1:1,000	Blotto 1%	Biozol
Goat anti mouse IgG: HRP	1:1,000	Blotto 1%	Southern Biotechnology
Goat anti-rabbit: HRP	1:1,000	Blotto 1%	Dianova
Alexa Fluor [®] 680 Goat anti-mouse IgG	1:10,000	Blotto 1%	Molecular Probes
Alexa Fluor [®] 680 Goat anti-rabbit IgG	1:10,000	Blotto 1%	Molecular Probes
IRDye [™] 800CW Goat anti-mouse IgG	1:20,000	Blotto 1%	LI-COR Biosciences
IRDye [™] 800CW Goat anti-rabbit IgG	1:20,000	Blotto 1%	LI-COR Biosciences

2.5 Electrophoretic mobility shift assay (EMSA)

2.5.1 Binding reaction and electrophoretic separation

The oligonucleotide for NF κ B with the consensus sequence 5'-AGT TGA GGG GAC TTT CCC AGG C-3' was purchased from Promega. Using the T4 polynucleotide kinase the oligonucleotides were 5' end-labeled with [γ -³²P]-ATP. Equal amounts of nuclear protein (1-2 μ g) were incubated with 2 μ g poly(dIdC) and 3 μ l of freshly prepared reaction buffer for 10 min at room temperature. The binding reaction was started by adding 1 μ l of the radioactive-labeled oligonucleotide and carried out for 30 min at

room temperature. The protein-oligonucleotide complexes were separated by gel electrophoresis (Power Tec™ HC, BioRad) with 0.25 x TBE buffer at 100 V for 60 minutes using non-denaturing polyacrylamide gels (5% PAA, 20% glycerol). After electrophoresis, gels were exposed to Cyclone Storage Phosphor Screens (Canberra-Packard, Schwadorf, Austria) for 24 hours, followed by analysis with a phosphor imager station (Cyclone Storage Phosphor System, Canberra-Packard).

Table 17 Buffers and gels for EMSA

5x Binding Buffer		Loading Buffer	
Tris/ HCl	50 mM	Tris/HCl	250 mM
NaCl	250 mM	Glycerol	40%
MgCl ₂	5.0 mM	Bromphenolblue	0.2%
EDTA	2.5 mM		
Glycerol	20%		
Reaction buffer		10x TBE, pH 8.3	
5x binding buffer	90%	Tris	890 mM
Loading buffer	10%	Boric acid	890 mM
DTT	2.6 mM	EDTA	20 mM
		H ₂ O	
Non-denaturing PAA gels 4.5%			
10 x TBE	5.3%		
Rotiphorese™ Gel 30	15.8%		
Glycerol	2.6%		
TEMED	0.05%		
APS	0.08%		
H ₂ O			

2.6 Flow cytometry

Flow cytometry has been used for the analysis of intercellular adhesion molecule-1 (ICAM-1) expression and for the quantification of apoptosis rate. All measurements

were performed on a FACSCanto II (Becton Dickinson, Heidelberg, Germany). Cells were illuminated by a blue argon laser (488 nm).

2.6.1 Analysis of ICAM-1 expression on cell surface

Cells were seeded in 24-well plates and grown to confluence and treated as indicated in the respective figure legends. Cells were washed with PBS twice, harvested by trypsination, and fixed in PBS/4% formalin for 10 min. Afterwards, cells were washed with PBS and 0.5 µg FITC-labeled CD54/ICAM-1 antibody (Biozol, Eching, Germany) was added for 45 min at RT. Cells were washed with PBS and 10,000 cells were measured by flow cytometry to detect the membrane expression of ICAM-1 as evidenced by a median shift in fluorescence intensity.

2.6.2 Determination of cell surface expression of CD11b

Granulocytes (10^6 cells/ml, 100 µl) were incubated with ABT 30 minutes before activating in HEPES buffer (pH 7.4) them for 15 min with fMLP (10^{-7} M). Then, cells were fixed with 4% formaldehyde and washed with PBS followed by incubation with saturating concentrations of FITC-labeled antibody against CD11b for 45 minutes at room temperature. Cells were washed once with PBS, resuspended in PBS and analyzed by flow cytometry. At least 5,000 events were acquired.

Table 18 Antibodies used for flow cytometry

Specificity	Format	Isotype	Dilution	Provider
CD11b	FITC	monocl. antibody	1:20	AbD Serotec
ICAM-1	FITC	monocl. antibody	1:25	BIOZOL

2.6.3 Determination of ROS production in granulocytes

ROS production in granulocytes was assessed by measuring the intracellular oxidation of dihydrorhodamine (DHR) to rhodamine. Therefore, the granulocytes (10^6 cells/ml, 100 µl) in suspension were primed with DHR (1 µM) for 10 min at 37°C. Afterwards cells were incubated with ABT for 30 min and activated with fMLP (10^{-7} M) for 15 min.

The reaction was stopped on ice and the DHR oxidation was analyzed by flow cytometry. At least 5,000 events were acquired.

2.6.4 Quantification of apoptosis rate

Cell cycle analysis and quantification of apoptosis rate was performed according to Nicoletti *et al.*¹²⁶ based on the fact that endonucleases, which are activated in apoptotic processes, cause DNA fragmentation. Therefore, an increasing subdiploid DNA content of cells indicates the induction of apoptosis. Cells were seeded in 24-well plates, grown to confluence and treated as indicated. After 24 h, or 48 h cells were trypsinized, washed three-times with PBS, and centrifugated at 600 g and 4°C for 10 min. For permeabilization and staining, cells were incubated in fluorochrome solution (FS) buffer containing propidium iodide (PI) to detect the DNA content of the cells. After incubation at 4°C overnight cells were analyzed by flow cytometry.

Table 19 FS buffer for Nicoletti assay

FS buffer	
Na ₃ -citrate	0.1%
Triton-X 100	0.1%
PBS	

2.7 Transfection of cells

For transient transfection with the indicated siRNA and plasmids, respectively, HUVECs were electroporated using the Nucleofector[®] II device in combination with the HUVEC Nucleofector[®] Kit (both from LONZA Cologne AG, Cologne, Germany).

2.7.1 Transfection with siRNA

In order to silence XIAP, HUVECs were transiently transfected with XIAP siRNA. XIAP On-TARGETplus SMARTPool siRNA consisting of four different siRNA sequences was used (Dharmacon, Lafayette, CO, USA). On-TARGETplus siCONTROL non-targeting

siRNA was used as a control. siRNAs were suspended in Dharmacon 1x siRNA buffer, aliquoted and stored at -80°C. The concentration of siRNA was verified using a NanoDrop (Wilmington, DE, USA). For each transfection, 2×10^6 HUVECs were suspended in 100 μ l HUVEC Nucleofector Solution and added to 3 μ g of the respective siRNA.

Table 20 On-TARGETplus SMARTPool XIAP siRNA

XIAP siRNA	Target sequence (5'-3')	Provider
1	GUAGAUAGAUGGCAAUAUG	Dharmacon
2	GAACUGGGCAGGUUGUAGA	
3	GAAAGAGAUUAGUACUGAA	
4	GGACUCUACUACACAGGUA	

The mixture of cells and siRNA was transferred to a cuvette and transfection was performed (program A-034). Immediately after electroporation, 900 μ l of prewarmed culture medium was added to the cuvette. Afterwards, cells were seeded into 24-well (500,000 cells per well) for FACS and Western blot analysis.

2.7.2 Transfection with plasmids

For the NF κ B reporter assay, HUVECs were transiently transfected with the plasmids pGL4.32[*luc2P/NF- κ B-RE/Hygro*] and pGL4.74[*hRluc/TK*] (both Promega, Mannheim, Germany) in the ratio 1:10. For each transfection, 1×10^6 HUVECs were suspended in 100 μ l HUVEC Nucleofector Solution and added to 0.5 μ g or 5 μ g of the respective plasmid. Electroporation was performed in analogy to the siRNA experiments. After transfection, cells were seeded into 96-well plates. Experiments were performed 16 h after transfection.

2.8 Dual Luciferase[®] Reporter Assay System

The reporter construct pGL4.32[*luc2P/NF- κ B-RE/Hygro*], a firefly luciferase reporter gene containing five copies of an NF κ B response element (NF κ B-RE) (Promega, Mannheim, Germany) and a plasmide coding for *Renilla reniformis* luciferase with

thymidine kinase (TK) promoter (pGL4.74[*hRluc*/TK] (Promega, Mannheim, Germany) used as a transfection control were co-transfected in the ratio of 1:10 by electroporation employing the Amaxa HUVEC Nucleofector kit (Amaxa GmbH, Koeln, Germany). Transfected 80,000 HUVECs per well were seeded in 96-well plates. After 24 h they were pretreated with the appropriate substances for 30 min followed by an incubation with TNF α for 6 h. The luciferase activity was determined using the Dual-Luciferase[®] Reporter Assay System (Promega, Mannheim, Germany). Cells were washed with PBS and, in order to lyse the cells, 20 μ l 1x passive lysis buffer (PLB) (1 x PLB diluted 1:5 from 5 x PLB, Promega, Mannheim, Germany) per well was added. After freezing the plates at -80 °C they were allowed to thaw under agitation for 15 min. The luciferase activity was determined in white 96 well plates using a luminometer (Berthold Orion II, Berthold Detection Systems, Pforzheim, Germany). The firefly luciferase reporter is measured by adding 100 μ l Luciferase Assay Reagent II per well (LAR II) (injector 1) to generate a luminescent signal lasting at least one minute. After quantifying the firefly luminescence, this reaction is quenched, and the *Renilla* luciferase reaction is initiated simultaneously by adding 100 μ l Stop & Glo[®] Reagent (injector 2) to the same sample. The luminometer was programmed to perform a 2-second measurement delay followed by a 10-second measurement read for both luciferase activities. The relative NF κ B transactivation activity was assessed as the x-fold change of firefly luciferase activity after normalization for *Renilla reniformis* luciferase activity.

2.9 Macromolecular permeability assay

HMECs (0.125×10^6 cells/well) were seeded on collagen G-coated 12-well Transwell[®] plate inserts (pore size 0.4 μ m, polyester membrane; Corning, New York, USA) and cultured for 48 h. FITC-dextran (40 kDa; 1 mg/ml; Sigma-Aldrich) was given to the upper compartment at t = 0 min. Cells were treated as indicated. Samples were taken from the lower compartment at t = 0, 5, 10, 15, 30 min. The fluorescence increase (ex 485/em 535) of the samples was detected with a fluorescence plate reader (SpectraFluor Plus, Tecan Deutschland GmbH). The mean fluorescence of untreated cells at t = 30 min was set as 100%. The data are expressed as percent increase of fluorescence versus the control.

2.10 Confocal microscopy

A Zeiss LSM 510 META confocal microscope (Zeiss, Oberkochen, Germany) was used for obtaining images of the translocation of the p65 subunit of NF κ B to the nucleus in fixed cells. HUVECs were cultured on ibidi μ -slides (8-well ibiTreat, ibidi GmbH, Munich, Germany) until reaching confluence. Afterwards, cells were treated as indicated, washed with PBS and fixed with 4% paraformaldehyde in PBS at room temperature (10 min), followed by permeabilization via incubation with 0.2% Triton X-100 (Sigma, Taufkirchen, Germany) in PBS (2 min). Cells were washed and unspecific binding was blocked with 0.2% BSA in PBS for 30 min. Afterwards, cells were incubated with a primary antibody against p65 (Santa-Cruz Biotechnology Inc., 1:200 in 0.2% BSA/PBS, rabbit polyclonal) for 1 h at room temperature. After three washing steps with PBS, cells were incubated with the AlexaFluor[®] Goat anti-rabbit secondary antibody (Invitrogen, 1:400 in 0.2% BSA) for 45 min at room temperature. Finally, the slides were again washed three times with PBS (5 min) and embedded in PermaFluor mounting medium (VWR, Darmstadt, Germany).

2.11 Leukocyte adhesion assay

2.11.1 Adhesion assay

HUVECs were seeded in 24-well plates and grown to confluence. They were treated with appropriate concentrations of ABT for 30 min before incubation with TNF α for 24 h. The medium was discarded and 10^5 freshly isolated granulocytes per well were added in a total volume of 500 μ l of granulocyte medium. The granulocytes (see 2.2.5) were allowed to adhere for 30 min. Then the wells were washed 3 times with PBS⁺ to remove non-adherent cells. After washing 100 μ l of lysis buffer (Table 21) per well was added and the plates were incubated for 30 min at 37°C.

2.11.2 Myeloperoxidase (MPO) activity

The amount of adhered neutrophils was analyzed by spectrometric measurement of the activity of the myeloperoxidase (MPO, an enzyme mainly occurring in neutrophils): 100 μ l of MPO substrate was added to 100 μ l of each lysate. The conversion of the

substrate was determined at 540 nm using SPECTRAFluor Plus plate reader. The number of adhered granulocytes was calculated from the gradient of the conversion curve of dianisidine.

Table 21 Buffer and medium for granulocyte adhesion assay

Phosphate buffer (pH 6.0)		Granulocyte medium	
KH ₂ PO ₄	9.08 g/l	M 199	500 ml
Na ₂ HPO ₄	11.88 g/l	FCS	10 ml
H ₂ O		Antibiotics	3.5 ml
MPO substrate		Lysis buffer	
Dianisidine	0.06%	HTAB (Hexadecyltrimethylammonium bromide)	1%
H ₂ O ₂	0.0009%	Phosphate buffer (pH 6.0)	
Phosphate buffer (pH 6.0)			

2.12 *In vivo* assays

2.12.1 Animals

Male C57BL/6 mice were purchased from Charles River (Sulzfeld, Germany). All experiments were performed with male mice at the age of 10-12 weeks. Animals were housed under conventional conditions with free access to food and water. All experiments were performed according to German legislation for the protection of animals and approved by the local government authorities.

2.12.2 Murine antigen-induced arthritis.

The antigen-induced arthritis experiment was performed as previously described by Veihelmann *et al.*¹²⁷ On day -21 and -14 C57BL/6 mice were subcutaneously immunized against methylated bovine serum albumine (mBSA) (Sigma-Aldrich, Deisenhofen, Germany) containing Freund's complete adjuvant and supplemented

with heat-killed *Mycobacterium tuberculosis* strain H37RA (Difco, Augsburg, Germany) in the left flank (day -21) and in the right flank (day -14). Simultaneously, the mice were injected intraperitoneally with heat killed *Bordetella pertussis* (2×10^9) (Institute of Microbiology, Berlin, Germany). On day 0, the mice were injected with mBSA into the left knee joint to cause arthritis. The right knee joint was treated with saline as an internal control. One part of the mice (six animals) was treated daily with intraperitoneally administered ABT (50 μ g per animal, diluted in PBS) The control group (five animals) was treated with the corresponding concentration of DMSO. The knee joint diameters, i.e. the transverse diameter of the knee joint measured by a caliper in units of 0.1 mm, were recorded from day -2 until the end of the experiment.

2.12.3 Analysis of leukocyte adhesion and transmigration by intravital microscopy of mouse cremaster muscle

This assay was kindly performed by Dr. Markus Rehberg from the group of Prof. Dr. Fritz Krombach, Walter-Brendel-Centre of Experimental Medicine, University of Munich, Germany.

The recruitment of leukocytes in the cremaster muscle of mice was induced by an intrascrotal injection of recombinant murine TNF α (500 ng per mouse) 4 h prior to intravital microscopic observation.

The surgical preparation was performed as originally described by Baez *et al.* with minor modifications.¹²⁸ Mice were anesthetized using a ketamine/xylazine mixture (100 mg/kg ketamine and 10 mg/kg xylazine). The right cremaster muscle was opened ventrally in a relatively avascular zone and spread over the transparent pedestal of a custom-made microscopic stage. Throughout the procedure as well as after surgical preparation during *in vivo* microscopy, the muscle was superfused with warm-buffered saline. In each animal, at least five single unbranched postcapillary venules with diameters of 17.5 to 35 μ m were analyzed. During a 15 min observation period, leukocyte rolling, adhesion and transendothelial migration were assessed by near-infrared reflected light oblique transillumination microscopy. Videotaped images were evaluated off-line using CAPIMAGE software (Zeintl, Heidelberg, Germany). Leukocyte rolling flux fraction is defined as the flux of rolling leukocytes in percent of total leukocyte flux. The total number of adherent leukocytes was determined for each venule segment (100 μ m) and is expressed per $10^4 \mu\text{m}^2$ of venule surface area. Emigrated cells were counted in an area reaching out 75 μ m to each side of a vessel

over a distance of 100 μm vessel length and are presented per $1.0 \times 10^4 \mu\text{m}^2$ tissue area. Centerline blood flow velocity was measured by using intra-arterial-administered microspheres (0.96 μm ; FluoSpheres; Invitrogen). The wall shear rate [s^{-1}] was estimated as $8 \times [V_b / d]$, where V_b refers to the mean blood flow velocity and d to the diameter of the vessel. Mean blood flow velocity, V_b , was approximated by multiplying the centerline blood flow velocity with 0.625^{129} . The number of leukocytes in whole blood was determined at the end of each experiment using Coulter A^CT Counter (Coulter Corp. Miami, FL, USA).

2.12.4 Statistical analysis

The number of independently performed experiments is stated in the respective figure legend. One representative image is shown. Bar graph data are mean values \pm SE. Statistical analysis was performed with the GraphPad Prism software version 3.03 (GraphPad Software, San Diego, CA, USA). Unpaired t test was used to compare two groups. To compare three or more groups, one-way ANOVA followed by Bonferroni post hoc test was used. Values of $P < 0.05$ were considered statistically significant.

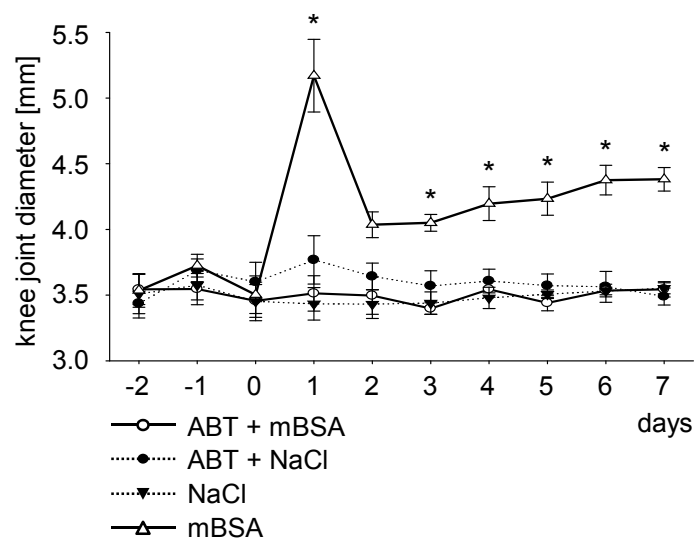
3 RESULTS

3.1 ABT abolishes antigen-induced arthritis in mice and inhibits leukocyte transmigration *in vivo*

Besides the interaction of IAPs with caspases, it is known that IAPs play a role in TNFR and NF κ B signaling^{7, 23} which led us to the hypothesis that IAPs are involved in inflammatory processes and therefore IAP antagonists might have an anti-inflammatory potential. We applied an antigen-induced arthritis mouse model to elucidate whether ABT shows anti-inflammatory effects in a clinically relevant *in vivo* model. Mice were immunized against methylated bovine serum albumin (mBSA). After immunization, arthritis was induced in one of the both knee joints. In contrast to the control group, mice that were medicated subcutaneously with 50 μ g ABT per day before and after induction of arthritis did not evolve any joint swelling in the mBSA-treated knee as depicted in Figure 9A.

Furthermore, to specifically investigate the *in vivo* action of ABT on endothelial activation and leukocyte endothelium interaction, we analyzed the TNF α -induced leukocyte rolling and adherence by intravital microscopy of the mouse cremaster muscle. The group of mice that was pretreated intraarterially with 0.5 μ g ABT showed a slight reduction of leukocyte adhesion and significant decrease in leukocyte transmigration in comparison to the control group (Figure 9B). The blood flow velocity, the leukocyte shear rate, and the total count of leukocytes were not influenced by ABT (data not shown).

A



B

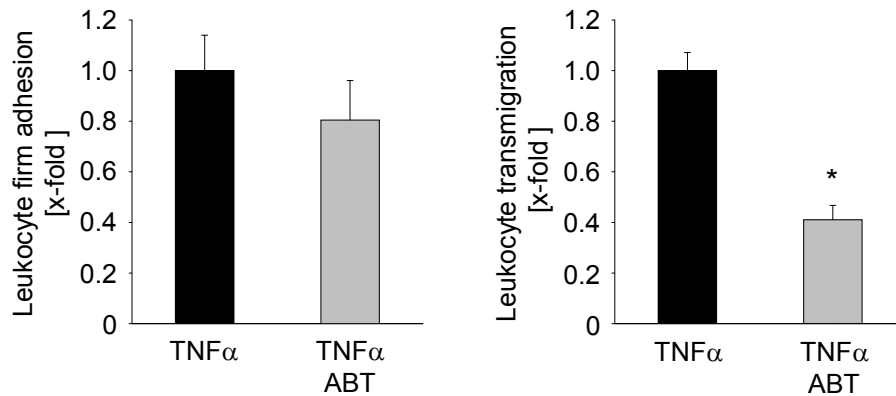


Figure 9 ABT inhibits inflammatory processes *in vivo*. A) For the arthritis model, mice were immunized with methylated BSA (mBSA). One group of the mice was additionally treated with 50 μ g ABT/mouse ip. every day beginning two days before the induction of arthritis with mBSA in the left knee joint. The right knee joints were used as internal control and were injected with NaCl solution. The knee joint diameter was determined daily starting 2 days before the induction of the arthritis until the end of the experiment 7 days later. Data are expressed as mean \pm S.E.M. (control mice: n = 5, ABT-treated mice n = 6). *, $p \leq 0.05$ versus TNF α . B) Leukocyte transmigration is impaired by ABT *in vivo*. Leukocyte extravasation in the cremaster muscle was induced by intra-scrotal injection of recombinant murine TNF α (500 ng) 4 h prior to intravital microscopic observation. The mice of the one group were injected intra-arterially with 0.5 μ g ABT/mouse 30 min before application of TNF α , the control group was treated with PBS. During a 15 min observation period, leukocyte adhesion and trans-endothelial migration were assessed. Data are expressed as mean \pm S.E.M. (control mice: n = 5, ABT-treated mice: n = 5). *, $p < 0.01$ versus TNF α . This assay was performed by Dr. Markus Rehberg from the group of Prof. Dr. Fritz Krombach, Walter-Brendel-Centre of Experimental Medicine, University of Munich, Germany

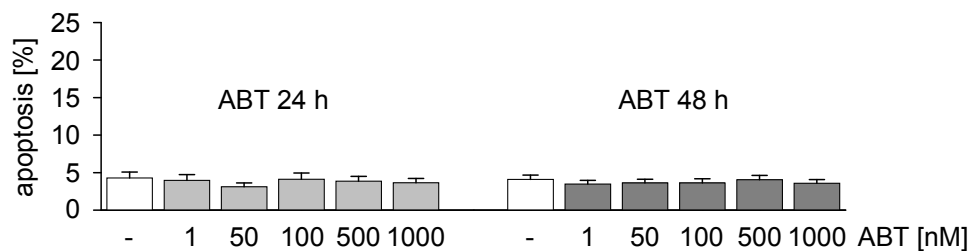
In summary, ABT potently inhibits antigen-induced arthritis and reduces leukocyte transmigration *in vivo*. Moreover, ABT was well tolerated in intra-peritoneal as well as in intra-arterial application.

3.2 ABT does not exert proapoptotic effects in HUVECs

The endothelium plays an important role in inflammatory processes.⁷⁹ Since the IAP antagonist shows anti-inflammatory effects *in vivo* we aimed at analyzing the actions of ABT on activated endothelial cells and uncovering the role of IAPs in inflammatory processes of endothelial cells *in vitro*. Because synthetic Smac mimetics are applied to induce apoptosis in cancer cells it was necessary to determine possible pro-apoptotic effects of the Smac mimetic ABT in endothelial cells. The treatment with ABT in concentrations ranging from 1 nM to 1 μ M did not evoke apoptosis (subdiploid DNA content) in HUVECs after 24 h or 48 h (Figure 10A). There also was no induction of apoptosis detectable in cells that were pretreated with ABT (3 nM to 3 μ M) before they were exposed to TNF α for 24h (Figure 10B).

These results indicate that the IAP antagonist ABT does not induce apoptosis in HUVECs, neither alone nor in combination with TNF α .

A



B

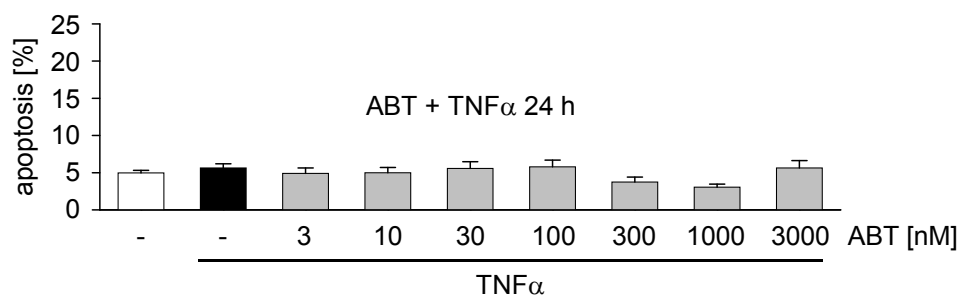


Figure 10 ABT does not induce apoptosis in HUVECs. Confluent cells were treated with the indicated concentrations of ABT for 24 h or 48 h (A) or they were pretreated with ABT for 30 min before incubation with TNF α for 24 h (B). After harvesting of the cells they were stained with PI and the subdiploid DNA content was determined by FACS analysis. Data are expressed as mean \pm S.E.M. (n = 3).

3.3 Influence of ABT on endothelial barrier function

The anti-inflammatory potential of the IAP antagonist *in vivo* gave rise for the exploration of effects of the IAP inhibitor and of the role of IAPs in inflammation-activated endothelial cells *in vitro*. Since the loss of endothelial barrier function is a hallmark of inflammatory processes,⁸⁰ we investigated if ABT has any impact on endothelial barrier function.

3.3.1 ABT inhibits macromolecular hyperpermeability

The endothelial macromolecular permeability was induced by thrombin and analyzed by a Transwell[®] assay. While the treatment of endothelial cells with thrombin increases their permeability to macromolecules, the pretreatment of the cells with ABT resulted in a clear reduction of thrombin-induced endothelial hyperpermeability (Figure 11).

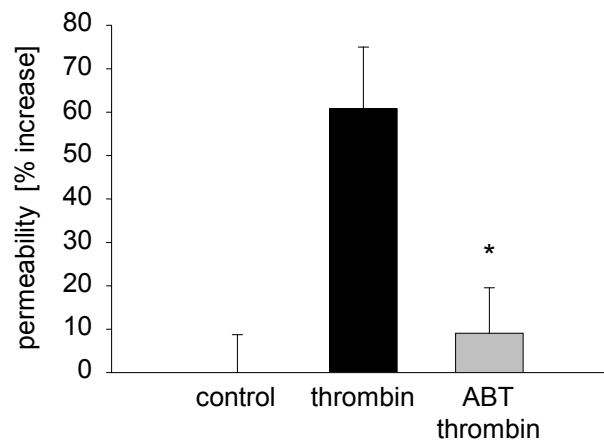


Figure 11 ABT restores endothelial barrier function. Macromolecular permeability of HMECs was measured by a Transwell[®] assay. The cells were seeded on Transwell[®] inserts and treated with thrombin (1 U/ml) after 30 min of preincubation with ABT (1 μ M). FITC-labeled dextran was used as a tracer and added to the upper compartment of the transwell chamber. After 5, 10, 15 and 30 min, the amount of FITC-dextran in the lower compartment of the chamber was determined. Data are expressed as mean \pm S.E.M. (n = 7). *, $p < 0.5$ versus thrombin.

3.3.2 Impact of ABT on adhesion junctions and the contractile machinery of endothelial cells

Endothelial barrier function is maintained by the balance between contractile and adhesive forces.⁸⁰ Therefore, we analyzed if ABT affects the contractile machinery or the endothelial adhesion junctions. There was no difference detectable in the thrombin-induced MLC2-phosphorylation irrespective of whether HUVECs were preincubated with ABT or not. In contrast, the thrombin-triggered phosphorylation of VE-cadherin was attenuated when cells were treated with ABT (Figure 12). Thus, the IAP antagonist seems not to influence the thrombin-induced activation of the contractile apparatus, but the signal initiating the destruction of adhesion junctions was decreased by the Smac mimetic.

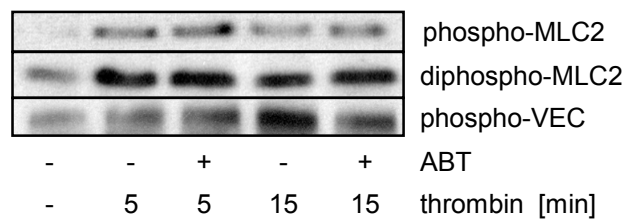


Figure 12 Influence of ABT on key parameters of endothelial barrier function. HUVECs were incubated with 1 μ M ABT before treatment with 1 U/ml thrombin for 5 min or 15 min. The phosphorylation of MLC2 and of VE-cadherin was analyzed by Western blot analysis. (n = 3).

ABT abrogates thrombin-induced hyperpermeability and influences the adhesion junctions in terms of abrogating the VE-cadherin phosphorylation but does not inhibit MLC2 activation.

3.4 Effects of ABT on leukocyte adhesion to endothelial cells

Adapted from our *in vivo* findings that ABT impairs the endothelial leukocyte interactions, we investigated the impact of the IAP antagonist on TNF α -induced adhesion of leukocytes to endothelial cells. The adhesion of neutrophil granulocytes to endothelial cells was reduced concentration dependently when the HUVECs were exposed to the IAP antagonist before treatment with TNF α (Figure 13).

The impairment of leukocyte adhesion to HUVECs could even be amplified when both, the neutrophils and the HUVECs, were treated with ABT (data not shown).

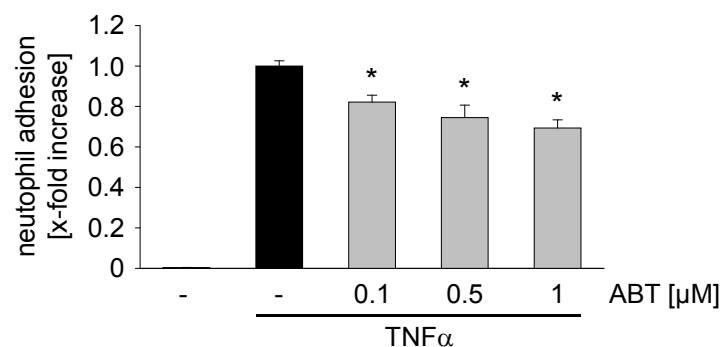


Figure 13 ABT influences the adhesion of leukocytes to HUVECs. HUVECs were seeded in 24-well plates and preincubated for 30 min with ABT (100 nM, 500 nM and 1 μ M) and after that treated with TNF α (10 ng/ml) for 24 h. Human neutrophil granulocytes were added (10^5 cells per well) and allowed to adhere for 45 min. MPO (an enzyme specific for granulocytes) activity was measured to determine the amount of adhered neutrophil granulocytes. Data are expressed as mean \pm S.E.M. (n = 7). *, $p < 0.05$ versus TNF α .

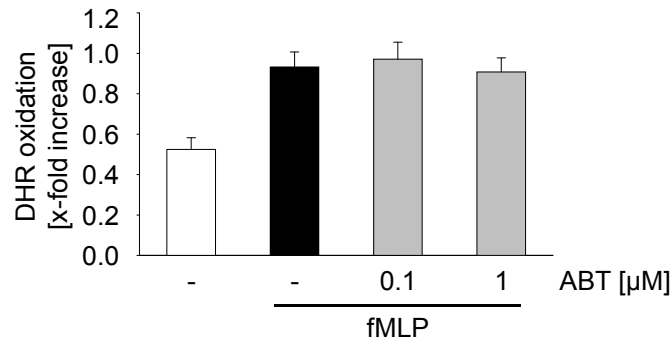
ABT decreases the TNF α -induced adhesion of leukocytes to endothelial cells and in this regard affects endothelial cells as well as leukocytes.

3.4.1 Influence of ABT on CD11b expression and oxidative burst of neutrophil granulocytes

Since the treatment of granulocytes with ABT additionally affects the interaction between granulocytes and HUVECs, we checked if ABT attenuates the activation of leukocytes by analyzing two markers for neutrophil activation: the fMLP-induced expression of CD11b and the oxidative burst. As depicted in Figure 14A, the treatment

of neutrophil granulocytes with ABT did not interfere with their property to execute oxidative burst. In contrast, the expression of the integrin CD11b was reduced when granulocytes were incubated with ABT (Figure 14B).

A



B

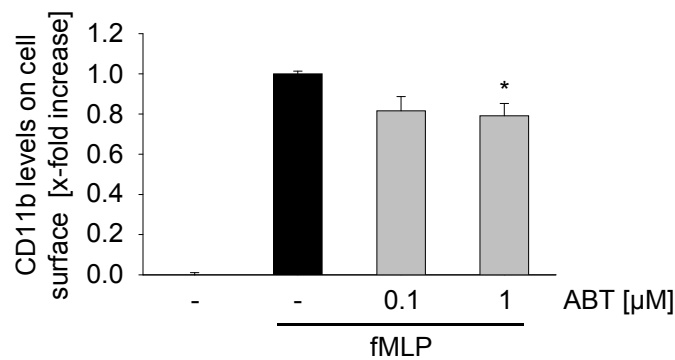


Figure 14 ABT does not affect oxidative burst of neutrophil granulocytes but reduces CD11b expression. Human neutrophil granulocytes were treated for 30 min with ABT (100 nM and 1 μM) before incubation with 10^{-7} M fMLP for 15 min. A) For the determination of the oxidative burst by FACS analysis, the granulocytes were preincubated with 10 μM dihydrorhodamine before the treatment with ABT and $\text{TNF}\alpha$. B) The expression of CD11b on the granulocyte cell surface was examined by staining with a CD11b antibody following FACS analysis. Data are expressed as mean \pm S.E.M. ($n = 3$). *, $p < 0.05$ versus $\text{TNF}\alpha$.

These results suggest that the IAP antagonist does not influence the granulocyte activation regarding their cytotoxic functions. It seems to selectively influence the cell surface expression of adhesion molecules.

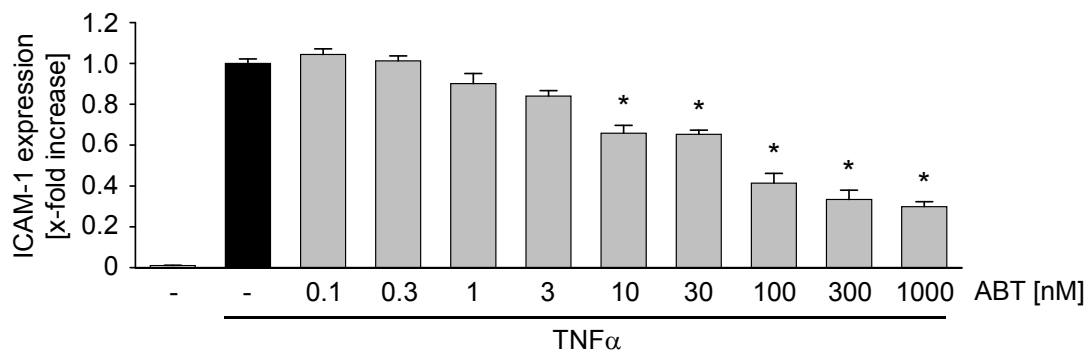
3.5 Role of IAPs in TNF α -induced adhesion molecule expression

Because the treatment of endothelial cells with ABT affected the adhesion of granulocytes, we investigated the influence of ABT on endothelial activation. Therefore, we analyzed the endothelial cell surface expression of intercellular adhesion molecule-1 (ICAM-1), which is involved in the firm adhesion of leukocytes to endothelial cells and the following diapedesis into the underlying tissue.^{92, 120}

3.5.1 ABT reduces TNF α -induced expression of an endothelial adhesion molecule

The expression of ICAM-1 was induced by TNF α and analyzed by flow cytometry. ABT impaired TNF α -induced expression of ICAM-1 on the cell surface of HUVECs dependently on the used concentrations (Figure 15A). Also the total cellular amount of ICAM-1 was diminished by treating the endothelial cells with ABT as indicated by Western blot analysis (Figure 15B).

A



B

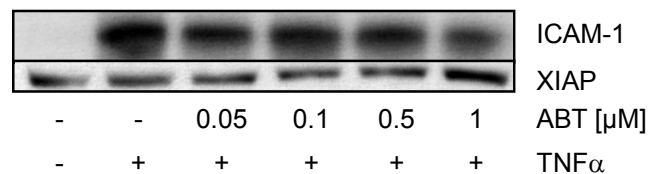


Figure 15 ABT reduces ICAM-1 expression in HUVECs. A) In order to investigate the TNF α -induced expression of the adhesion molecule ICAM-1 on HUVECs, they were

preincubated with ABT (100 pM–1 μ M) for 30 min and then treated with TNF α (10 ng/ml) for 24 h. The levels of ICAM-1 on the cell surface were determined by flow cytometry. Data are expressed as mean \pm S.E.M. (n = 3). *, $p < 0.05$ versus TNF α . B) For the Western blot analysis of the total cellular amount of ICAM-1, HUVECs were treated for 6 h with TNF α (10 ng/ml) after pretreatment with ABT.

3.5.2 The IAP inhibitors Smac066 and Smac085 are capable of reducing TNF α -induced expression of ICAM-1

To ensure that the effects of ABT on the inflammatory activation of endothelial cells arise from targeting the IAPs and to exclude off-target effects of ABT, we compared its influence on the TNF α -evoked adhesion molecule expression with the structurally different IAP antagonists Smac066 and Smac085 (figure 17).^{68, 120} Similar results were obtained for the monovalent Smac mimetic Smac066 and the homodimeric Smac mimetic Smac085 as for ABT regarding the reduction of TNF α -evoked ICAM-1 expression (Figure 16), suggesting that molecules that mimic the interaction of Smac with IAPs have an anti-inflammatory potential.

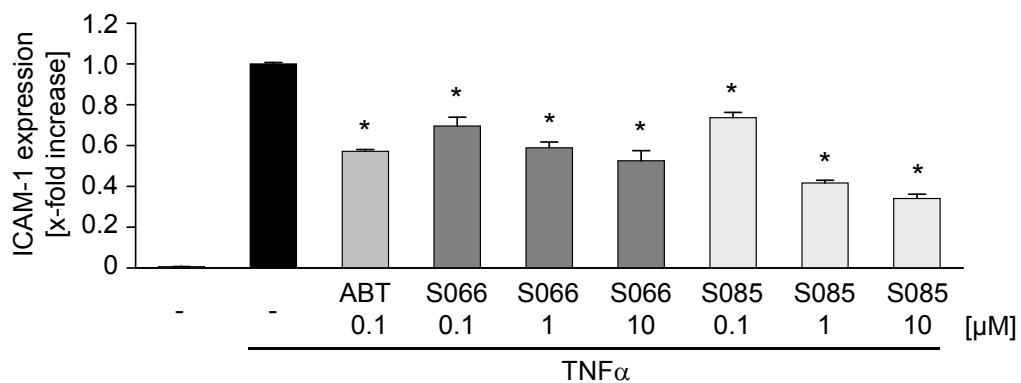


Figure 16 Influence of Smac066 and Smac085 on ICAM-1 expression. HUVECs were treated with Smac066 or Smac085 (100 nM–1 μ M) for 30 min before incubation with TNF α (10 ng/ml) for 24 h. The levels of ICAM-1 on the cell surface were determined by flow cytometry. Data are expressed as mean \pm S.E.M. (n = 3). *, $p < 0.05$ versus TNF α .

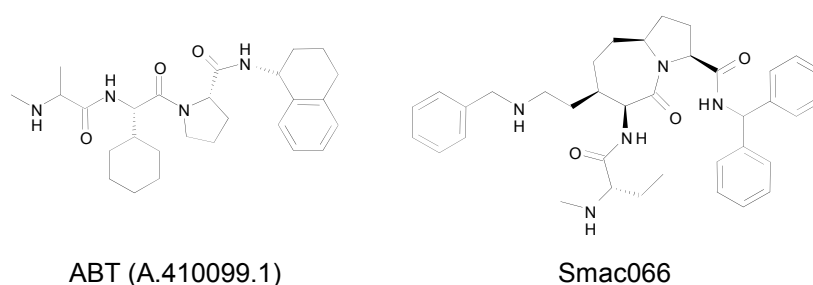


Figure 17 Structurally different Smac mimetics. ABT (A410099.1) Oost *et al.*⁶ and Smac066 (compound 40d) Seneci *et al.*¹²⁰ The structure of Smac085 is unpublished.

3.5.3 Impact of the pan-caspase inhibitor Q-VD-OPh on ICAM-1 expression induced by TNF α

Smac mimetics have originally been designed to abrogate the inhibitory interaction of IAPs with caspases.⁶⁸ Therefore, we tested if the activation of caspases participates in the effect of ABT on the TNF α -induced ICAM-1 expression. The application of a pan-caspase inhibitor had no impact on the ABT-mediated reduction of expression of ICAM-1 on endothelial cells (Figure 18), indicating that the ICAM-reducing effect of ABT is independent of caspases

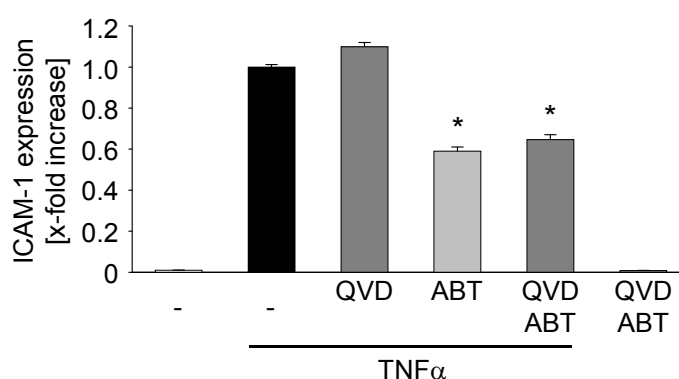


Figure 18 The role of caspases in the ABT-induced reduction of ICAM-1 expression. Cells were preincubated with the pan-caspase inhibitor Q-VD-OPh (QVD) (10 μ M, 30 min) to examine the role of caspases before treating them with ABT (100 nM) for 30 min and TNF α (10 ng/ml) for 24 h. The ICAM-1 expression on HUVECs was analyzed by flow cytometry. Data are means \pm S.E.M. (n = 3). *, $p < 0.05$ versus TNF α .

Taken together, our results clearly suggest that Smac mimetics influence the interactions between leukocytes and endothelial cells by reducing the endothelial adhesion molecule expression. Moreover, the prevention of endothelial activation as a result of targeting IAPs by Smac mimetics is not due to an activation of caspases and points to a considerable role of IAPs in the context of inflammatory processes.

3.6 Interactions of ABT with the NF κ B signaling

Since the activation of the transcription factor NF κ B is involved in the TNF α -induced increase of adhesion molecule expression¹¹⁹, we consequentially explored the influence of ABT on different stages of NF κ B activation.

3.6.1 ABT does not influence phosphorylation and degradation of I κ B α

ABT did neither reduce the TNF α -induced phosphorylation of the IKK inhibitor I κ B α nor did it result in a degradation of I κ B α (Figure 19).

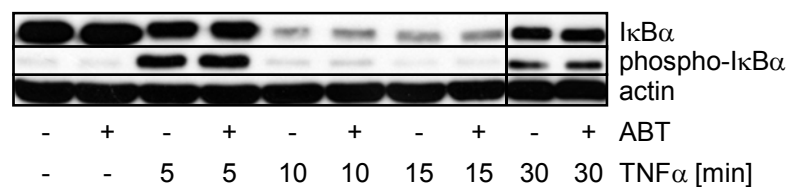


Figure 19 ABT does not significantly influence NF κ B activation. The phosphorylation and the degradation of I κ B α was induced by incubating the cells with 10 ng/ml TNF α for 15 min, 30 min and 60 min after they were treated with ABT (100 nM) for 30 min. The levels of I κ B α and phospho-I κ B α were examined by analysis blot (n=3).

3.6.2 The translocation of p65 is not impaired by ABT

In accordance to these findings, the TNF α -induced translocation of the NF κ B p65 subunit to the nucleus was not influenced by ABT (Figure 20).

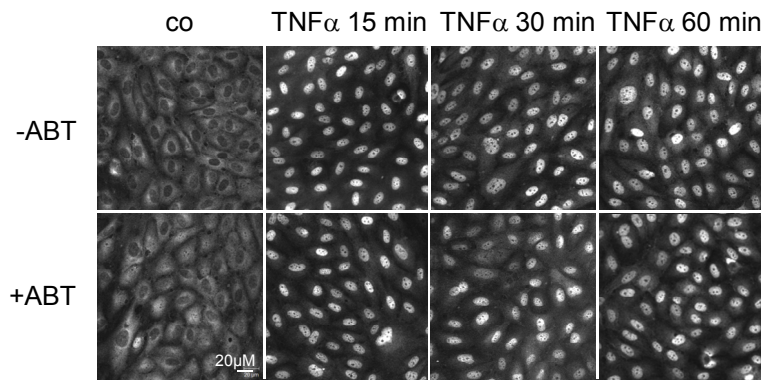


Figure 20 The translocation of the NF κ B p65 subunit is not affected by ABT. For immunocytochemical analysis of the translocation of the p65 subunit to the nucleus, cells were treated with TNF α (10 ng/ml) for 15 min, 30 min and 60 min following to a 30 min preincubation with ABT (100 nM) (n = 3).

3.6.3 ABT does not affect the DNA-binding capacity of NF κ B

Moreover, the IAP antagonist did not interfere with the increase in the DNA-binding capacity of NF κ B evoked by TNF α (Figure 21). The DNA-binding capacity of NF κ B is neither reduced by ABT after short term treatment nor after long term treatment of the endothelial cells with TNF α (data not shown).

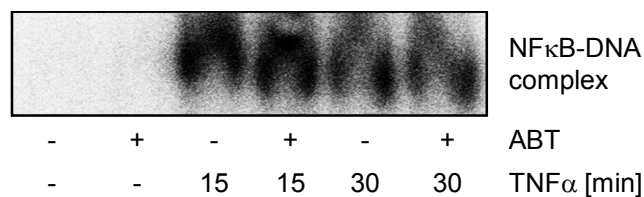


Figure 21 ABT does not influence DNA-binding capacity of NF κ B in electrophoretic mobility shift assay (EMSA). In order to determine the effect of ABT on DNA-binding capacity of NF κ B, HUVECs were treated with ABT (100 nM or 1 μ M) for 30 min followed by TNF α (10 ng/ml, 15 min and 30 min). Nuclear proteins were isolated. P³²-labeled NF κ B consensus sequence oligonucleotides were added and an electrophoretic mobility shift assay was performed (n = 3).

3.6.4 NF κ B-dependent promoter activity is not influenced by ABT

Since ABT did not influence the NF κ B activation cascade, we finally checked impact of ABT on the transcriptional activity of NF κ B dependent genes. The NF κ B reporter gene assay indicated no significant effect of ABT on NF κ B-dependent promoter activity (Figure 22).

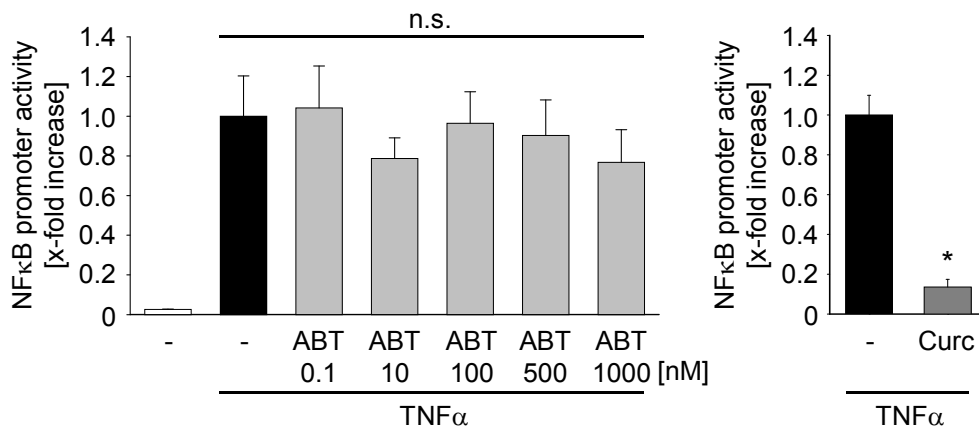


Figure 22 ABT does not attenuate the NF κ B promoter activity. For the Dual Luciferase[®] NF κ B reporter assay, HUVECs were transfected with plasmids coding for *Renilla* luciferase (determination of transfection efficiency) and firefly luciferase (coupled to NF- κ B promoter). 16 h after transfection ABT (100 nM to 1 μ M) was added and 30 min later cells were treated with TNF α (10 ng/ml) for 6 h (left diagram). Curcumin (20 μ M) in combination with TNF α was used as a positive control (right diagram). The luciferase activity was assayed by spectrofluorometry. Data are expressed as means \pm S.E.M. (n = 3).

Summarizing the results from above, ABT does not significantly affect the TNF α -induced activation cascade of NF κ B.

3.7 Interactions of ABT with MAPK signaling

Since the ABT-dependent reduction of TNF α -induced ICAM-1 expression is not due to an effect on NF κ B signaling, we analyzed if the anti-inflammatory effect of ABT on endothelial cells is based on an interaction with the proinflammatory MAPK signaling.

3.7.1 ABT affects TNF α -induced activation of MAPKs

Figure 23 shows that ABT diminished the TNF α -induced phosphorylation of the MAPKs p38 and JNK that both are known to participate in pro-inflammatory signaling. In contrast, the IAP antagonist had no impact on the TNF α -mediated phosphorylation of ERK1. The protein levels of the MAPK phosphatase MKP-1 were not altered by ABT as well.

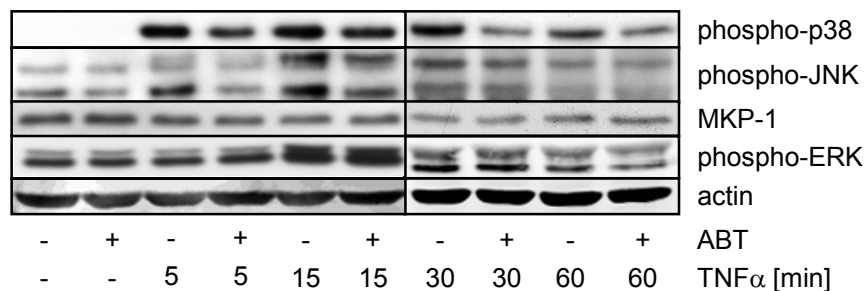


Figure 23 ABT influences the TNF α -induced activation of MAPKs. HUVECs were incubated with 100 nM ABT for 30 min before treating them with 10 ng/ml TNF α for 5, 15, 30 and 60 min. Levels of phospho-JNK, phospho-p38, phospho-ERK and MKP-1 were determined via Western blot (n = 3).

3.7.2 Inhibition of p38 and JNK influence ICAM-1 expression

To test whether the anti-inflammatory effect of ABT is based on the inhibition of the p38- and JNK activity, the influence of the p38 inhibitor SB203580 and the JNK inhibitor SB600125 on the TNF α -evoked ICAM-1 expression on HUVECs was analyzed. The treatment of the cells with the p38- as well as with the JNK inhibitor resulted in a significant decrease of TNF α -induced ICAM-1 expression (Figure 24). The effect of SB600125 was more pronounced than the impact of SB203580. The added levels of

ICAM-1 reduction caused by SB203580 and by SP600125 correspond to the effect of ABT on TNF α -induced ICAM-1 expression.

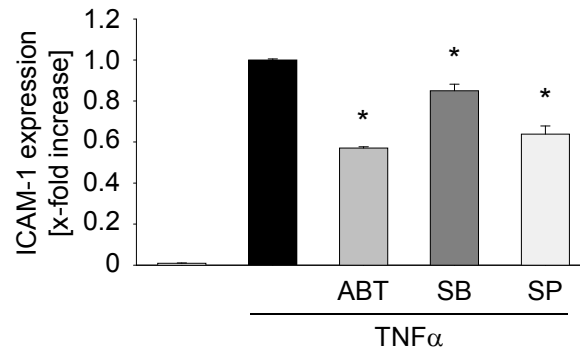


Figure 24 The influence of a p38- and a JNK inhibitor on the expression of ICAM-1. The cells were incubated with the SB203580 (20 μ M), SP600125 (10 μ M), or with ABT (100 nM) for 30 min and for another 24 h with TNF α (10ng/ml). Levels of ICAM-1 expression were determined by flow cytometry. Data are expressed as mean \pm S.E.M. (n = 3). *, $p < 0.05$ versus TNF α .

3.7.3 ABT controls the activity of the MAP3K TAK1

Due to the inhibitory impact of the IAP antagonist on the activation of p38 and JNK, we analyzed the interaction of ABT with the MAPK signaling cascade upstream of JNK and p38. The MAP3K TAK1 is phosphorylated immediately upon activation by TNF α . This phosphorylation was reduced when cells were pretreated with the IAP antagonist as shown in Figure 25.

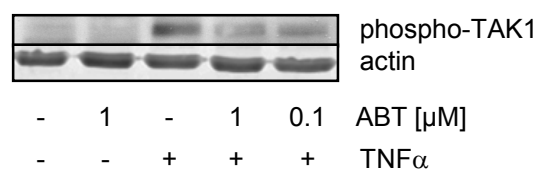


Figure 25 ABT reduces the phosphorylation of TAK1. The activation of the MAP3K TAK1 was determined by Western blot analysis after preincubation of HUVECs with ABT (100 nM and 1 μ M, 30 min) and following treatment with TNF α (10 ng/ml, 5 min) (n = 3).

3.7.4 Impact of ABT on the interactions of TAK1 binding protein (TAB1) with XIAP

The activation of TAK1 can (among others) be influenced by the interaction between the BIR1 domain of XIAP and TAK1 via the TAK1 binding protein TAB1⁷. Smac, the intrinsic IAP antagonist, is able to affect the interaction of XIAP and TAB1.⁷ Immunoprecipitations of TAB1 with following Western blot analysis of co-precipitated XIAP indicated that the interaction of XIAP and TAB1 in HUVECs is very weak in contrary to cancer cells (data not shown). Neither ABT nor TNF α nor a combination of both influenced the amount of XIAP that is co-precipitated with TAB1 (Figure 26).

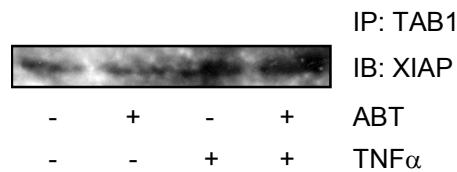


Figure 26 ABT does not influence the XIAP-TAB1 interaction. Cells were pretreated with ABT (1 μ M, 30 min) and incubated with 10 ng/ml TNF α for 5 min. TAB1 was immunoprecipitated and the amount of co-precipitated XIAP was detected by Western blot analysis (n = 3).

Taking together all results from above, ABT strongly reduces the TNF α -induced activation of the MAPKs p38 and JNK which are involved in the TNF α -evoked expression of ICAM-1 but not by an increase of MKP-1 levels. The activity of the upstream MAP3K TAK1 was also affected by the IAP antagonist, while this effect seems not to be based on an abrogation of the interaction between XIAP and TAK1.

3.8 Silencing of XIAP does not reduce ICAM-1 expression

ABT is modeled on the basis of the interaction of the endogenous IAP antagonist Smac with the BIR3 domain of XIAP. Because of this fact and the finding that ABT does not block the activation of TAK1 by an abrogation of the interaction of XIAP with TAB1 we investigated the role of XIAP for the anti-inflammatory impact of ABT.

We tested if the down-regulation of XIAP levels results in similar effects on ICAM-1 expression as treating the cells with the IAP-antagonist. Unexpectedly, silencing of XIAP in HUVECs did not cause a reduction of ICAM-1 expression but even increased it as shown in Figure 27A. Moreover, in cells where XIAP was down-regulated, ABT still was capable of reducing TNF α -caused ICAM-1 expression. The Western blot analysis exhibited a clear reduction of XIAP protein levels in those cells that were transfected with XIAP siRNA, while at the same time cIAP1 and cIAP2 protein levels were significantly up-regulated (Figure 27B).

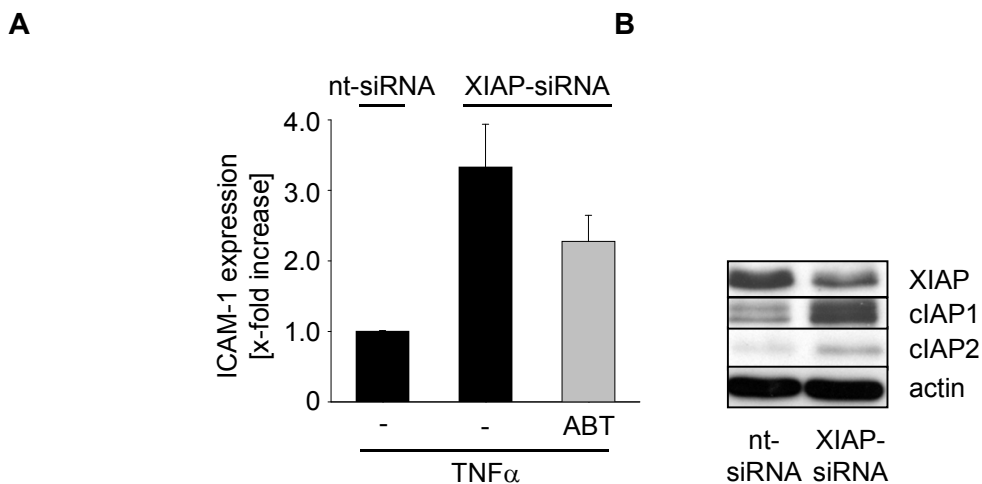


Figure 27 Silencing of XIAP does not reduce ICAM-1 expression. XIAP was silenced in HUVECs by XIAP siRNA. 24 h after transfection of cells with XIAP siRNA or non-targeting siRNA, the respectively cells were exposed to ABT (100 nM, 30 min) and to TNF α (10 ng/ml, 24 h). The ICAM-1 expression was determined by flow cytometry. Data are expressed as mean \pm S.E.M. (n = 3). XIAP protein levels and the content of cIAP1 and cIAP2 were studied by Western blot analysis.

The presence of XIAP is not required for the anti-inflammatory impact of the IAP antagonist. Instead, the reduction of XIAP levels in endothelial cells induces a counteraction in terms of an increased cIAP1 and cIAP2 expression.

3.9 Interactions of ABT with the TNF receptor signaling

Since ABT does not influence the TAK1 activation by inhibiting the interaction of XIAP and TAB1 and since silencing of XIAP does not cause any anti-inflammatory effect in HUVECs, the question raised in which way the Smac mimetic influences the pro-inflammatory activation of the MAPKs.

3.9.1 ABT induces degradation of cIAP1 and cIAP2

The analysis of XIAP and cIAP1 protein levels showed a very fast and long lasting reduction of cIAP1 levels in endothelial cells treated with ABT. In contrast, the amount of XIAP remained constant as it is known for the cellular IAP antagonist Smac⁷⁵ (Figure 28A). The protein levels of cIAP2 are only detectable if its expression is activated by TNF α as described by Harlin *et al.*²⁶ They appear to be similarly influenced by ABT as cIAP1 levels (Figure 28B).

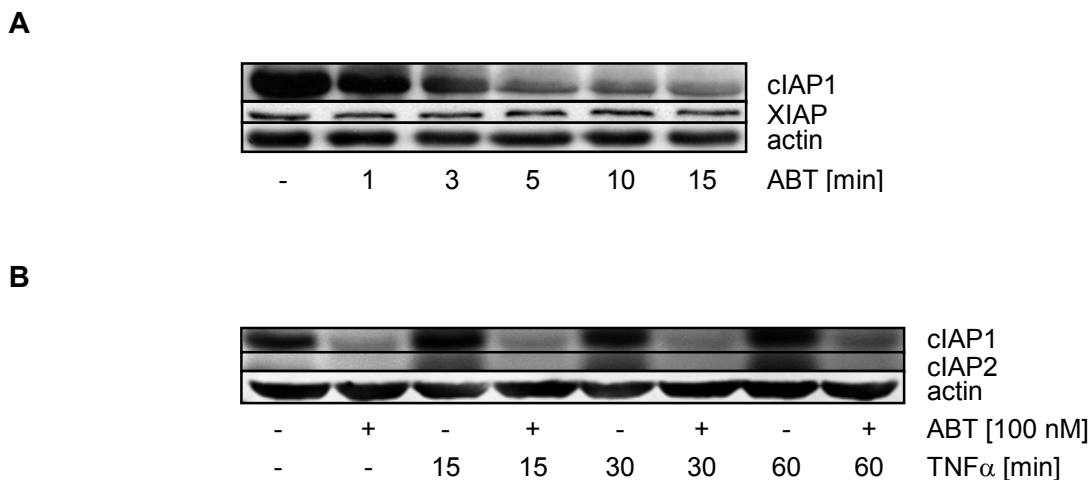
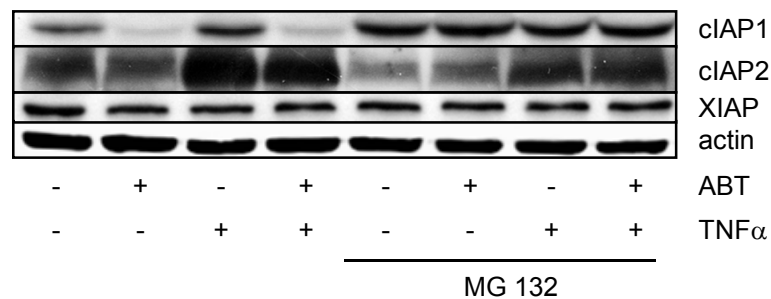


Figure 28 Degradation of cIAP1 and cIAP2 induced by ABT. Cells were treated with ABT (100 nM) for 1 min, 3 min, 5 min, 10 min or 15 min (A) or cells were incubated with ABT (100 μ M) before treatment with TNF α (10 ng/ml) (B). The effect of ABT on the total cellular levels of XIAP, cIAP1 and cIAP2 was determined by Western blot analysis (n = 3).

3.9.2 The proteasomal degradation of cIAP1 and cIAP2 is responsible for the anti-inflammatory effect of ABT

Because of the knowledge that cIAP1 and cIAP2 participate in TNF receptor signaling¹² we investigated if their downregulation caused by ABT is responsible for the reduction TNF α -evoked signs of inflammation. The degradation of cIAP1 and cIAP2 activated by ABT was inhibited by the proteasome inhibitor MG132 as shown in Figure 29A. The analysis of the TNF α -induced ICAM-1 expression showed that abolishing the proteasomal activity by MG132 abrogates the attenuating effect of ABT on the expression of ICAM-1 (Figure 29B).

A



B

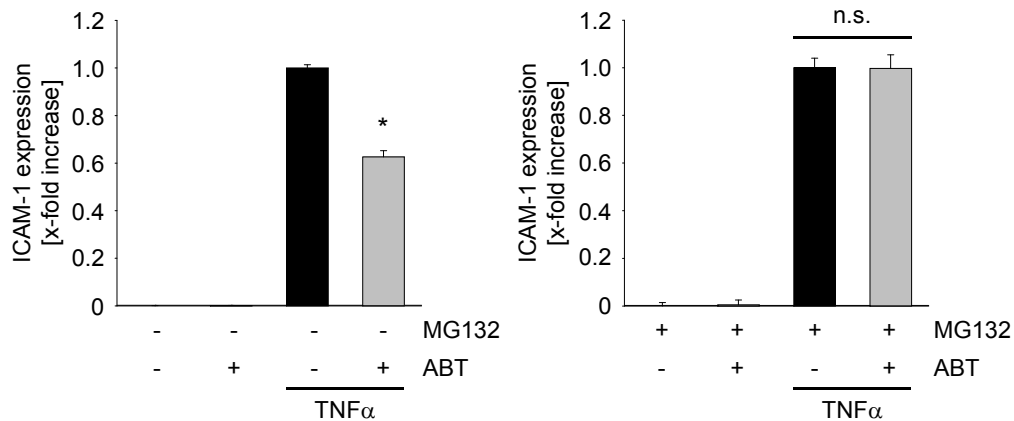


Figure 29 Inhibition of the proteasome abrogates the anti-inflammatory effect of ABT. In order to analyze the involvement of proteasomal degradation the HUVECs were preincubated with the proteasome inhibitor MG132 (10 μ M, 30 min) before treatment with ABT (1 μ M) for 30 min and TNF α (10 ng/ml) for 24 h. The levels of cIAP1, cIAP2 and XIAP were determined by Western blot analysis (A) and the ICAM-1 expression on HUVECs was analyzed by flow cytometry (B). Data are mean values of \pm S.E.M. (n = 3). *, $p < 0.05$ versus TNF α .

3.9.3 Influence of ABT on the participants of the TNFR1-associated complex TRAF2 and TRAF5

In order to investigate the role of the ABT-induced proteasomal degradation of cIAP1 and cIAP2 in the inflammation-inducing signaling of TNF α , we analyzed the influence of the IAP antagonist on TRAF2, a member of the TNF receptor associated signaling complex. TRAF2 mediates the activation of NF κ B and of the MAP3K (TAK1) signaling⁶¹ and it is known to interact with cIAP1 and cIAP2 in the TNFR1-associated complex⁶⁴. Upon treatment of endothelial cells with ABT, the levels of TRAF2 in the membrane fraction (where the TNF receptor associated signaling complex is located) decreased immediately. In contrast, the amount of TRAF5, which is known to compensate the loss of TRAF2 only in terms of activation of the NF κ B signaling,^{130, 131} remained constant (Figure 30).

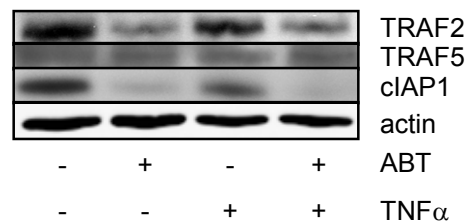


Figure 30 ABT influences the amount of TRAF2 but not of TRAF5 in the membrane fraction. Western blot analysis of the membrane fractionation of HUVECs pretreated with ABT (1 μ M, 30 min) and exposed to 10 ng/ml TNF α for 5 min shows the amount of TRAF2, TRAF5 and cIAP1 in the membrane fraction (n = 3).

Our data strongly indicate an as yet unknown role of cIAP1 and cIAP2 in the TNF α -induced inflammatory signaling of endothelial cells. Moreover, they evidence an impact of ABT on these signaling processes by influencing TRAF2 in the TNFR-associated signaling complex.

4 DISCUSSION

4.1 The link between IAPs and inflammation

Activation of inflammatory processes is crucial for the host defense against infections or for repairing tissue damage, but it shows destructive properties in pathologies like atherosclerosis or sepsis or in ischemic tissue. The administration of conventional anti-inflammatory drugs is not always effective and may often cause undesirable side effects. Therefore, inflammation is still a very important subject of research in terms of unraveling signaling interconnections to reveal new therapeutical strategies.

Since the transcription factor NF κ B regulates the expression of adhesion molecules and cytokines in inflammatory processes as well as the expression of anti-apoptotic genes like IAPs or Bcl-2, inflammation and the regulation of cell death are often closely connected.¹³² For example, the up-regulation of IAPs in atherosclerotic plaques of patients with carotid stenosis seems to be involved in the stabilization of symptomatic atheromatous plaques by preventing apoptosis.¹³³

Cancer as well is associated with inflammatory processes. On the one hand inflammatory diseases increase the risk of many types of cancer¹³⁴ and on the other hand inflammatory cells and cytokines are present in the microenvironment of many tumors from the early stages of development.¹³⁵

Despite these associations between inflammation and cancer, and the fact that XIAP is known to activate NF κ B signaling⁷ as well as that cIAP1 and cIAP2 participate in TNFR1-associated signaling,^{23, 64} current research is only illuminating the role of IAPs in TNFR and NF κ B signaling concerning apoptotic processes.

In our work, we for the first time demonstrate that targeting IAPs has the potential of a completely new and promising anti-inflammatory approach.

4.2 Anti-inflammatory effects of ABT *in vivo*

Until now, IAP antagonists have only been applied in tumor models to proof them as promising candidates for cancer therapy.⁶⁸ ABT, for example, was effectively used in a breast cancer xenograft tumor model.⁶ This is for our best knowledge the first study investigating the effects of an IAP antagonist *in vivo* in an inflammatory context.

Rheumatoid arthritis (RA), the most common form of arthritis, concerns millions of people world wide and is associated with chronic pain and reduced quality of life.¹³⁶ It is a process of chronic inflammation and involves the infiltration of neutrophils, monocytes

and lymphocytes into the inflamed tissue. The infiltration of joints results in synovial proliferation, pannus formation, cartilage destruction and subchondral bone erosion.¹³⁷ The antigen-induced arthritis in mice is a well established model for the investigation of RA.¹³⁸ We found a highly potent action of ABT on mBSA-induced arthritis: a complete abrogation of knee joint swelling, elucidating for the first time an anti-inflammatory potential of an IAP antagonist in a clinically relevant *in vivo* model.

The activated endothelium is a crucial player in the process of arthritis because it facilitates the transit of more and more leukocytes to the inflamed tissue, which is also supported by an increased angiogenesis.¹³⁶ Thereby, cytokines like TNF α activate the endothelium to express a large amount of the adhesion molecules ICAM-1 and E-selectin as found in the synovial tissue of arthritic patients. Elevated expression of adhesion molecules on neutrophils had been demonstrated as well.¹³⁹

The convincing protective effect of ABT in a model of a disease that crucially involves endothelium leukocyte interactions encouraged us to pass on to the detailed analysis of the influence of ABT on these interactions *in vivo* by intravital microscopy of the mouse cremaster muscle. The significant ABT-dependent abrogation of the leukocyte transmigration indicated an effect of the IAP antagonist on the leukocyte endothelium interaction and on the activation of the leukocytes and/or the endothelium.

Thus, we for the first time showed a promising anti-inflammatory action of an IAP antagonist *in vivo*, which called for a detailed analysis of the underlying mechanisms on inflammation-activated cells *in vitro*.

4.3 Effects of ABT on endothelial activation *in vitro*

4.3.1 Functional *in vitro* assays

Under normal physiological circumstances, the vascular endothelium exhibits a quiescent phenotype that modulates permeability, coagulation and vasodilation. However, when the endothelium is exposed to inflammatory mediators derived from a local infection, the endothelium becomes activated to a state that expresses chemokines and adhesive receptors facilitating the recruitment of pro-inflammatory leukocytes. The influence of the IAP antagonist on this state was investigated by several functional assays.

4.3.1.1 Endothelial permeability

Inflammatory cytokines and the process of leukocyte transmigration activate endothelial cells in terms of weakening the endothelial barrier function and lead to an increase of endothelial permeability. Thus, endothelial hyperpermeability is a hallmark of inflammatory processes and seriously assists the progression of the disease when it gets down to an excessive extravasation of fluid and leukocytes to the tissue. A total collapse of endothelial barrier function, like in sepsis, contributes to its life-threatening complications.^{88,90,89}

The strong barrier protective effect of ABT indicates that the IAP antagonist counteracts endothelial activation *in vitro*. The abrogation of the thrombin-induced hyperpermeability seems not to rely on an influence of ABT on the contractile machinery but on a prevention of adhesion junction disassembly, indicated by a reduction of VE-cadherin phosphorylation. These data are in line with our *in vivo* findings regarding the ABT-mediated abrogation of leukocyte transmigration because the phosphorylation of VE-cadherin is required in the diapedesis process of leukocytes through the endothelial cell monolayer.^{96, 140, 141}

Although a participation of IAPs in TNFR signaling is known, it is totally unknown how IAPs are involved in the thrombin-mediated activation of endothelial cells or how an IAP antagonist could interfere with endothelial hyperpermeability activated by the thrombin receptor PAR. Hence, it would be a very interesting task to investigate the link between the IAPs and the PAR receptor signaling and to analyze possible effects of ABT on keyregulators of endothelial barrier function (RhoA, Rac1, Ca²⁺ signaling, PKA/cAMP, PKC and the cytoskeleton). This project is currently pursued.

4.3.1.2 ICAM-1 mediated endothelium leukocyte interactions

The inflammatory activation of endothelial cells induces, besides barrier dysfunction, the upregulation of adhesion molecules and mediates the leukocyte endothelium interactions.⁹² The attenuation of ICAM-1 expression attests the IAP antagonist to have an anti-inflammatory potential *in vitro* by preventing TNF α -mediated endothelial activation. Since ICAM-1 is engaged in the firm adhesion- and the diapedesis-step of leukocyte transmigration,^{141, 142} the ICAM-1 reducing effect of ABT explains the attenuation of neutrophil adhesion to endothelial cells *in vitro* as well as the inhibition of leukocyte transmigration *in vivo*. This effect might also contribute to the impact of ABT

on antigen-induced arthritis because a strong increase in ICAM-1 expression is reported to be vital for the disease progression in arthritis.¹³⁶

Moreover, the influence of ABT seems not to be limited on endothelial activation. It also appears to act on the adhesive properties of leukocytes as the additional reduction of leukocyte adhesion to the endothelium indicates when the leukocytes as well (not only the endothelial cells) were treated with the Smac mimetic. This is supported by our finding of a reduction of the ICAM-1-interacting adhesion molecule CD11b on ABT treated neutrophils. Since the activation of leukocytes employs similar signaling pathways (for example regarding the TNFR1 signaling and the engagement of MAPK signaling) as endothelial activation,¹⁴³ supposedly the IAPs also play a role in leukocyte activation. Uncovering the participation of IAPs in the inflammatory activation of leukocytes and the contribution of the ABT-mediated attenuation of this activation to the impairment of leukocyte recruitment constitutes an interesting field of research.

However, in order to investigate the signaling mechanisms that underly the influence of ABT on endothelial activation and to uncover the role of IAPs in inflammation we concentrated our research activities on endothelial cells.

The IAP antagonist attenuates the inflammatory activation of endothelial cells by two means: It stabilizes endothelial barrier functions and prevents endothelial adhesion molecule expression which protects from leukocyte endothelium interactions.

4.3.1.3 Specificity of the ICAM-1-attenuating effect of ABT

Since ABT is designed on the model of the interaction between Smac and the BIR3 domain of XIAP⁶ it is rather unlikely that the IAP antagonist exerts its anti-inflammatory effects by the inhibition of other targets than IAPs. Though off-target effects can not be ruled out completely, the parallel effects of structurally completely different IAP antagonists on the TNF α -activated ICAM-1 expression allayed the concerns and underlined the role of IAPs in inflammatory events.

The intention for the design of Smac mimetics was to kill cancer cells by activating caspases.^{6, 120, 144} In endothelial cells, there was no induction of apoptosis detectable by ABT. Even in the combination with TNF α , which is reported to be necessary to sensitize some cancer cell lines for IAP antagonist-mediated apoptosis, ABT did not increase cell death. This might be due to the fact that endothelial cells are in comparison to cancer cells not highly active and proliferative cells and therefore react differently to death-propagating stimuli. Our findings ensured that the anti-inflammatory

effects of the IAP antagonist are not due to an induction of apoptotic processes and indicated that the role of IAPs in endothelial cells must exceed the regulation of cell death.

Besides acting in apoptosis, caspases can be involved in inflammatory processes. As participants of the inflammasome, the caspases 1, 4, and 5 contribute to the maturation of cytokines.¹⁴⁵ Moreover, Wu *et al.* described a connection of the caspases-3 and -8 and inflammatory activation of endothelial cells, in particular in the TNF α -mediated ICAM-1 expression.¹⁴⁶ However, we could clearly exclude that the anti-inflammatory effect of ABT is due to an influence on caspase activity pointing to a different signaling mechanism for the anti-inflammatory effect of ABT.

Our functional *in vitro* assays indicate that the IAP antagonist attenuates inflammatory activation of endothelial cells by two means: It stabilizes endothelial barrier functions and prevents endothelial adhesion molecule expression which protects from leukocyte endothelium interactions.

In summary, our *in vivo* findings and the functional *in vitro* assays regarding the endothelial activation for the first time characterize an IAP antagonist as a potent anti-inflammatory drug and indicate a participation of IAPs in the inflammatory activation of endothelial cells. The exclusion of apoptosis or caspases as mediators of the anti-inflammatory effect of ABT favors the assumption that the IAP antagonist exerts its effects via influencing the TNFR or NF κ B signaling.

4.3.2 Signaling

On the basis of the effects of ABT on endothelial activation, we investigated the signaling mechanisms underlying the protective impact of ABT and the role of IAPs in inflammation-activated endothelial cells.

4.3.2.1 NF κ B/MAPK signaling

So far, the existing data about the function of IAPs in endothelial cells only refer to the aspect that IAPs, as NF κ B dependent genes, protect endothelial cells from TNF α -induced apoptosis.^{147, 148}

Interestingly, the activation of the pro-inflammatory transcription factor NF κ B is not the major target of the anti-inflammatory action of ABT in endothelial cells. This is somewhat surprising because on the one hand, NF κ B is one of the main responsible

transcription factors for the TNF α -induced expression of the adhesion molecule ICAM-1,¹¹⁹ and on the other hand, it is described that IAPs are involved in the TNF α -mediated activation of NF κ B.^{12, 68} However, the reported effects of IAP antagonists on NF κ B signaling are not coincident. It is referred that the autoubiquitination-dependent loss of cIAP1 and cIAP2 induced by IAP antagonists does not influence¹¹ or completely abrogates NF κ B signaling,^{56, 58} while others found that degradation of cIAP1 and cIAP2 activated by a Smac mimetic stimulates NF κ B signaling.^{59, 149} Nevertheless, we found in HUVECs that not the NF κ B signaling but the activation of the MAPKs p38 and JNK is attenuated by ABT. JNK and p38 are crucial mediators of TNF α signaling and strongly involved in the regulation of cellular adhesion molecules such as ICAM-1¹³ as we were able to demonstrate in our cell system as well. By the activation of pro-inflammatory transcription factors, namely of AP-1, but also ATF-2, CREB, SP-1, STAT-1 and STAT-3, they contribute to driving the expression of ICAM-1.^{13, 119} Moreover, p38 is known to be involved in endothelial activation and enhances neutrophil recruitment.¹⁴¹ Corresponding to the inhibition of p38 and JNK, the IAP antagonist blocks the activation of the upstream MAP3K TAK1, which is regulated by TNFR signaling and by XIAP. TAK1 is a MAP3K for p38 and JNK but not for ERK, whose activity was accordingly not influenced by ABT. The finding that ABT does not influence the levels of the MAPK phosphatase MKP-1, which is responsible for the deactivation of MAPKs, also points towards an ABT-mediated inhibition of TAK1 and its upstream signaling.

For that reason we propose that an inhibition of IAPs in inflammation-activated endothelial cells blocks cellular adhesion molecule expression for the most part via an inhibition of the MAPK signaling.

4.3.2.2 Role of XIAP

XIAP is known to mediate the activation of TAK1 by its interaction with TAB1. Thus, the most obvious explanation for the influence of ABT on TAK1 activation would be the interruption of the interaction between XIAP and TAB1 as it is described for the cellular IAP antagonist Smac.⁷ However, the interaction of XIAP and TAB1 in HUVECs seems to be very weak in contrast to cancer cells (data not shown) and moreover the IAP antagonist did not influence this interaction. Furthermore, silencing of XIAP did not result in an inhibition of endothelial activation. In contrast, it even increased TNF α -induced ICAM-1 expression. Importantly, downregulation of XIAP went along with a rise of cIAP1 and cIAP2 levels. A compensatory up-regulation of cIAP1 and cIAP2 has

also been reported for XIAP knockout mice.²⁶ These findings led us to the presumption that XIAP is at least not the main target of the IAP antagonist in the inflammatory context even though the IAP antagonist was modeled to the BIR3 domain of XIAP. Therefore, XIAP does not seem to play a predominant role in the inflammatory activation of endothelial cells but cIAP1 and cIAP2 might be of importance.

Furthermore, the results regarding the XIAP silencing also point out that the downregulation of a protein by silencing does not always have to be in accordance with the interactions of an inhibitor with this protein. Silencing results in the disappearance of the target protein and can result in an upregulation of functionally related proteins (as cIAP1 and cIAP2 upon silencing of XIAP). An inhibitor for example may just inhibit a special function of the protein but the protein is still present (like XIAP). Thus, the protein is still able to interact with other proteins via structurally not influenced sites. Moreover, the inhibitor can influence special functions of the protein like the ubiquitination processes of cIAP1 and cIAP2. Therefore, it is not trivial to compare findings in literature that were achieved by silencing or overexpression of XIAP, cIAP1 and cIAP2 or by using a Smac mimetic. Since IAP antagonists mimic the actions of the cellular protein Smac, they are valuable tools for the investigation of the role of IAPs by comprising the complex interplay of the IAPs.

4.3.2.3 Role of cIAP1 and cIAP2

ABT mediates the loss of cIAP1 and cIAP2 but not of XIAP as it is described for other IAP antagonists that were designed to mimic the Smac AVPI-binding motif and target the XIAP-BIR3 domain. These IAP antagonists not only interact with XIAP but also exhibit high affinities to cIAP1 and cIAP2,⁶⁹ which triggers of the proteasomal degradation of cIAP1 and cIAP2.^{26, 59, 74} Our results evidence that the anti-inflammatory effect of ABT does not necessarily arise from antagonizing XIAP but results from the loss of cIAP1 and cIAP2 because the ICAM-1 reducing effect of the Smac mimetic was reversible by inhibition of the proteasome. This notion is supported by the fact that cIAP1 and cIAP2 upregulation that results from XIAP silencing increases the proinflammatory activation of the endothelium. Moreover, we found that the reduction of cIAP1 and cIAP2 protein levels influences TNF receptor signaling which consequently alters the activation of the MAP3K TAK1.¹²

4.3.2.4 TNFR-associated signaling

The TNF α -induced activation of TNFR1 involves the assembly of the TNFR1-associated signaling complex containing TRAF2 and cIAP1/2. The ubiquitination activity of cIAP1 and cIAP2 is essential for the recruitment and the activation of the IKK/NEMO and the TAB/TAK complex.^{12, 106} Via their BIR1 domain cIAP1 and cIAP2 directly interact with the adaptor protein TRAF2,⁶⁴ which participates in NF κ B as well as in MAPK signaling.^{8, 74, 150, 151} In our experiments the treatment of HUVECs with an IAP antagonist resulted in a proteasome-dependent degradation of cIAP1 and cIAP2 and we detected a loss of TRAF2 in the membrane fraction. This result led us to the assumption that the degradation of cIAP1 and cIAP2 influences the TNF α -induced MAPK activation by affecting TRAF2 in the TNFR1-associated signaling complex and leaves the question why NF κ B signaling is not affected. Yeh *et al.* reported that a loss of TRAF2 prevents TNF α -caused activation of JNK.¹³⁰ In contrast to the levels of TRAF2, the amount of TRAF5 in the membrane fraction was not changed. TRAF5 is reported to compensate the absence of TRAF2 concerning the activation of the NF κ B signaling by TNF α while MAPK signaling is impaired.^{130, 131} This supports our hypothesis that the loss of cIAP1 and cIAP2 in the TNFR associated signaling complex goes along with an impaired TRAF2-mediated initiation of MAPK signaling and explains why the inflammatory activation of endothelial cells is abrogated, although NF κ B signaling is not affected.

Our findings point toward an important role of cIAP1 and cIAP2 in inflammation. Unfortunately, a cIAP1 and cIAP2 double knockout mouse that could reflect the effects of ABT still doesn't exist. cIAP1 or cIAP2 knockout mice are, beside an increased susceptibility of macrophages to LPS-induced apoptosis, asymptomatic. This is presumably due to the fact that for each cIAP knockout the corresponding cIAP is up-regulated and each cIAP can compensate for the other cIAP because of their redundant functions.^{152, 153}

Altogether, this study not only demonstrates for the first time that IAPs play an important regulatory role in inflammatory processes of endothelial cells but also highlights a clear anti-inflammatory potential of an IAP antagonist *in vitro* and *in vivo*.

5 SUMMARY AND CONCLUSION

The IAPs are in the focus of current recent research regarding their role in apoptotic processes and in tumor progression. IAP antagonists are not only promising new therapeutic substances but, moreover, serve as important tools for the investigation of IAP-mediated signaling in apoptosis.

The human IAPs, XIAP, cIAP1 and cIAP2, not only interact with caspases but also participate in TNFR and NF κ B signaling. The NF κ B and TNFR signaling is, besides its involvement in the regulation of cell death, vital for the inflammatory activation of endothelial cells, a prerequisite and fundament of many common and life-threatening pathologies like atherosclerosis, arthritis, diabetes or sepsis. Since there is still a need for efficient treatments of these diseases, it is necessary to dig deeper into the investigation of the underlying signaling mechanisms and to search for new appropriate targets.

Interestingly, despite the importance of NF κ B and TNFR signaling in inflammation, the role of IAPs in these signaling pathways is only elucidated concerning apoptotic processes. Our hypothesis was that IAPs are crucial mediators of inflammation and that therefore IAP antagonists should exhibit an anti-inflammatory potential.

To uncover the link between IAPs and inflammation we applied the IAP antagonist A-410099.1 (ABT) and investigated its role in inflammatory processes.

We, for the first time, demonstrated profound anti-inflammatory actions of an IAP antagonist *in vivo* in an antigen-induced arthritis mouse model as well as the prevention of leukocyte extravasation in mice.

Functional *in vitro* assays showed an ABT-mediated attenuation of endothelial hyperpermeability and a reduced leukocyte adhesion to TNF α -activated endothelial cells accompanied by an abrogation of the expression of the endothelial cell adhesion molecule ICAM-1.

Mechanistically, we found that ABT does not influence endothelial NF κ B signaling, but decreased the TNF α -induced activation of the pro-inflammatory MAPK signaling cascade consisting of the MAP3K TAK1 and the MAPKs p38 and JNK. The activity of p38 and JNK was shown to be involved in TNF α -mediated ICAM-1 expression.

Most importantly, ABT seems not to exert its anti-inflammatory effect by an inhibition of XIAP but by the induction of the proteasomal degradation of cIAP1 and cIAP2. The downregulation of cIAP1 and cIAP2 affects the TNF receptor-associated signaling upstream of the MAPKs and NF κ B in terms of a reduction of the levels of TRAF2. This presumably accounts for the inhibition of the MAPKs, while the activation of the NF κ B

signaling might be compensated by TRAF5, whose levels were not influenced by the loss of cIAP1 and cIAP2 (Figure 31).

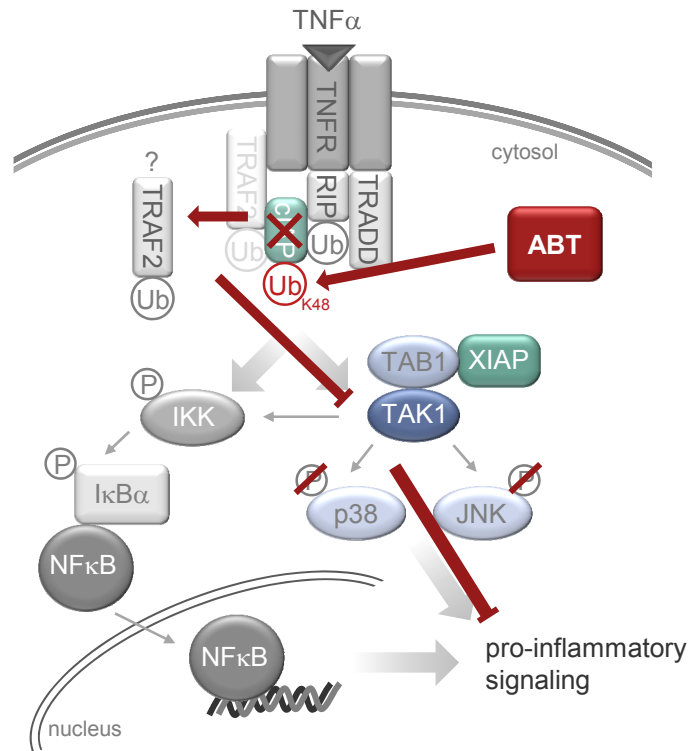


Figure 31 Effects of ABT on TNF α -induced inflammatory signaling in endothelial cells.

In conclusion:

1. We, for the first time, discovered a profound **anti-inflammatory potential** of an **IAP antagonist** *in vivo* and *in vitro*.
2. Our work highlights **IAPs as regulators in inflammatory processes**, i.e.: in leukocyte endothelium interactions and of endothelial activation.

6 ANP

Atrial natriuretic peptide (ANP), a hormone firstly found to be produced in the cardiac atria, plays a role in the regulation of natriuresis, diuresis and vasodilation and therefore contributes to cardiovascular homeostasis. In the last years it has been shown that diverse tissues express receptors for ANP or produce ANP. For example several components of the immune system are influenced by ANP like polymorphonuclear cells, macrophages or the endothelial cells.¹⁵⁴ The endothelium is, besides its functions in cardiovascular homeostasis, an important player in the regulation of immune response in inflammatory processes. Kiemer *et al.* found that ANP reduces inflammation-induced activation of endothelial cells.¹⁵⁵ Moreover, a protective effect on the endothelial barrier function of TNF α -activated endothelial cells was reported.¹⁵⁶

Since the underlying molecular mechanisms of the barrier protective effect of ANP were not known, we aimed at investigating the actions of ANP on histamine-induced hyperpermeability.

At first we proofed that ANP significantly inhibits vascular leakage *in vivo*. Our *in vitro* assays demonstrated that ANP modulates the barrier disrupting effects of histamine by an inhibition of adhesion junction disassembly and by a reduction of cell contraction. Moreover, we could determine the receptor subtype by which the ANP-caused barrier protective effects were mediated

Thus, our results highlighted ANP as a barrier-protecting agent that directly targets key regulators of endothelial permeability and therefore might open a novel therapeutic strategy for inflammatory diseases.

This study was completed in 2007 and published in 2008 as an accelerated communication in *Mol Pharmacol.*:

Atrial natriuretic peptide protects against histamine-induced endothelial barrier dysfunction *in vivo*. Robert Fürst, Martin F. Bubik, Peter Bihari, Bettina A. Mayer, Alexander G. Khandoga, Florian Hoffmann, Markus Rehberg, Fritz Krombach, Stefan Zahler and Angelika M. Vollmar. *Mol Pharmacol.* 2008;74(1):1-8.

Recent publications strongly confirm our findings about the barrier protective effect of ANP as an inhibitor of the contractile machinery and a protector of adhesion junctions.^{157, 158}

The manuscript of our study is subsequently added.

Atrial natriuretic peptide protects against histamine-induced endothelial barrier dysfunction *in vivo*

Robert Fürst, Martin F. Bubik, Peter Bihari, Bettina A. Mayer, Alexander G. Khandoga, Florian Hoffmann, Markus Rehberg, Fritz Krombach, Stefan Zahler, and Angelika M. Vollmar

Department of Pharmacy, Pharmaceutical Biology, University of Munich, Germany (R.F., M.F.B., B.A.M., F.H., S.Z., A.M.V.); Institute for Surgical Research, University of Munich, Germany (P.B., A.G.K., M.R., F.K.)

Running title: ANP protects against endothelial barrier dysfunction in vivo

Address all correspondence to:

Robert Fürst, Ph.D.

Department of Pharmacy, Pharmaceutical Biology, University of Munich

Butenandtstr. 5-13, 81377 Munich, Germany

Phone: +49-89-2180-77189; Fax: +49-89-2180-77170

E-mail: robert.fuerst@cup.uni-muenchen.de

Number of text pages: 21

Number of tables: 0

Number of figures: 4

Number of references: 30

Number of words in the *Abstract*: 216

Number of words in the *Introduction*: 441

Number of words in the *Discussion*: 1,140

Nonstandard abbreviations: AJ, adherens junctions; ANP, atrial natriuretic peptide; NPR, natriuretic peptide receptor; VE-cadherin, vascular endothelial-cadherin; MLC myosin light chain; HUVEC, human umbilical vein endothelial cells; MCP, monocyte chemoattractant protein; VEGF, vascular endothelial growth factor; MAPK, mitogen-activated protein kinase.

Abstract

Endothelial barrier dysfunction is a hallmark of many severe pathologies including sepsis or atherosclerosis. The cardiovascular hormone atrial natriuretic peptide (ANP) has increasingly been suggested to counteract endothelial leakage. Surprisingly, the precise *in vivo* relevance of these observations has never been evaluated. Thus, we aimed to clarify this issue and, moreover, to identify the permeability-controlling subcellular systems that are targeted by ANP. Histamine was used as important pro-inflammatory, permeability-increasing stimulus. Measurements of FITC-dextran extravasation from venules of the mouse cremaster muscle and rat hematocrit values were performed to judge changes of endothelial permeability *in vivo*. Importantly, ANP strongly reduced the histamine-evoked endothelial barrier dysfunction *in vivo*. *In vitro*, ANP blocked the breakdown of transendothelial electrical resistance (TEER) induced by histamine. Moreover, as judged by immunocytochemistry and Western blot analysis, ANP inhibited changes of vascular endothelial (VE)-cadherin, β -catenin, and p120^{ctn} morphology, VE-cadherin and myosin light chain 2 (MLC2) phosphorylation, and F-actin stress fiber formation. These changes seem to be predominantly mediated by the natriuretic peptide receptor (NPR)-A, but not by NPR-C. In summary, we revealed ANP as a potent endothelial barrier protecting agent *in vivo* and identified adherens junctions and the contractile apparatus as subcellular systems targeted by ANP. Thus, our study highlights ANP as an interesting pharmacological compound opening new therapeutic options for preventing endothelial leakage.

Introduction

The endothelium crucially participates in the regulation of important physiological functions, such as blood pressure, coagulation, or host defense, and it represents a barrier that controls the passage of cells, macromolecules, and fluid between the blood and the adjacent tissue interstitium. Beyond its physiological role, the endothelium is also involved in pathological conditions: Endothelial barrier dysfunction is a hallmark of inflammatory processes and still poses an important therapeutical challenge, since a causal pharmacological treatment is as yet widely lacking.

Endothelial barrier function is mainly governed by the balance between interendothelial cell adhesion. Adherens junctions (AJs) are important subcellular structures responsible for endothelial cell-cell attachment and they represent multiprotein complexes that consist of vascular endothelial (VE)-cadherin, β -catenin, and p120^{ctn}. Under inflammatory conditions VE-cadherin junctions disassemble, thus facilitating paracellular passage, and show an increased tyrosine phosphorylation. Endothelial cell retraction is caused by the activation of the contractile machinery, i.e. the interaction between actin and myosin, which is controlled by phosphorylation of the myosin light chain (MLC). These two regulatory systems could be targets of a successful therapeutic principle.

The cardiovascular hormone atrial natriuretic peptide (ANP) is secreted by the cardiac atria as response to an increased plasma volume. In general, ANP binds to the guanylate cyclase-coupled natriuretic peptide receptor (NPR)-A and NPR-C, which lacks guanylate cyclase function. ANP exerts a hypotensive effect by its natriuretic, diuretic, and vasodilating action. The role of ANP as an important regulator of the cardiovascular system is highlighted by the fact that ANP (carperitide, HANP[®]) has been approved as drug for the treatment of acute heart failure in Japan. Recently, however, ANP has been recognized to possess important additional functions beyond blood pressure regulation: ANP is expressed by macrophages and is able to influence these immune cells by attenuating their inflammatory response (Kiemer and Vollmar, 2001). Most importantly, ANP exerts anti-inflammatory properties in the endothelium (Kiemer et al., 2005). Thus, we posed the working hypothesis that ANP could open new therapeutical options for protecting against endothelial barrier dysfunction. In fact, some evidence is given from *in vitro* and *ex vivo* experiments that ANP influences an inflammation-increased permeability (Kiemer et al., 2002a; Lofton et al., 1991; Inomata et al., 1987). However, data precisely demonstrating a beneficial effect of administered ANP on inflammation-induced endothelial barrier dysfunction *in vivo* are lacking. Moreover, data concerning the effect of ANP on subcellular systems that control permeability are missing.

Therefore, aim of the study was (i) to examine the *in vivo* potential of ANP as pharmacological agent counteracting endothelial leakage and (ii) to investigate the influence of ANP on key regulators of endothelial permeability, i.e. the endothelial cell adhesion (VE-cadherin) and contraction system (MLC).

Materials and Methods

Measurement of vascular permeability in the mouse cremaster muscle *in vivo*. Male C57BL/6NCrl mice (Charles River, Sulzfeld, Germany) with 23-25 g bodyweight were used. All experiments were performed according to the German legislation for the protection of animals. Surgery was performed as described by Baez (Baez, 1973). Vascular permeability was analyzed according to Hatakeyama *et al.* (Hatakeyama *et al.*, 2006). Briefly, mice were anesthetized *i.p.* using a ketamine (Pfizer, Karlsruhe, Germany)/xylazine (Bayer, Leverkusen, Germany) mixture. Fluorescein isothiocyanate-dextran (150 kDa, Sigma-Aldrich, Taufkirchen, Germany), Ringer solution (control) and ANP (bolus sufficient to reach 200 nM plasma concentration, AnaSpec/MoBiTec, Göttingen, Germany) were applied into the left femoral artery. 20 min after ANP application, the cremaster was superfused with histamine (30 μ M, Sigma-Aldrich) for 10 min. Dexamethasone 21-phosphate (disodium salt, Sigma-Aldrich) was administered *i.p.* (10 mg/kg bodyweight) 2 h before histamine. Postcapillary venules with diameters of 18-30 μ m were analyzed. Ten regions of interests (50x50 μ m²) in the interstitial tissue (approx. 50 μ m distant from the venule) were randomly selected. Intravital microscopic images were recorded with an IMAGO S/N 382KLO345 CCD-camera (TILL Photonics, Gräfelfing, Germany) and subjected to digital image analysis (TILLvisiON 4.0, TILL Photonics).

Measurement of rat hematocrit. Male Sprague-Dawley rats (Charles River) with 190-240 g bodyweight were used. All experiments were performed according to the German legislation for the protection of animals. Rats were anesthetized *i.p.* using a fentanyl (Jansen-Cilag, Neuss, Germany)/midazolam (Ratiopharm, Ulm, Germany) mixture and anesthesia was maintained by 1.5% isoflurane (Abbott, Wiesbaden, Germany). Rats were pre-treated for 15 min with ANP (bolus sufficient to reach 200 nM plasma concentration) or PBS, followed by histamine (bolus sufficient to reach 1 μ M plasma concentration). Reagents were applied into the jugular vein. 30 min after administration of histamine, blood samples were collected *via* a jugular artery catheter and hematocrit was determined by centrifugation in hematocrit capillaries.

Cell culture. Human umbilical vein endothelial cells (HUVECs) were prepared as previously described (Kiemer *et al.*, 2002a) and cultured in Endothelial Cell Growth Medium (Provitro, Berlin, Germany) containing 10% FBS (Biochrom, Berlin, Germany). Cells were used for experiments at passages 1-3.

Measurement of transendothelial electric resistance (TEER). HUVECs were cultured on collagen A (Biochrom)-coated Millicell 12 mm PCF inserts (Millipore, Schwalbach, Germany). TEER measurements were performed with an Ussing-type chamber. The incubation fluid (HEPES-buffer containing 10% FBS) was circulated by means of humidified air streams at 37°C. A custom-built voltage/current clamp unit in connection with a computer-aided evaluation program was used. Bidirectional square current pulses of 50 μ A and 200 ms duration were applied across the monolayer every 2 second. The resistance of the monolayer was calculated by Ohm's law from the induced deflection of the transendothelial voltage.

Immunocyto/histochemistry and confocal laser scanning fluorescence microscopy. HUVECs were cultured on collagen-treated μ -Slides (ibidi, Martinsried, Germany). The NPR-A/B antagonist HS-142-1 (Morishita *et al.*, 1991) was kindly provided by Dr. Y. Matsuda, Kyowa Hakko Kogyo Co., Ltd. (Shizuoka, Japan). cANP was from Bachem (Weil am Rhein, Germany). HUVECs and samples of the mouse cremaster muscle (immediately dissected after histamine treatment) were analyzed immunocyto/ histochemically and by confocal fluorescence microscopy as previously described (Fürst *et al.*, 2005). The following antibodies and reagents were used: mouse monoclonal anti-VE-cadherin (Santa Cruz, Heidelberg, Germany), rabbit polyclonal anti-phospho-Tyr⁷³¹-VE-cadherin (Biosource/Invitrogen, Karlsruhe, Germany), rabbit

polyclonal anti-phospho-MLC2 (Thr¹⁸/Ser¹⁹) (Cell Signaling/New England Biolabs, Frankfurt a. M., Germany), rhodamine phalloidin (Invitrogen, Karlsruhe, Germany), Alexa Fluor 633-linked goat anti-mouse (Invitrogen), and Alexa Fluor 488-linked goat anti-rabbit (Invitrogen).

Western blot analysis. HUVEC were cultured in collagen-treated 6-well plates or 60 mm-dishes. Western blot analysis was performed as previously described (Kiemer et al., 2002a). The following antibodies were used: rabbit polyclonal anti-phospho-Tyr⁷³¹-VE-cadherin (Biosource), mouse monoclonal anti-VE-cadherin (Santa Cruz), rabbit polyclonal anti-phospho-MLC2 (Thr¹⁸/Ser¹⁹) (Cell Signaling), and MLC2 (Santa Cruz).

Statistical analysis. Statistical analysis was performed with the GraphPad Prism software version 3.03 (GraphPad Software, San Diego, CA). Unpaired *t* test was used to compare two groups. To compare three or more groups, one-way ANOVA followed by Newman-Keuls post hoc test was used.

Results

ANP protects against an inflammation-impaired endothelial barrier function *in vivo*. To judge endothelial permeability *in vivo*, we measured the extravasation of FITC-dextran (150 kDa) *via* intravital fluorescence microscopy in postcapillary venules of the mouse cremaster muscle. 20 min after *i.a.*-application of ANP (bolus sufficient to reach 200 nM plasma concentration), histamine (30 μ M) was superfused for 10 min. Histamine evoked a strong leak of FITC-dextran from the blood into the adjacent tissue. ANP clearly abrogated the histamine-induced extravasation (Figure 1A, upper panel). Movies of this extravasation are presented as supplemental data (movie1: control; movie2: histamine; movie3: ANP+histamine). ANP alone (at least in the observed 20 min pre-treatment) seems to slightly increase basal permeability (please note the different ordinate scales in Figure 1A), but this effect is statistically not significant (Figure 1A, lower left panel). Moreover, we aimed to appraise the therapeutical impact of ANP by comparing its beneficial effect to that of a strong anti-inflammatory drug. Thus, we treated mice with a high dose of dexamethasone (*i.p.*, 10 mg/kg, 2 h) before applying histamine (30 μ M). The glucocorticoid completely prevented the histamine-induced extravasation of FITC-dextran.

As a second approach for detecting changes of endothelial permeability *in vivo*, we measured hematocrit levels. Rats were treated with histamine (*i.v.* bolus sufficient to reach 1 μ M plasma concentration) and hematocrit was determined after 30 min. Due to a reduction of plasma volume, i.e. augmented fluid extravasation, histamine evoked a strong hematocrit increase. ANP (bolus injection sufficient to reach 200 nM plasma concentration, 15 min pre-treatment) significantly reduced the permeability-increasing effect of histamine (Figure 1B).

Characterization of the barrier protecting effect of ANP *in vitro*. Data about an influence of ANP on histamine-induced endothelial leakage *in vitro* are completely lacking. Thus, we first aimed to verify the effect of ANP in human umbilical vein endothelial cells (HUVECs). To judge permeability changes, transendothelial electrical resistance (TEER) was measured. Upon applying histamine, the electrical resistance of a HUVEC monolayer rapidly drops within seconds and recovers after approx. 10 min. The extent of this effect depends on the histamine concentration used: the resistance is lowered to 55% by 10 μ M and to 85% by 1 μ M histamine (Figure 1C, left). ANP (1 μ M, 30 min pre-treatment) attenuates the drop-down of electrical resistance evoked by histamine (Figure 1C, middle). The statistic analysis of all experiments (*n* = 4) performed is depicted in the right panel of Figure 1C. The large variability of the ANP+histamine group expresses the fact that in 2 of the 4 experiments ANP did not only attenuate the effect of histamine, but even increased the endothelial resistance, i.e. led to a less permeable endothelium, even if compared to the basal resistance under control conditions. In summary, ANP strongly alleviates endothelial barrier dysfunction induced by histamine *in vitro*. This warrants the usage of this system for the following investigations into the action of ANP on adherens junctions and the contractile machinery.

ANP abolishes the histamine-evoked changes of adherens junction morphology and inhibits the histamine-induced VE-cadherin tyrosine phosphorylation. Histamine (1 μ M)

leads to strong changes of AJ morphology: the VE-cadherin, β -catenin, and p120^{ctn} seam, properly build in untreated endothelial cells (control), becomes fringy, indicating an AJ disassembly, i.e. the retraction of the inter-endothelial VE-cadherin homodimers and/or an intramembranous lateral shift (Figure 2 A-C). Endothelial cells treated with ANP alone did not show any effect on AJs. Most importantly, ANP (1 μ M, 30 min pretreatment) clearly abolishes the detrimental effects induced by histamine (Figure 2, A-C).

To clarify which natriuretic peptide receptor is involved in mediating the beneficial actions of ANP, we treated cells with the NPR-A/B antagonist HS-142-1 (10 μ g/ml, 10 min before ANP) and found that the effects on VE-cadherin disassembly were prevented by this inhibitor. The NPR-C receptor agonist cANF (1 μ M, 30 min before histamine) was not able to mimic the effects of ANP (Figure 2A). Compared to NPR-B, NPR-A binds ANP with a much higher affinity. Thus, our results suggest that the action of ANP is mainly transduced by NPR-A. The C-receptor seems not to be involved.

Phosphorylation of the VE-cadherin Tyr⁷³¹ residue is associated with AJ disassembly and strong endothelial leakage *in vitro* (Potter et al., 2005). First, we verified that Tyr⁷³¹ is also phosphorylated by histamine *in vivo*: Vessels of the mouse cremaster muscle show a strong increase of Tyr⁷³¹ phosphorylation induced by histamine (30 μ M, 10 min, Figure 3A) and the same pronounced localization at cell fringes (Figure 3A, longitudinal vessel section) as in the *in vitro* situation (Figure 3B). Most importantly, as shown both by microscopic (Figure 3B) and by Western blot analysis (Figure 3C), ANP completely blocked the histamine-induced VE-cadherin Tyr⁷³¹ phosphorylation. ANP alone did not evoke any alterations of the phosphorylation (Figure 2B). Our data clearly point towards a protecting effect of ANP on the integrity of endothelial adherens junctions.

ANP reduces the histamine-evoked activation of myosin light chain (MLC) and the formation of F-actin stress fibers. The generation of contractile forces (interaction of actin and myosin) is governed by MLC Thr¹⁸/Ser¹⁹-phosphorylation. Histamine treatment time-dependently leads to a strong phosphorylation of MLC, which was analyzed microscopically (Figure 4A) and by Western blotting (Figure 4B). Moreover, histamine evokes a strong change in F-actin organization. While quiescent endothelial cells show a cortical F-actin localization, histamine induces the formation of long, cell-spanning stress fibers (Figure 4C). ANP clearly reduces both MLC phosphorylation (Figure 4, A and B) and F-actin stress fiber formation (Figure 4C). ANP alone had no effect on these parameters (Figure 4, A-C). These results indicate that ANP prevents histamine-evoked activation of the endothelial cell contraction system.

Furthermore, we investigated which NP receptor subtype was involved in mediating these effects. The NPR-A/B inhibitor HS-142-1 (10 μ g/ml, 10 min before ANP) blocked the effects of ANP on MLC phosphorylation (Figure 4A) and stress fiber formation (Figure 4C). The NPR-C agonist cANF (1 μ M, 30 min) was not able to show beneficial effects (Figure 4, A and C). Thus, NPR-A/B could be regarded as the major receptors for transducing the actions of ANP in our setting.

Discussion

Many severe pathologies like sepsis or atherosclerosis are associated with an inflammation-impaired endothelial barrier function leading to an increased plasma extravasation, and thus edema formation (Volk and Kox, 2000; Poredos, 2001). Proinflammatory mediators, such as TNF- α or histamine, are involved in the pathogenesis of these disorders and are strong inducers of vascular leakage. Current therapies against an inflammation-evoked barrier dysfunction (e.g. the administration of glucocorticoids or antihistamines) are often insufficient or even fail (van Nieuw Amerongen and van Hinsbergh, 2002). Therefore, new therapeutical options are needed. Strong progress has been made in the recent years concerning the mechanisms involved in the regulation of endothelial permeability (Mehta and Malik, 2006). However, substances that counteract an inflammation-induced vascular leakage by specifically influencing these mechanisms are still largely lacking (van Nieuw Amerongen and van Hinsbergh, 2002).

Initially, the physiological action of the cardiovascular hormone ANP, i.e. the reduction of blood pressure, was mainly ascribed to its natriuretic, diuretic, and vasodilating action. However, ANP was also found to increase endothelial permeability (Huxley et al., 1987). Recently, this effect was proven to be crucial for the chronic control of plasma volume by ANP (Sabrane et al., 2005). Beyond these permeability increasing effects on *quiescent* endothelial cells, ANP has increasingly been recognized to possess barrier protecting actions on an inflammation-*activated* endothelium: We could demonstrate that ANP attenuates the TNF- α -induced expression of adhesion molecules and monocyte chemoattractant protein-1 (MCP-1) by inhibiting NF- κ B activation and p38 mitogen-activated protein kinase (MAPK) signaling (Weber et al., 2003; Kiemer et al., 2002b). In this context, we showed that ANP protects against TNF- α -evoked endothelial barrier dysfunction in HUVECs (Kiemer et al., 2002a). ANP was also shown to lower endothelial leakage *in vitro* induced by the pro-inflammatory stimuli thrombin (Baron et al., 1989) and VEGF (Pedram et al., 2002).

Thus, ANP has commonly been suggested to work as a barrier protecting agent. Surprisingly, an obvious question has as yet not been answered precisely: Can ANP be used as pharmacological agent to prevent endothelial barrier dysfunction *in vivo*? This issue is of special interest, since the drug ANP (carperitide, HANP[®]) could open new therapeutical options for protecting endothelial barrier function. In the present study, we for the first time show that ANP administered at a pharmacological concentration is able to prevent endothelial leakage in a (histamine-induced) inflammatory setting *in vivo*. Different aspects of endothelial permeability were used as read-out parameters and were all beneficially influenced by ANP: macromolecular permeability (FITC-dextran extravasation), plasma volume/fluid changes (hematocrit), and electrical resistance (TEER measurement). Compared to the maximal increase of FITC-dextran extravasation induced by histamine (time point 45 min in Figure 1A), ANP led to approx. 65% reduction. Due to this pronounced effect, a therapeutical impact of ANP is not unlikely. A complete blockage of the deleterious effect of histamine was observed in the presence of an extraordinary high dosage of the glucocorticoid dexamethasone, a highly potent anti-inflammatory drug.

Former studies dealing with ANP and vascular permeability served as valuable hints toward an *in vivo* relevance of ANP as barrier protecting agent. However, these reports did not concisely test the hypothesis that administered ANP exerts beneficial effects on endothelial barrier dysfunction *in vivo*, because they (i) either used *ex vivo* models or (ii) focused on the *endogenous* ANP system: (i) Three older reports demonstrate that pharmacological concentrations of ANP attenuate changes of pulmonary wet weight induced by toxic agents like reactive oxygen metabolites, paraquat, or arachidonic acid in *ex vivo* models of isolated-perfused lungs from rabbits or guinea pigs (Lofton et al., 1991; Inomata et al., 1987; Imamura et al., 1988). (ii) Blockade of *endogenous* ANP was shown to deteriorate pulmonary edema formation in rats suffering from high altitude-induced (Irwin et al., 2001) or HCl-evoked (Wakabayashi et al., 1990) pulmonary vascular leakage, whereas mice lacking the major ANP-degrading enzyme neutral endopeptidase were found to be less susceptible for pulmonary leakage (Irwin et al., 2005a). Interestingly, Pedram *et al.* showed that VEGF-induced vascular leakage is attenuated in ANP-overexpressing mice, whereas these mice are not protected against histamine-evoked leakage (Pedram et al., 2002). This might be due to the much lower ANP levels in these animals (plasma level: ~40 pM) compared to our setting, in which ANP is exogenously supplied to reach a pharmacological plasma concentration of 200 nM. Recently, our group could demonstrate that ANP-treated mice (plasma level: ~35 nM) are protected against LPS-induced septic shock (Ladetzki-Baehs et al., 2007). Since endothelial hyperpermeability is an important pathological feature of sepsis, it can be speculated that the barrier protecting effect of ANP contributes to the beneficial action in the mouse septic shock model. Our results suggest that pharmacological concentrations of ANP show additional, highly valuable effects beyond its action as an endogenous regulator of permeability.

Adherens junctions and the contractile apparatus are key players in the regulation of endothelial permeability. Both the loss of VE-cadherin function and the activation of MLC result in decreased transendothelial electrical resistance (Garcia et al., 1997; van Buul et al., 2005) and increased macromolecular permeability (Nwariaku et al., 2002; Garcia et al., 1995). Studies investigating the action of ANP on these key systems are as yet completely lacking. We provide for the first time evidence that ANP interacts with these systems, since we showed that ANP attenuates both adherens junction disassembly (morphological changes and Tyr⁷³¹

phosphorylation of VE-cadherin) and activation of the contractile apparatus (phosphorylation of MLC and rearrangement of F-actin) induced by histamine. Furthermore, we could demonstrate that ANP exerts these effects predominantly via the natriuretic peptide receptor (NPR)-A. Since these receptors represent particulate guanylate cyclases, it can be speculated that the actions of ANP might be mediated via the second messenger cyclic guanosine monophosphate (cGMP). Our results add further support to the hypothesis that ANP is an endothelium protecting agent, since it directly counteracts the detrimental effects of proinflammatory mediators on endothelial barrier function.

Only few data exist about the action of ANP on subcellular systems contributing to permeability regulation. We and others could demonstrate that ANP inhibits F-actin stress fiber formation induced by TNF- α (Kierner et al., 2002a; Irwin et al., 2005b) or VEGF (Pedram et al., 2002). Interestingly, one study reports that ANP influences tight junctions in bovine aortic endothelial cells (Pedram et al., 2002). In contrast to the dense aortic endothelium, the occurrence of tight junctions is limited in the venous endothelium (Ogunrinade et al., 2002), which represents the predominant site of endothelial hyperpermeability and was investigated in the present study.

In summary, we have revealed ANP as a potent endothelial barrier protecting agent *in vivo*. Moreover, we have identified adherens junctions and the contractile apparatus as important subcellular systems targeted by ANP. Most importantly, our study highlights ANP as an interesting pharmacological compound opening a new therapeutic option for the prevention of vascular leakage. This warrants further efforts aiming for an expansion of the therapeutic indications of natriuretic peptides.

References

- Baez S (1973) An Open Cremaster Muscle Preparation for the Study of Blood Vessels by *in Vivo* Microscopy. *Microvasc Res* **5**:384-394.
- Baron DA, Lofton CE, Newman WH and Currie MG (1989) Atriopeptin Inhibition of Thrombin-Mediated Changes in the Morphology and Permeability of Endothelial Monolayers. *Proc Natl Acad Sci U S A* **86**:3394-3398.
- Fürst R, Brueckl C, Kuebler WM, Zahler S, Krötz F, Görlach A, Vollmar AM and Kierner AK (2005) Atrial Natriuretic Peptide Induces Mitogen-Activated Protein Kinase Phosphatase-1 in Human Endothelial Cells Via Rac1 and NAD(P)H Oxidase/Nox2-Activation. *Circ Res* **96**:43-53.
- Garcia JG, Davis HW and Patterson CE (1995) Regulation of Endothelial Cell Gap Formation and Barrier Dysfunction: Role of Myosin Light Chain Phosphorylation. *J Cell Physiol* **163**:510-522.
- Garcia JG, Schaphorst KL, Shi S, Verin AD, Hart CM, Callahan KS and Patterson CE (1997) Mechanisms of Ionomycin-Induced Endothelial Cell Barrier Dysfunction. *Am J Physiol* **273**:L172-L184.
- Hatakeyama T, Pappas PJ, Hobson RW, Boric MP, Sessa WC and Duran WN (2006) Endothelial Nitric Oxide Synthase Regulates Microvascular Hyperpermeability *in Vivo*. *J Physiol* **574**:275-281.
- Huxley VH, Tucker VL, Verburg KM and Freeman RH (1987) Increased Capillary Hydraulic Conductivity Induced by Atrial Natriuretic Peptide. *Circ Res* **60**:304-307.
- Imamura T, Ohnuma N, Iwasa F, Furuya M, Hayashi Y, Inomata N, Ishihara T and Noguchi T (1988) Protective Effect of Alpha-Human Atrial Natriuretic Polypeptide (Alpha-HANP) on Chemical-Induced Pulmonary Edema. *Life Sci* **42**:403-414.
- Inomata N, Ohnuma N, Furuya M, Hayashi Y, Kanai Y, Ishihara T, Noguchi T and Matsuo H (1987) Alpha-Human Atrial Natriuretic Peptide (Alpha-HANP) Prevents Pulmonary Edema Induced by Arachidonic Acid Treatment in Isolated Perfused Lung From Guinea Pig. *Jpn J Pharmacol* **44**:211-214.
- Irwin DC, Patot MT, Tucker A and Bowen R (2005a) Neutral Endopeptidase Null Mice Are Less Susceptible to High Altitude-Induced Pulmonary Vascular Leak. *High Alt Med Biol* **6**:311-319.
- Irwin DC, Rhodes J, Baker DC, Nelson SE and Tucker A (2001) Atrial Natriuretic Peptide Blockade Exacerbates High Altitude Pulmonary Edema in Endotoxin-Primed Rats. *High Alt Med Biol* **2**:349-360.

- Irwin DC, Tissot van Patot MC, Tucker A and Bowen R (2005b) Direct ANP Inhibition of Hypoxia-Induced Inflammatory Pathways in Pulmonary Microvascular and Macrovascular Endothelial Monolayers. *Am J Physiol Lung Cell Mol Physiol* **288**:L849-L859.
- Kiemer AK, Fürst R and Vollmar AM (2005) Vasoprotective Actions of the Atrial Natriuretic Peptide. *Curr Med Chem Cardiovasc Hematol Agents* **3**:11-21.
- Kiemer AK and Vollmar AM (2001) The Atrial Natriuretic Peptide Regulates the Production of Inflammatory Mediators in Macrophages. *Ann Rheum Dis* **60 Suppl 3**:iii68-iii70.
- Kiemer AK, Weber NC, Fürst R, Bildner N, Kulhanek-Heinze S and Vollmar AM (2002a) Inhibition of P38 MAPK Activation Via Induction of MKP-1: Atrial Natriuretic Peptide Reduces TNF- α -Induced Actin Polymerization and Endothelial Permeability. *Circ Res* **90**:874-881.
- Kiemer AK, Weber NC and Vollmar AM (2002b) Induction of I κ B: Atrial Natriuretic Peptide As a Regulator of the NF- κ B Pathway. *Biochem Biophys Res Commun* **295**:1068-1076.
- Ladetzki-Baehs K, Keller M, Kiemer AK, Koch E, Zahler S, Wendel A and Vollmar AM (2007) Atrial Natriuretic Peptide, a Regulator of Nuclear Factor- κ B Activation in Vivo. *Endocrinology* **148**:332-336.
- Lofton CE, Baron DA, Heffner JE, Currie MG and Newman WH (1991) Atrial Natriuretic Peptide Inhibits Oxidant-Induced Increases in Endothelial Permeability. *J Mol Cell Cardiol* **23**:919-927.
- Mehta D and Malik AB (2006) Signaling Mechanisms Regulating Endothelial Permeability. *Physiol Rev* **86**:279-367.
- Morishita Y, Sano T, Ando K, Saitoh Y, Kase H, Yamada K and Matsuda Y (1991) Microbial Polysaccharide, HS-142-1, Competitively and Selectively Inhibits ANP Binding to Its Guanylyl Cyclase-Containing Receptor. *Biochem Biophys Res Commun* **176**:949-957.
- Nwariaku FE, Liu Z, Zhu X, Turnage RH, Sarosi GA and Terada LS (2002) Tyrosine Phosphorylation of Vascular Endothelial Cadherin and the Regulation of Microvascular Permeability. *Surgery* **132**:180-185.
- Ogunrinade O, Kameya GT and Truskey GA (2002) Effect of Fluid Shear Stress on the Permeability of the Arterial Endothelium. *Ann Biomed Eng* **30**:430-446.
- Pedram A, Razandi M and Levin ER (2002) Deciphering Vascular Endothelial Cell Growth Factor/Vascular Permeability Factor Signaling to Vascular Permeability. Inhibition by Atrial Natriuretic Peptide. *J Biol Chem* **277**:44385-44398.
- Poredos P (2001) Endothelial Dysfunction in the Pathogenesis of Atherosclerosis. *Clin Appl Thromb Hemost* **7**:276-280.
- Potter MD, Barbero S and Cheresh DA (2005) Tyrosine Phosphorylation of VE-Cadherin Prevents Binding of P120- and Beta-Catenin and Maintains the Cellular Mesenchymal State. *J Biol Chem* **280**:31906-31912.
- Sabrane K, Kruse MN, Fabritz L, Zetsche B, Mitko D, Skryabin BV, Zwiener M, Baba HA, Yanagisawa M and Kuhn M (2005) Vascular Endothelium Is Critically Involved in the Hypotensive and Hypovolemic Actions of Atrial Natriuretic Peptide. *J Clin Invest* **115**:1666-1674.
- van Buul JD, Anthony EC, Fernandez-Borja M, BurrIDGE K and Hordijk PL (2005) Proline-Rich Tyrosine Kinase 2 (Pyk2) Mediates Vascular Endothelial-Cadherin-Based Cell-Cell Adhesion by Regulating Beta-Catenin Tyrosine Phosphorylation. *J Biol Chem* **280**:21129-21136.
- van Nieuw Amerongen GP and van Hinsbergh VW (2002) Targets for Pharmacological Intervention of Endothelial Hyperpermeability and Barrier Function. *Vascul Pharmacol* **39**:257-272.
- Volk T and Kox WJ (2000) Endothelium Function in Sepsis. *Inflamm Res* **49**:185-198.
- Wakabayashi G, Ueda M, Aikawa N, Naruse M and Abe O (1990) Release of ANP and Its Physiological Role in Pulmonary Injury Due to HCl. *Am J Physiol* **258**:R690-R696.
- Weber NC, Blumenthal SB, Hartung T, Vollmar AM and Kiemer AK (2003) ANP Inhibits TNF- α -Induced Endothelial MCP-1 Expression - Involvement of P38 MAPK and MKP-1. *J Leukoc Biol* **74**:932-941.

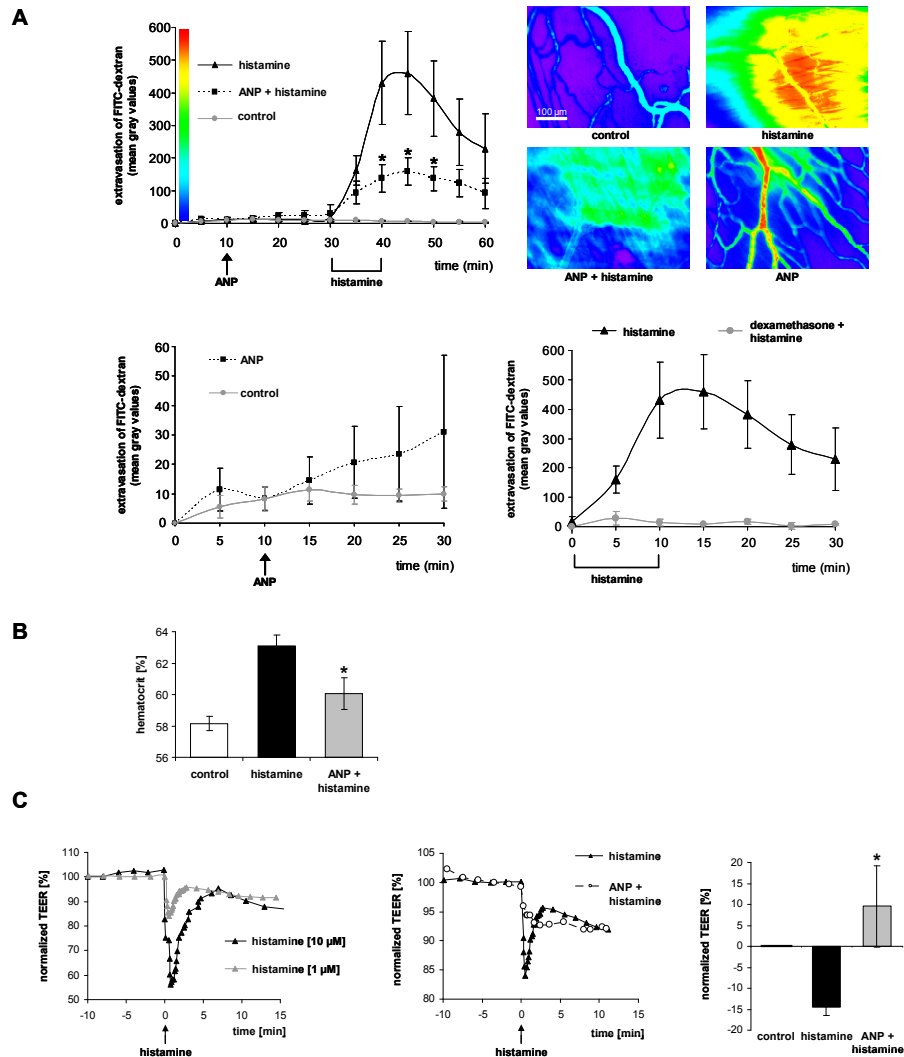


Figure 1. ANP attenuates histamine-induced increase of endothelial permeability *in vivo* and *in vitro*. **A**, Extravasation of FITC-dextran (150 kDa) from venules of the mouse cremaster muscle was measured. Upper left panel: Mice were pre-treated with Ringer solution (control and histamine group), or with ANP (*i.a.* bolus injection sufficient to reach 200 nM plasma concentration). After 20 min, histamine (30 μ M) was superfused for 10 min (histamine and ANP+histamine group). Data are expressed as mean \pm SEM ($n = 6$). $p < 0.05$ vs. histamine. Upper right panel: One representative image is shown for each group of treatment (at time point 45 min for control, histamine, and histamine+ANP; at time point 30 min for ANP alone). Videos showing this FITC-dextran extravasation (movie1: control; movie2: histamine; movie3: ANP+histamine) are available as supplemental data. Lower left panel: Mice were treated with Ringer solution (control group) or with ANP (*i.a.* bolus injection sufficient to reach 200 nM plasma concentration). Data are expressed as mean \pm SEM ($n = 6$). Lower right panel: Mice were pre-treated with Ringer solution (histamine group) or with dexamethasone (*i.p.*, 10 mg/kg bodyweight) for 2 h. Histamine (30 μ M) was superfused for 10 min. Data are expressed as mean \pm SEM ($n = 2$). **B**, Plasma volume changes were determined by measuring hematocrit values. Rats were pre-treated with PBS (control) or with ANP (*i.v.*, bolus injection sufficient to reach 200 nM plasma concentration). After 15 min, histamine was applied (*i.v.*, bolus injection sufficient to reach 1 μ M plasma concentration). 30 min later, blood samples were taken and hematocrit was measured. Data are expressed as mean \pm SEM ($n = 3$). $p < 0.05$ vs. histamine. **C**, Transendothelial electrical resistance (TEER) was used to judge changes in endothelial permeability of HUVECs. Left panel: Histamine concentration-dependently decreases TEER values. Middle panel: ANP (1 μ M, 30 min pre-treatment) attenuates the histamine-induced decrease of electrical resistance. One representative graph out of 4 independent experiments is shown, each. Right panel: Statistical analysis of all experiments performed ($n = 4$). Data are expressed as mean \pm SEM. $p < 0.05$ vs. histamine.

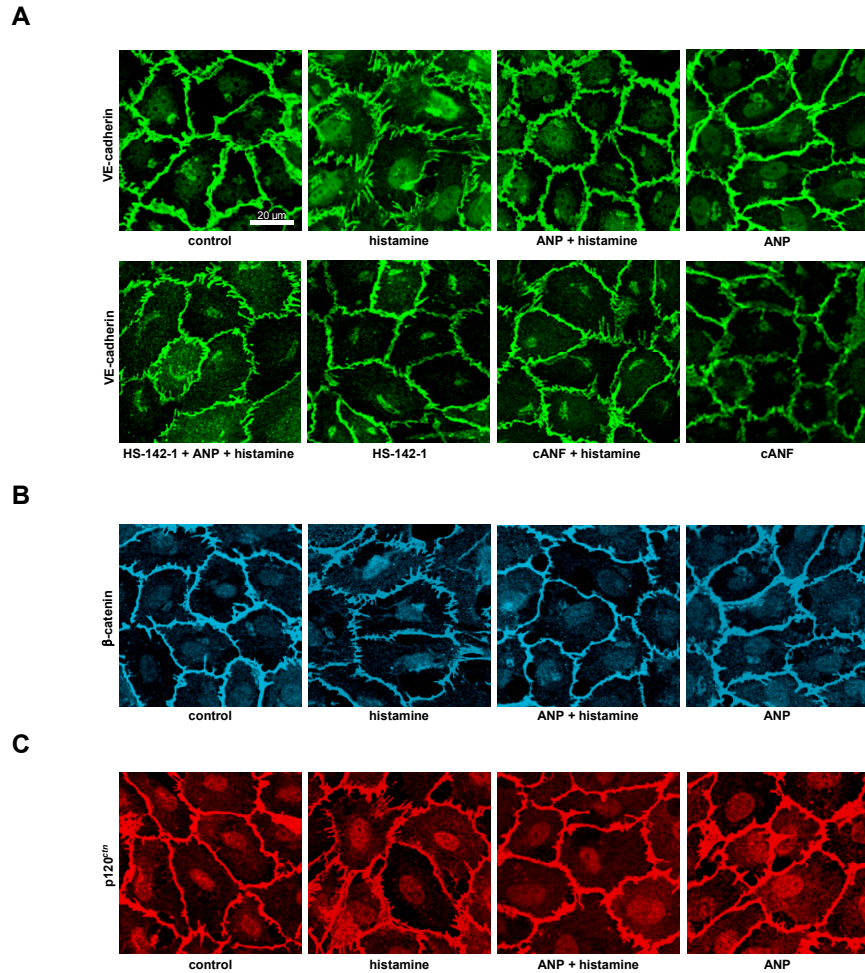


Figure 2. ANP inhibits the histamine-evoked morphological changes of adherens junctions. HUVECs were left untreated (control) or were treated with histamine (1 μ M, 2 min) alone or in combination with ANP (1 μ M, 30 min pre-treatment) or the NPR-C agonist cANF (1 μ M, 30 min pre-treatment). The NPR-A/B receptor antagonist HS142-1 (10 μ g/ml) was given 10 min before ANP. Immunocytochemistry and confocal fluorescence microscopy were performed to analyze morphological changes of (A) VE-cadherin, (B) β -catenin, and (C) p120^{cas}. One representative image out of three independent experiments is shown, each.

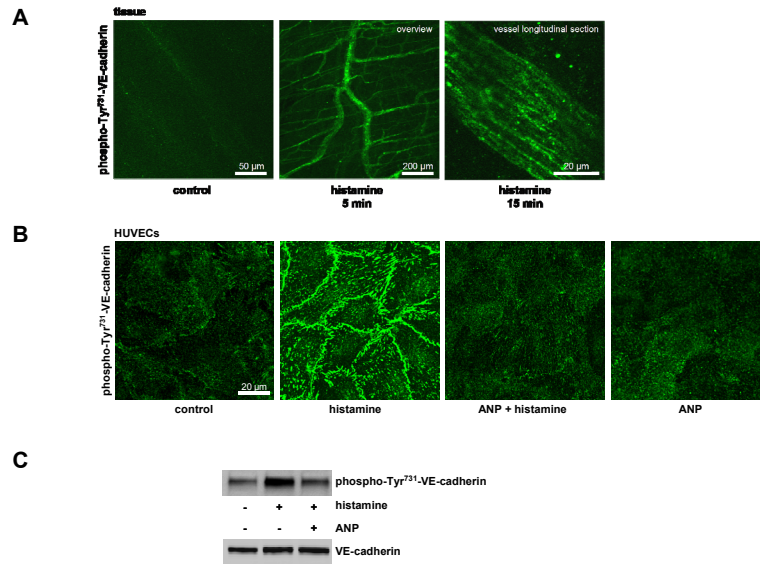


Figure 3. ANP blocks histamine-induced VE-cadherin Tyr⁷³¹-phosphorylation. A, Histamine induces phosphorylation of VE-cadherin at Tyr⁷³¹ *in vivo*. Mice were treated as described in Figure 1A. Samples of the mouse cremaster muscle were analyzed via immunohistochemistry and confocal fluorescence microscopy. Histamine (30 μM) was superfused for the indicated times. One representative image out of 3 independent experiments is shown. B-C, ANP inhibits histamine-induced VE-cadherin Tyr⁷³¹-phosphorylation *in vitro*. HUVECs were left untreated (control), were treated with histamine (1 μM, 5 min) or ANP (1 μM, 30 min) alone, or with ANP (1 μM) 30 min before histamine was applied. The VE-cadherin Tyr⁷³¹-phosphorylation was analyzed via immunocytochemistry and confocal fluorescence microscopy (B, *n* = 3) or biochemically via Western blot (C, *n* = 2).

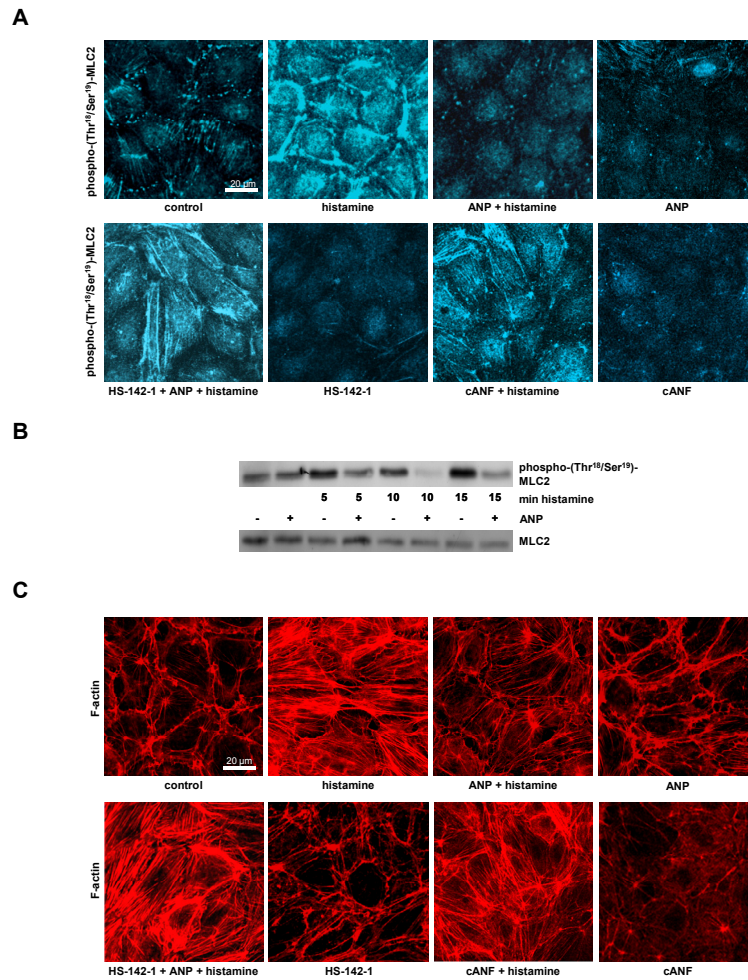


Figure 4. ANP inhibits histamine-induced MLC2 Thr¹⁸/Ser¹⁹-phosphorylation and stress fiber formation. A-C, HUVECs were left untreated (control) or were treated with histamine (1 μ M, 5 min) alone or in combination with ANP (1 μ M, 30 min pre-treatment) or the NPR-C agonist cANF (1 μ M, 30 min pre-treatment). The NPR-A/B receptor antagonist HS142-1 (10 μ g/ml) was given 10 min before ANP. MLC2 Thr¹⁸/Ser¹⁹-phosphorylation and F-actin were analyzed via immunocytochemistry and confocal fluorescence microscopy (A, C). MLC2 Thr¹⁸/Ser¹⁹-phosphorylation was additionally analyzed via Western blot (B). One representative image out of at least three independent experiments is shown, each.

7 REFERENCES

1. Scott FL, Denault JB, Riedl SJ, Shin H, Renatus M, Salvesen GS. XIAP inhibits caspase-3 and -7 using two binding sites: evolutionarily conserved mechanism of IAPs. *EMBO J*. Feb 9 2005;24(3):645-655.
2. Shiozaki EN, Chai J, Rigotti DJ, et al. Mechanism of XIAP-mediated inhibition of caspase-9. *Mol Cell*. Feb 2003;11(2):519-527.
3. Krepela E, Dankova P, Moravcikova E, et al. Increased expression of inhibitor of apoptosis proteins, survivin and XIAP, in non-small cell lung carcinoma. *Int J Oncol*. Dec 2009;35(6):1449-1462.
4. Sung KW, Choi J, Hwang YK, et al. Overexpression of X-linked inhibitor of apoptosis protein (XIAP) is an independent unfavorable prognostic factor in childhood de novo acute myeloid leukemia. *J Korean Med Sci*. Aug 2009;24(4):605-613.
5. Liu Z, Sun C, Olejniczak ET, et al. Structural basis for binding of Smac/DIABLO to the XIAP BIR3 domain. *Nature*. Dec 21-28 2000;408(6815):1004-1008.
6. Oost TK, Sun C, Armstrong RC, et al. Discovery of potent antagonists of the antiapoptotic protein XIAP for the treatment of cancer. *J Med Chem*. Aug 26 2004;47(18):4417-4426.
7. Lu M, Lin SC, Huang YH, et al. XIAP induces NF-kappa B activation via the BIR1/TAB1 interaction and BIR1 dimerization. *Molecular Cell*. Jun 8 2007;26(5):689-702.
8. Varfolomeev E, Wayson SM, Dixit VM, Fairbrother WJ, Vucic D. The inhibitor of apoptosis protein fusion c-IAP2.MALT1 stimulates NF-kappaB activation independently of TRAF1 AND TRAF2. *J Biol Chem*. Sep 29 2006;281(39):29022-29029.
9. Vince JE, Chau D, Callus B, et al. TWEAK-FN14 signaling induces lysosomal degradation of a cIAP1-TRAF2 complex to sensitize tumor cells to TNF alpha. *Journal of Cell Biology*. Jul 14 2008;182(1):171-184.
10. Yang Y, Fang S, Jensen JP, Weissman AM, Ashwell JD. Ubiquitin protein ligase activity of IAPs and their degradation in proteasomes in response to apoptotic stimuli. *Science*. May 5 2000;288(5467):874-877.
11. Bertrand MJ, Milutinovic S, Dickson KM, et al. cIAP1 and cIAP2 facilitate cancer cell survival by functioning as E3 ligases that promote RIP1 ubiquitination. *Mol Cell*. Jun 20 2008;30(6):689-700.
12. Haas TL, Emmerich CH, Gerlach B, et al. Recruitment of the Linear Ubiquitin Chain Assembly Complex Stabilizes the TNF-R1 Signaling Complex and Is Required for TNF-Mediated Gene Induction. *Molecular Cell*. Dec 11 2009;36(5):831-844.
13. Lin SJ, Shyue SK, Hung YY, et al. Superoxide dismutase inhibits the expression of vascular cell adhesion molecule-1 and intracellular cell adhesion molecule-1 induced by tumor necrosis factor-alpha in human endothelial cells

- through the JNK/p38 pathways. *Arterioscler Thromb Vasc Biol.* Feb 2005;25(2):334-340.
14. Lockshin RA, Zakeri Z. Cell death in health and disease. *J Cell Mol Med.* Nov-Dec 2007;11(6):1214-1224.
 15. Fuentes-Prior P, Salvesen GS. The protein structures that shape caspase activity, specificity, activation and inhibition. *Biochem J.* Dec 1 2004;384(Pt 2):201-232.
 16. Ashkenazi A, Dixit VM. Death receptors: signaling and modulation. *Science.* Aug 28 1998;281(5381):1305-1308.
 17. Crook NE, Clem RJ, Miller LK. An apoptosis-inhibiting baculovirus gene with a zinc finger-like motif. *J Virol.* Apr 1993;67(4):2168-2174.
 18. LaCasse EC, Baird S, Korneluk RG, MacKenzie AE. The inhibitors of apoptosis (IAPs) and their emerging role in cancer. *Oncogene.* Dec 24 1998;17(25):3247-3259.
 19. Liston P, Roy N, Tamai K, et al. Suppression of apoptosis in mammalian cells by NAIP and a related family of IAP genes. *Nature.* Jan 25 1996;379(6563):349-353.
 20. Cheung HH, Lynn Kelly N, Liston P, Korneluk RG. Involvement of caspase-2 and caspase-9 in endoplasmic reticulum stress-induced apoptosis: a role for the IAPs. *Exp Cell Res.* Jul 15 2006;312(12):2347-2357.
 21. Silke J, Brink R. Regulation of TNFRSF and innate immune signalling complexes by TRAFs and cIAPs. *Cell Death Differ.* Jan;17(1):35-45.
 22. Duckett CS, Nava VE, Gedrich RW, et al. A conserved family of cellular genes related to the baculovirus iap gene and encoding apoptosis inhibitors. *EMBO J.* Jun 3 1996;15(11):2685-2694.
 23. Rothe M, Pan MG, Henzel WJ, Ayres TM, Goeddel DV. The TNFR2-TRAF signaling complex contains two novel proteins related to baculoviral inhibitor of apoptosis proteins. *Cell.* Dec 29 1995;83(7):1243-1252.
 24. Uren AG, Pakusch M, Hawkins CJ, Puls KL, Vaux DL. Cloning and expression of apoptosis inhibitory protein homologs that function to inhibit apoptosis and/or bind tumor necrosis factor receptor-associated factors. *Proc Natl Acad Sci U S A.* May 14 1996;93(10):4974-4978.
 25. Dubrez-Daloz L, Dupoux A, Cartier J. IAPs: more than just inhibitors of apoptosis proteins. *Cell Cycle.* Apr 15 2008;7(8):1036-1046.
 26. Harlin H, Reffey SB, Duckett CS, Lindsten T, Thompson CB. Characterization of XIAP-deficient mice. *Mol Cell Biol.* May 2001;21(10):3604-3608.
 27. Potts PR, Singh S, Knezek M, Thompson CB, Deshmukh M. Critical function of endogenous XIAP in regulating caspase activation during sympathetic neuronal apoptosis. *J Cell Biol.* Nov 24 2003;163(4):789-799.

28. Potts MB, Vaughn AE, McDonough H, Patterson C, Deshmukh M. Reduced Apaf-1 levels in cardiomyocytes engage strict regulation of apoptosis by endogenous XIAP. *J Cell Biol.* Dec 19 2005;171(6):925-930.
29. Hinds MG, Norton RS, Vaux DL, Day CL. Solution structure of a baculoviral inhibitor of apoptosis (IAP) repeat. *Nat Struct Biol.* Jul 1999;6(7):648-651.
30. Sun C, Cai M, Gunasekera AH, et al. NMR structure and mutagenesis of the inhibitor-of-apoptosis protein XIAP. *Nature.* Oct 21 1999;401(6755):818-822.
31. Mace PD, Shirley S, Day CL. Assembling the building blocks: structure and function of inhibitor of apoptosis proteins. *Cell Death Differ.* Jan;17(1):46-53.
32. Eckelman BP, Salvesen GS. The human anti-apoptotic proteins cIAP1 and cIAP2 bind but do not inhibit caspases. *J Biol Chem.* Feb 10 2006;281(6):3254-3260.
33. Eckelman BP, Salvesen GS, Scott FL. Human inhibitor of apoptosis proteins: why XIAP is the black sheep of the family. *EMBO Rep.* Oct 2006;7(10):988-994.
34. Riedl SJ, Renatus M, Schwarzenbacher R, et al. Structural basis for the inhibition of caspase-3 by XIAP. *Cell.* Mar 9 2001;104(5):791-800.
35. Chai J, Shiozaki E, Srinivasula SM, et al. Structural basis of caspase-7 inhibition by XIAP. *Cell.* Mar 9 2001;104(5):769-780.
36. Srinivasula SM, Ashwell JD. IAPs: what's in a name? *Mol Cell.* Apr 25 2008;30(2):123-135.
37. Samuel T, Welsh K, Lober T, Togo SH, Zapata JM, Reed JC. Distinct BIR domains of cIAP1 mediate binding to and ubiquitination of tumor necrosis factor receptor-associated factor 2 and second mitochondrial activator of caspases. *Journal of Biological Chemistry.* Jan 13 2006;281(2):1080-1090.
38. Zheng C, Kabaleeswaran V, Wang Y, Cheng G, Wu H. Crystal structures of the TRAF2: cIAP2 and the TRAF1: TRAF2: cIAP2 complexes: affinity, specificity, and regulation. *Mol Cell.* Apr 9;38(1):101-113.
39. Mace PD, Smits C, Vaux DL, Silke J, Day CL. Asymmetric recruitment of cIAPs by TRAF2. *J Mol Biol.* May 3.
40. Martin SJ. Dealing the CARDS between life and death. *Trends Cell Biol.* May 2001;11(5):188-189.
41. Park HH, Lo YC, Lin SC, Wang L, Yang JK, Wu H. The death domain superfamily in intracellular signaling of apoptosis and inflammation. *Annu Rev Immunol.* 2007;25:561-586.
42. Huang H, Joazeiro CA, Bonfoco E, Kamada S, Levenson JD, Hunter T. The inhibitor of apoptosis, cIAP2, functions as a ubiquitin-protein ligase and promotes in vitro monoubiquitination of caspases 3 and 7. *J Biol Chem.* Sep 1 2000;275(35):26661-26664.

43. Morizane Y, Honda R, Fukami K, Yasuda H. X-linked inhibitor of apoptosis functions as ubiquitin ligase toward mature caspase-9 and cytosolic Smac/DIABLO. *J Biochem.* Feb 2005;137(2):125-132.
44. Li X, Yang Y, Ashwell JD. TNF-RII and c-IAP1 mediate ubiquitination and degradation of TRAF2. *Nature.* Mar 21 2002;416(6878):345-347.
45. Suzuki Y, Nakabayashi Y, Takahashi R. Ubiquitin-protein ligase activity of X-linked inhibitor of apoptosis protein promotes proteasomal degradation of caspase-3 and enhances its anti-apoptotic effect in Fas-induced cell death. *Proc Natl Acad Sci U S A.* Jul 17 2001;98(15):8662-8667.
46. Silke J, Kratina T, Chu D, et al. Determination of cell survival by RING-mediated regulation of inhibitor of apoptosis (IAP) protein abundance. *Proc Natl Acad Sci U S A.* Nov 8 2005;102(45):16182-16187.
47. Dikic I, Wakatsuki S, Walters KJ. Ubiquitin-binding domains - from structures to functions. *Nat Rev Mol Cell Biol.* Oct 2009;10(10):659-671.
48. Tait SW, de Vries E, Maas C, Keller AM, D'Santos CS, Borst J. Apoptosis induction by Bid requires unconventional ubiquitination and degradation of its N-terminal fragment. *J Cell Biol.* Dec 31 2007;179(7):1453-1466.
49. Tang ED, Wang CY, Xiong Y, Guan KL. A role for NF-kappaB essential modifier/IkappaB kinase-gamma (NEMO/IKKgamm) ubiquitination in the activation of the IkappaB kinase complex by tumor necrosis factor-alpha. *J Biol Chem.* Sep 26 2003;278(39):37297-37305.
50. Varfolomeev EE, Ashkenazi A. Tumor necrosis factor: an apoptosis JuNKie? *Cell.* Feb 20 2004;116(4):491-497.
51. Feldmann M, Maini RN. Lasker Clinical Medical Research Award. TNF defined as a therapeutic target for rheumatoid arthritis and other autoimmune diseases. *Nat Med.* Oct 2003;9(10):1245-1250.
52. Chen G, Goeddel DV. TNF-R1 signaling: a beautiful pathway. *Science.* May 31 2002;296(5573):1634-1635.
53. Hayden MS, Ghosh S. Shared principles in NF-kappaB signaling. *Cell.* Feb 8 2008;132(3):344-362.
54. Wallach D, Varfolomeev EE, Malinin NL, Goltsev YV, Kovalenko AV, Boldin MP. Tumor necrosis factor receptor and Fas signaling mechanisms. *Annu Rev Immunol.* 1999;17:331-367.
55. Wajant H, Pfizenmaier K, Scheurich P. Tumor necrosis factor signaling. *Cell Death Differ.* Jan 2003;10(1):45-65.
56. Mahoney DJ, Cheung HH, Mrad RL, et al. Both cIAP1 and cIAP2 regulate TNFalpha-mediated NF-kappaB activation. *Proc Natl Acad Sci U S A.* Aug 19 2008;105(33):11778-11783.

57. Shu HB, Takeuchi M, Goeddel DV. The tumor necrosis factor receptor 2 signal transducers TRAF2 and c-IAP1 are components of the tumor necrosis factor receptor 1 signaling complex. *Proc Natl Acad Sci U S A*. Nov 26 1996;93(24):13973-13978.
58. Varfolomeev E, Goncharov T, Fedorova AV, et al. c-IAP1 and c-IAP2 are critical mediators of tumor necrosis factor alpha (TNFalpha)-induced NF-kappaB activation. *J Biol Chem*. Sep 5 2008;283(36):24295-24299.
59. Vince JE, Wong WWL, Khan N, et al. IAP antagonists target cIAP1 to induce TNF alpha- dependent apoptosis. *Cell*. Nov 16 2007;131(4):682-693.
60. Hsu H, Xiong J, Goeddel DV. The TNF receptor 1-associated protein TRADD signals cell death and NF-kappa B activation. *Cell*. May 19 1995;81(4):495-504.
61. Devin A, Cook A, Lin Y, Rodriguez Y, Kelliher M, Liu ZG. The distinct roles of TRAF2 and RIP in IKK activation by TNF-R1: TRAF2 recruits IKK to TNF-R1 while RIP mediates IKK activation. *Immunity*. Apr 2000;12(4):419-429.
62. Kelliher MA, Grimm S, Ishida Y, Kuo F, Stanger BZ, Leder P. The death domain kinase RIP mediates the TNF-induced NF-kappaB signal. *Immunity*. Mar 1998;8(3):297-303.
63. Wu H, Tschopp J, Lin SC. Smac mimetics and TNFalpha: a dangerous liaison? *Cell*. Nov 16 2007;131(4):655-658.
64. Vince JE, Pantaki D, Feltham R, et al. TRAF2 Must Bind to Cellular Inhibitors of Apoptosis for Tumor Necrosis Factor (TNF) to Efficiently Activate NF-kappa B and to Prevent TNF-induced Apoptosis. *Journal of Biological Chemistry*. Dec 18 2009;284(51):35906-35915.
65. Varfolomeev E, Vucic D. (Un)expected roles of c-IAPs in apoptotic and NFkappaB signaling pathways. *Cell Cycle*. Jun 1 2008;7(11):1511-1521.
66. Wang CY, Mayo MW, Korneluk RG, Goeddel DV, Baldwin AS, Jr. NF-kappaB antiapoptosis: induction of TRAF1 and TRAF2 and c-IAP1 and c-IAP2 to suppress caspase-8 activation. *Science*. Sep 11 1998;281(5383):1680-1683.
67. Wang L, Du F, Wang X. TNF-alpha induces two distinct caspase-8 activation pathways. *Cell*. May 16 2008;133(4):693-703.
68. LaCasse EC, Mahoney DJ, Cheung HH, Plenchette S, Baird S, Korneluk RG. IAP-targeted therapies for cancer. *Oncogene*. Oct 20 2008;27(48):6252-6275.
69. Mannhold R, Fulda S, Carosati E. IAP antagonists: promising candidates for cancer therapy. *Drug Discov Today*. Jan 21.
70. Du C, Fang M, Li Y, Li L, Wang X. Smac, a mitochondrial protein that promotes cytochrome c-dependent caspase activation by eliminating IAP inhibition. *Cell*. Jul 7 2000;102(1):33-42.

71. Verhagen AM, Ekert PG, Pakusch M, et al. Identification of DIABLO, a mammalian protein that promotes apoptosis by binding to and antagonizing IAP proteins. *Cell*. Jul 7 2000;102(1):43-53.
72. Chai J, Du C, Wu JW, Kyin S, Wang X, Shi Y. Structural and biochemical basis of apoptotic activation by Smac/DIABLO. *Nature*. Aug 24 2000;406(6798):855-862.
73. Srinivasula SM, Hegde R, Saleh A, et al. A conserved XIAP-interaction motif in caspase-9 and Smac/DIABLO regulates caspase activity and apoptosis. *Nature*. Mar 1 2001;410(6824):112-116.
74. Varfolomeev E, Blankenship JW, Wayson SM, et al. IAP antagonists induce autoubiquitination of c-IAPs, NF-kappaB activation, and TNFalpha-dependent apoptosis. *Cell*. Nov 16 2007;131(4):669-681.
75. Yang QH, Du C. Smac/DIABLO selectively reduces the levels of c-IAP1 and c-IAP2 but not that of XIAP and livin in HeLa cells. *J Biol Chem*. Apr 23 2004;279(17):16963-16970.
76. Dineen SP, Roland CL, Greer R, et al. Smac mimetic increases chemotherapy response and improves survival in mice with pancreatic cancer. *Cancer Res*. Apr 1;70(7):2852-2861.
77. Nikolovska-Coleska Z, Meagher JL, Jiang S, et al. Design and characterization of bivalent Smac-based peptides as antagonists of XIAP and development and validation of a fluorescence polarization assay for XIAP containing both BIR2 and BIR3 domains. *Anal Biochem*. Mar 1 2008;374(1):87-98.
78. Cossu F, Mastrangelo E, Milani M, et al. Designing Smac-mimetics as antagonists of XIAP, cIAP1, and cIAP2. *Biochem Biophys Res Commun*. Jan 9 2009;378(2):162-167.
79. Cines DB, Pollak ES, Buck CA, et al. Endothelial cells in physiology and in the pathophysiology of vascular disorders. *Blood*. May 15 1998;91(10):3527-3561.
80. Mehta D, Malik AB. Signaling mechanisms regulating endothelial permeability. *Physiol Rev*. Jan 2006;86(1):279-367.
81. Galley HF, Webster NR. Physiology of the endothelium. *Br J Anaesth*. Jul 2004;93(1):105-113.
82. Acosta D, Adelman J, Affolder T, et al. Evidence for B0 s-->phipi decay and measurements of branching ratio and A(CP) for B+ -->phiK+. *Phys Rev Lett*. Jul 15 2005;95(3):031801.
83. Konstantoulaki M, Kouklis P, Malik AB. Protein kinase C modifications of VE-cadherin, p120, and beta-catenin contribute to endothelial barrier dysregulation induced by thrombin. *Am J Physiol Lung Cell Mol Physiol*. Aug 2003;285(2):L434-442.
84. Lampugnani MG, Corada M, Caveda L, et al. The molecular organization of endothelial cell to cell junctions: differential association of plakoglobin, beta-

- catenin, and alpha-catenin with vascular endothelial cadherin (VE-cadherin). *J Cell Biol.* Apr 1995;129(1):203-217.
85. Essler M, Amano M, Kruse HJ, Kaibuchi K, Weber PC, Aepfelbacher M. Thrombin inactivates myosin light chain phosphatase via Rho and its target Rho kinase in human endothelial cells. *J Biol Chem.* Aug 21 1998;273(34):21867-21874.
 86. Coughlin SR. Thrombin signalling and protease-activated receptors. *Nature.* Sep 14 2000;407(6801):258-264.
 87. Volk T, Kox WJ. Endothelium function in sepsis. *Inflamm Res.* May 2000;49(5):185-198.
 88. Aird WC. The role of the endothelium in severe sepsis and multiple organ dysfunction syndrome. *Blood.* May 15 2003;101(10):3765-3777.
 89. Kumar P, Shen Q, Pivetti CD, Lee ES, Wu MH, Yuan SY. Molecular mechanisms of endothelial hyperpermeability: implications in inflammation. *Expert Rev Mol Med.* 2009;11:e19.
 90. van Zonneveld AJ, de Boer HC, van der Veer EP, Rabelink TJ. Inflammation, vascular injury and repair in rheumatoid arthritis. *Ann Rheum Dis.* Jan;69 Suppl 1:i57-60.
 91. Janeway CA, Travers, P., Walport, M., Shlomchik, M.J. *Immuno Biology: the immune system in health and disease.* 6 ed. New York and London: Garland Sciences, Churchill Livingstone; 2005.
 92. Wittchen ES. Endothelial signaling in paracellular and transcellular leukocyte transmigration. *Front Biosci.* 2009;14:2522-2545.
 93. Kansas GS. Selectins and their ligands: current concepts and controversies. *Blood.* Nov 1 1996;88(9):3259-3287.
 94. Eriksson EE, Xie X, Werr J, Thoren P, Lindbom L. Importance of primary capture and L-selectin-dependent secondary capture in leukocyte accumulation in inflammation and atherosclerosis in vivo. *J Exp Med.* Jul 16 2001;194(2):205-218.
 95. McEver RP, Cummings RD. Role of PSGL-1 binding to selectins in leukocyte recruitment. *J Clin Invest.* Dec 1 1997;100(11 Suppl):S97-103.
 96. Ley K, Laudanna C, Cybulsky MI, Nourshargh S. Getting to the site of inflammation: the leukocyte adhesion cascade updated. *Nat Rev Immunol.* Sep 2007;7(9):678-689.
 97. Chesnutt BC, Smith DF, Raffler NA, Smith ML, White EJ, Ley K. Induction of LFA-1-dependent neutrophil rolling on ICAM-1 by engagement of E-selectin. *Microcirculation.* Mar 2006;13(2):99-109.
 98. Kinashi T. Intracellular signalling controlling integrin activation in lymphocytes. *Nat Rev Immunol.* Jul 2005;5(7):546-559.

99. Giagulli C, Scarpini E, Ottoboni L, et al. RhoA and zeta PKC control distinct modalities of LFA-1 activation by chemokines: critical role of LFA-1 affinity triggering in lymphocyte in vivo homing. *Immunity*. Jan 2004;20(1):25-35.
100. Campbell JJ, Hedrick J, Zlotnik A, Siani MA, Thompson DA, Butcher EC. Chemokines and the arrest of lymphocytes rolling under flow conditions. *Science*. Jan 16 1998;279(5349):381-384.
101. Millan J, Ridley AJ. Rho GTPases and leucocyte-induced endothelial remodelling. *Biochem J*. Jan 15 2005;385(Pt 2):329-337.
102. Vestweber D. Regulation of endothelial cell contacts during leukocyte extravasation. *Curr Opin Cell Biol*. Oct 2002;14(5):587-593.
103. Wang S, Dangerfield JP, Young RE, Nourshargh S. PECAM-1, alpha6 integrins and neutrophil elastase cooperate in mediating neutrophil transmigration. *J Cell Sci*. May 1 2005;118(Pt 9):2067-2076.
104. Bradley JR. TNF-mediated inflammatory disease. *J Pathol*. Jan 2008;214(2):149-160.
105. Locksley RM, Killeen N, Lenardo MJ. The TNF and TNF receptor superfamilies: integrating mammalian biology. *Cell*. Feb 23 2001;104(4):487-501.
106. Bianchi K, Meier P. A tangled web of ubiquitin chains: breaking news in TNF-R1 signaling. *Mol Cell*. Dec 11 2009;36(5):736-742.
107. Sprague AH, Khalil RA. Inflammatory cytokines in vascular dysfunction and vascular disease. *Biochem Pharmacol*. Sep 15 2009;78(6):539-552.
108. Hayden MS, Ghosh S. Signaling to NF-kappaB. *Genes Dev*. Sep 15 2004;18(18):2195-2224.
109. Perkins ND. Integrating cell-signalling pathways with NF-kappaB and IKK function. *Nat Rev Mol Cell Biol*. Jan 2007;8(1):49-62.
110. Skaug B, Jiang X, Chen ZJ. The role of ubiquitin in NF-kappaB regulatory pathways. *Annu Rev Biochem*. 2009;78:769-796.
111. Xu P, Duong DM, Seyfried NT, et al. Quantitative proteomics reveals the function of unconventional ubiquitin chains in proteasomal degradation. *Cell*. Apr 3 2009;137(1):133-145.
112. Chang L, Karin M. Mammalian MAP kinase signalling cascades. *Nature*. Mar 1 2001;410(6824):37-40.
113. Brown MD, Sacks DB. Protein scaffolds in MAP kinase signalling. *Cell Signal*. Apr 2009;21(4):462-469.
114. Aiyer HS, Vadhanam MV, Stoyanova R, Caprio GD, Clapper ML, Gupta RC. Dietary berries and ellagic Acid prevent oxidative DNA damage and modulate expression of DNA repair genes. *Int J Mol Sci*. Mar 2008;9(3):327-341.

115. Broom OJ, Widjaya B, Troelsen J, Olsen J, Nielsen OH. Mitogen activated protein kinases: a role in inflammatory bowel disease? *Clin Exp Immunol*. Dec 2009;158(3):272-280.
116. Karin M, Gallagher E. TNFR signaling: ubiquitin-conjugated TRAF6 signals control stop-and-go for MAPK signaling complexes. *Immunol Rev*. Mar 2009;228(1):225-240.
117. Thalhamer T, McGrath MA, Harnett MM. MAPKs and their relevance to arthritis and inflammation. *Rheumatology (Oxford)*. Apr 2008;47(4):409-414.
118. Brown MD, Sacks DB. Compartmentalised MAPK pathways. *Handb Exp Pharmacol*. 2008(186):205-235.
119. Roebuck KA, Finnegan A. Regulation of intercellular adhesion molecule-1 (CD54) gene expression. *J Leukoc Biol*. Dec 1999;66(6):876-888.
120. Seneci P, Bianchi A, Battaglia C, et al. Rational design, synthesis and characterization of potent, non-peptidic Smac mimics/XIAP inhibitors as proapoptotic agents for cancer therapy. *Bioorg Med Chem*. Aug 15 2009;17(16):5834-5856.
121. Li H, Oehrlein SA, Wallerath T, et al. Activation of protein kinase C alpha and/or epsilon enhances transcription of the human endothelial nitric oxide synthase gene. *Mol Pharmacol*. Apr 1998;53(4):630-637.
122. Smith PK, Krohn RI, Hermanson GT, et al. Measurement of protein using bicinchoninic acid. *Anal Biochem*. Oct 1985;150(1):76-85.
123. Bradford MM. A rapid and sensitive method for the quantitation of microgram quantities of protein utilizing the principle of protein-dye binding. *Anal Biochem*. May 7 1976;72:248-254.
124. Laemmli UK. Cleavage of structural proteins during the assembly of the head of bacteriophage T4. *Nature*. Aug 15 1970;227(5259):680-685.
125. Kurien BT, Scofield RH. Protein blotting: a review. *J Immunol Methods*. Mar 1 2003;274(1-2):1-15.
126. Nicoletti I, Migliorati G, Pagliacci MC, Grignani F, Riccardi C. A rapid and simple method for measuring thymocyte apoptosis by propidium iodide staining and flow cytometry. *J Immunol Methods*. Jun 3 1991;139(2):271-279.
127. Veihelmann A, Hofbauer A, Krombach F, et al. Differential function of nitric oxide in murine antigen-induced arthritis. *Rheumatology*. May 2002;41(5):509-517.
128. Baez S. An open cremaster muscle preparation for the study of blood vessels by in vivo microscopy. *Microvasc Res*. May 1973;5(3):384-394.
129. Wegmann F, Petri B, Khandoga AG, et al. ESAM supports neutrophil extravasation, activation of Rho, and VEGF-induced vascular permeability. *J Exp Med*. Jul 10 2006;203(7):1671-1677.

130. Yeh WC, Shahinian A, Speiser D, et al. Early lethality, functional NF-kappaB activation, and increased sensitivity to TNF-induced cell death in TRAF2-deficient mice. *Immunity*. Nov 1997;7(5):715-725.
131. Tada K, Okazaki T, Sakon S, et al. Critical roles of TRAF2 and TRAF5 in tumor necrosis factor-induced NF-kappa B activation and protection from cell death. *J Biol Chem*. Sep 28 2001;276(39):36530-36534.
132. Karin M. Nuclear factor-kappaB in cancer development and progression. *Nature*. May 25 2006;441(7092):431-436.
133. Moran EP, Agrawal DK. Increased expression of inhibitor of apoptosis proteins in atherosclerotic plaques of symptomatic patients with carotid stenosis. *Exp Mol Pathol*. Aug 2007;83(1):11-16.
134. Balkwill F, Charles KA, Mantovani A. Smoldering and polarized inflammation in the initiation and promotion of malignant disease. *Cancer Cell*. Mar 2005;7(3):211-217.
135. Coussens LM, Werb Z. Inflammation and cancer. *Nature*. Dec 19-26 2002;420(6917):860-867.
136. Lee DM, Weinblatt ME. Rheumatoid arthritis. *Lancet*. Sep 15 2001;358(9285):903-911.
137. Joseph A, Brasington R, Kahl L, Ranganathan P, Cheng TP, Atkinson J. Immunologic rheumatic disorders. *J Allergy Clin Immunol*. Feb;125(2 Suppl 2):S204-215.
138. Brackertz D, Mitchell GF, Mackay IR. Antigen-induced arthritis in mice. I. Induction of arthritis in various strains of mice. *Arthritis Rheum*. Apr 1977;20(3):841-850.
139. Schaible UE, Vestweber D, Butcher EG, Stehle T, Simon MM. Expression of endothelial cell adhesion molecules in joints and heart during *Borrelia burgdorferi* infection of mice. *Cell Adhes Commun*. Dec 1994;2(6):465-479.
140. Turowski P, Martinelli R, Crawford R, et al. Phosphorylation of vascular endothelial cadherin controls lymphocyte emigration. *J Cell Sci*. Jan 1 2008;121(Pt 1):29-37.
141. Sumagin R, Sarelius IH. Intercellular Adhesion Molecule-1 Enrichment near Tricellular Endothelial Junctions Is Preferentially Associated with Leukocyte Transmigration and Signals for Reorganization of These Junctions To Accommodate Leukocyte Passage. *J Immunol*. Apr 2.
142. Madge LA, Pober JS. TNF signaling in vascular endothelial cells. *Exp Mol Pathol*. Jun 2001;70(3):317-325.
143. Kato T, Kitagawa S. Regulation of neutrophil functions by proinflammatory cytokines. *Int J Hematol*. Oct 2006;84(3):205-209.

144. Sun H, Nikolovska-Coleska Z, Yang CY, et al. Structure-based design, synthesis, and evaluation of conformationally constrained mimetics of the second mitochondria-derived activator of caspase that target the X-linked inhibitor of apoptosis protein/caspase-9 interaction site. *J Med Chem.* Aug 12 2004;47(17):4147-4150.
145. Schroder K, Tschopp J. The inflammasomes. *Cell.* Mar 19;140(6):821-832.
146. Wu X, Guo R, Chen P, Wang Q, Cunningham PN. TNF induces caspase-dependent inflammation in renal endothelial cells through a Rho- and myosin light chain kinase-dependent mechanism. *Am J Physiol Renal Physiol.* Aug 2009;297(2):F316-326.
147. Furusu A, Nakayama K, Xu Q, Konta T, Kitamura M. MAP kinase-dependent, NF-kappaB-independent regulation of inhibitor of apoptosis protein genes by TNF-alpha. *J Cell Physiol.* Mar 2007;210(3):703-710.
148. Stehlik C, de Martin R, Kumabashiri I, Schmid JA, Binder BR, Lipp J. Nuclear factor (NF)-kappaB-regulated X-chromosome-linked iap gene expression protects endothelial cells from tumor necrosis factor alpha-induced apoptosis. *J Exp Med.* Jul 6 1998;188(1):211-216.
149. Ndubaku C, Varfolomeev E, Wang L, et al. Antagonism of c-IAP and XIAP proteins is required for efficient induction of cell death by small-molecule IAP antagonists. *ACS Chem Biol.* Jul 17 2009;4(7):557-566.
150. Wu CJ, Conze DB, Li T, Srinivasula SM, Ashwell JD. Sensing of Lys 63-linked polyubiquitination by NEMO is a key event in NF-kappaB activation [corrected]. *Nat Cell Biol.* Apr 2006;8(4):398-406.
151. Ea CK, Deng L, Xia ZP, Pineda G, Chen ZJ. Activation of IKK by TNFalpha requires site-specific ubiquitination of RIP1 and polyubiquitin binding by NEMO. *Mol Cell.* Apr 21 2006;22(2):245-257.
152. Conte D, Holcik M, Lefebvre CA, et al. Inhibitor of apoptosis protein cIAP2 is essential for lipopolysaccharide-induced macrophage survival. *Mol Cell Biol.* Jan 2006;26(2):699-708.
153. Conze DB, Albert L, Ferrick DA, et al. Posttranscriptional downregulation of c-IAP2 by the ubiquitin protein ligase c-IAP1 in vivo. *Mol Cell Biol.* Apr 2005;25(8):3348-3356.
154. Mohapatra SS. Role of natriuretic peptide signaling in modulating asthma and inflammation. *Can J Physiol Pharmacol.* Jul 2007;85(7):754-759.
155. Kierner AK, Weber NC, Vollmar AM. Induction of IkappaB: atrial natriuretic peptide as a regulator of the NF-kappaB pathway. *Biochem Biophys Res Commun.* Aug 2 2002;295(5):1068-1076.
156. Kierner AK, Weber NC, Furst R, Bildner N, Kulhanek-Heinze S, Vollmar AM. Inhibition of p38 MAPK activation via induction of MKP-1: atrial natriuretic peptide reduces TNF-alpha-induced actin polymerization and endothelial permeability. *Circ Res.* May 3 2002;90(8):874-881.

-
157. Birukova AA, Zagranichnaya T, Alekseeva E, Bokoch GM, Birukov KG. Epac/Rap and PKA are novel mechanisms of ANP-induced Rac-mediated pulmonary endothelial barrier protection. *J Cell Physiol.* Jun 2008;215(3):715-724.
 158. Xing J, Birukova AA. ANP attenuates inflammatory signaling and Rho pathway of lung endothelial permeability induced by LPS and TNFalpha. *Microvasc Res.* Jan;79(1):56-62.

8 APPENDIX

8.1 Publications

8.1.1 Original publications

Mayer BA, Rehberg M, Reichel CA, Krombach F, Zahler S, Vollmar AM, Fürst R. Inhibitor of apoptosis proteins (IAPs) as novel targets in inflammatory processes of endothelial cells. In preparation.

Heermann R, Weber A, Mayer BA, Ott M, Hauser E, Gabriel G, Pirch T, Jung K. The universal stress protein UspC scaffolds the KdpD/KdpE signaling cascade of *Escherichia coli* under salt stress. J Mol Biol. 2009 Feb 13;386(1):134-48. Epub 2008 Dec 11.

Fürst R, Bubik MF, Bihari P, Mayer BA, Khandoga AG, Hoffmann F, Rehberg M, Krombach F, Zahler S, Vollmar AM. Atrial natriuretic peptide protects against histamine-induced endothelial barrier dysfunction *in vivo*. Mol Pharmacol. 2008 Jul;74(1):1-8. Epub 2008 Apr 15.

8.1.2 Abstracts

Mayer BA, Rehberg M, Reichel CA, Krombach F, Zahler S, Vollmar AM, Fürst R. Inhibitor of apoptosis proteins (IAPs) as novel targets in inflammatory processes of endothelial cells. IVBM 2010, June 20-24, Los Angeles, CA, USA

Mayer BA, Reichel CA, Krombach F, Zahler S, Vollmar AM, Fürst R. Inhibitor of apoptosis proteins (IAPs) as novel targets in inflammatory processes of endothelial cells. WorldPharma 2010, July 17-23, Copenhagen, Denmark.

Mayer BA, Rehberg M, Reichel CA, Krombach F, Zahler S, Vollmar AM, Fürst R. Inhibitor of apoptosis proteins (IAPs) as novel targets in inflammatory processes of endothelial cells. 51st Annual Meeting of the Deutsche Gesellschaft für Experimentelle und Klinische Pharmakologie und Toxikologie, March 23-25, 2010, Mainz, Germany. Naunyn Schmiedeberg's Arch Pharmacol. 2010;381 Abs. 161.

Mayer BA, Schmerwitz UK, Zahler S, Vollmar AM, Fürst R. Inhibitor of apoptosis proteins (IAPs) as novel targets for the impairment of inflammatory processes in endothelial cells. 7th international Symposium on the biology of endothelial cells 2009, September 2-5, Vienna, Austria.

Mayer BA, Bubik MF, Ammer H, Zahler S, Vollmar AM, Fürst R. ANP protects against endothelial leakage by influencing endothelial cell contraction signaling. 50st Annual Meeting of the Deutsche Gesellschaft für Experimentelle und Klinische Pharmakologie und Toxikologie, March 10-12, 2009, Mainz, Germany. Naunyn Schmiedeberg's Arch Pharmacol. 2009;379 Abs. 165.

8.1.3 Grants

LMUexcellent Mentoring

Oktober 2007-recent, Ludwig Maximilians Universität Munich, Germany

8.2 Curriculum vitae

Personal data

Name	Bettina Angela Mayer
Date of birth	6 th January 1981
Place of birth	Bad Reichenhall
Marital status	single

Academic education

June 2006-June 2010	PhD thesis at the department of pharmacy, pharmaceutical biology, LMU Munich, Prof. Dr. A.M. Vollmar
January 2005-October 2005	Diploma thesis "Die Bedeutung der universellen Stressproteine UspC und UspD in <i>E. coli</i> : Der Einfluss auf das KdpD-System und die Interaktion von UspC mit KdpD" at the department of biology, microbiology, LMU Munich, Prof. Dr. K. Jung
September 2000-October 2005	Study of biology, LMU Munich, Diploma

School education

1991-2000	Karls-gymnasium, Bad Reichenhall
1987-1991	Primary school, Feldkirchen

8.3 Acknowledgements

First of all, I would like to thank Prof. Dr. Angelika M. Vollmar for giving me the opportunity to carry out my PhD thesis in her working group, for her great mentoring and for continuously motivating me. I also highly appreciated that she trusted in my ideas and my opinion and that she always took the time for her PhD students.

Equally, I would like to show my gratitude to Dr. Robert Fürst for his excellent and competent supervision, for our discussions and exchange and his input also beyond the technical knowledge.

Furthermore I am very grateful to PD Dr. Stefan Zahler for his technical advice in difficult situations and for his suggestions and estimations in our meetings and last but not least for acting as a second examiner on my thesis.

I also want to thank Prof. Dr. Fritz Krombach, Prof. Dr. Christian Wahl-Schott, PD Dr. Manfred Ogris and Prof. Dr. Franz F. Paintner for being members of my thesis committee.

Sincere thanks are given to the group of Prof. Dr. Fritz Krombach. I thank Dr. Markus Rehberg for performing the mouse cremaster assays and Dr. Christoph Reichel for supervising the arthritis experiment.

I am also very indebted to Jana, Bianca and Frau Schnegg for their great help and for our stimulating conversations. I want to thank all my former and recent lab members for the fun we had and the pleasant ambiance which made it easier to endure lean times. I thank Hanna for her support, her advice, the conversations and for having a very nice time in Vienna. I enjoyed the coffee times with the members of the pre-PhD team (Ulla, Nina, Christine and Ruth) and of course the “sushi meetings” and leisure time activities. Moreover, I want to thank Elisabeth and Sabine for the pleasant company in our lab and their extra-support in the last student lab class.

I am deeply thankful to my family for offering me the opportunity for my development, for their never ending support and understanding and for being there when I need them.

Many thanks go to Lutz for his appreciation and encouragement and for having a very exhilarating time together.